NASACR134853

EXPERIMENTAL CLEAN COMBUSTOR PROGRAM

Noise Measurement Addendum

PHASE I FINAL REPORT

by

J. J. Emmerling

GENERAL ELECTRIC COMPANY

Prepared For

National Aeronautics and Space Administration

NASA-Lewis Research Center
Contract NAS 3-16830

1. Report No.	2. Government Accession No.	3. Recipient's Catalog No.
CR 134853		

4. Title and Subtitle	5. Report Date
Experimental Clean Combustor Program Noise Measurement Addendum - Phase I Final Report	July, 1975
	6. Performing Organization Code
7. Author(s)	8. Performing Organization Report No.
J.J. Emmerling	GE 75AEG315
	10. Work Unit No.
9. Performing Organization Name and Address	
General Electric Company Aircraft Engine Group Cincinnati, Ohio 45215	11. Contract or Grant No. NAS3-16830
	13. Type of Report and Period Covered
12. Sponsoring Agency Name and Address	Contractor Report
National Aeronautics and Space Administration Washington, D.C. 20546	14. Sponsoring Agency Code

15. Supplementary Notes

Project Manager, R.G. Huff, V/STOL and Noise Division
NASA-Lewis Research Center, Cleveland, Ohio

16. Abstract

The test results of combustor noise measurements taken with waveguide probes have been presented. Waveguide probes were shown to be a viable measurement technique for determining high sound pressure level broadband noise. A total of six full-scale annular combustors were tested and included the three advanced combustor designs: Swirl-Can, Radial/Axial and Double Annular.

17. Key Words (Suggested by Author(s))	18. Distribution Statement
Noise Combustor Noise Waveguide Acoustic Probe Core Engine Noise	

19. Security Classif. (of this report)	20. Security Classif. (of this page)	21. No. of Pages	22. Price*
Unclassified	Unclassified		

* For sale by the National Technical Information Service, Springfield, Virginia 22151

TABLE OF CONTENTS

LIST OF ILLUSTRATIONS

LIST OF ILLUSTRATIONS (Continued)

LIST OF ILLUSTRATIONS (Continued)

LIST OF ILLUSTRATIONS (Continued)

LIST OF ILLUSTRATIONS (Concluded)

LIST OF TABLES

LIST OF TABLES (Concluded)

SECTION 1.0

SUMMARY

Combustor noise has been suspected of being a significant contributor to an aircraft gas turbine's acoustic signature at the lower power settings. It is therefore desirable to measure combustor noise independent of the other engine noise sources in order to better understand the characteristics of this component's acoustic signature. Acoustic measurements using waveguide probes were taken on six of the combustor configurations that were tested during Phase I of the Experimental Clean Combustor Program.

SECTION 2.0

INTRODUCTION

The principle objective of this Noise Measurement Addendum to Phase I of the Experimental Clean Combustor Program was to observe and record the differences in spectrum shape and level between the combustor configurations over a range of inlet aerodynamic conditions.

Acoustic waveguide probes were placed upstream and downstream of the combustors. A top-half cross section of the combustor test rig layout can be seen in Figure 1. Detailed information that has not been included in this report concerning the test facility or the aerodynamic instrumentation can be found in the Experimental Clean Combustor Program Phase I Final Report (Reference 1).

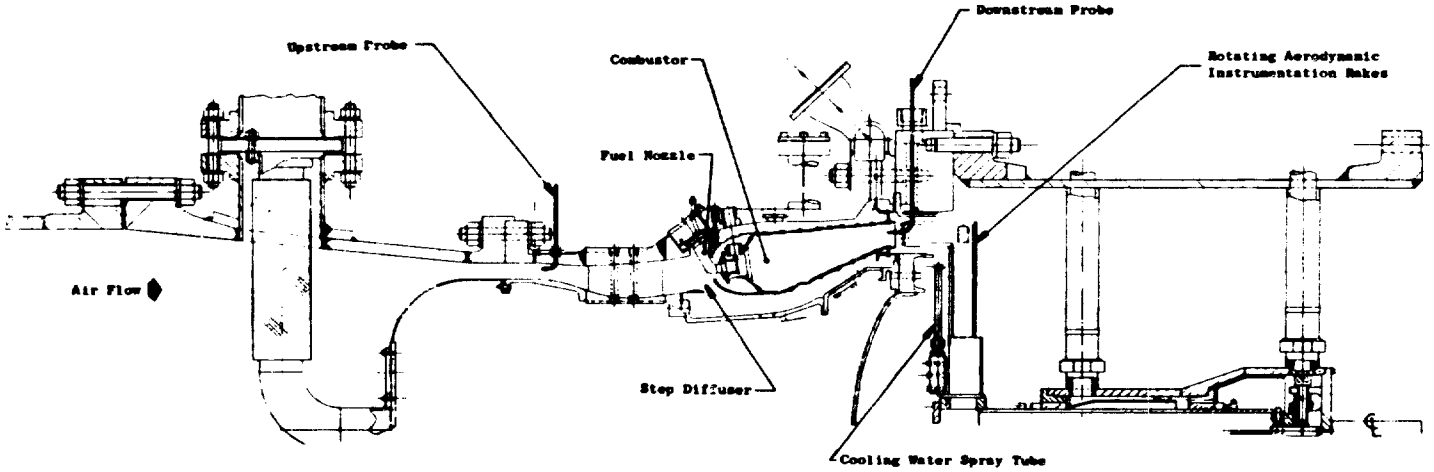

Figure 1. Combustor Test Rig Layout.

SECTION 3.0

INSTRUMENTATION

3.1 PROBE DESIGN

There was an initial question as to whether a wall static or a waveguide probe could be used to measure combustor noise. A comparison was made of the relative levels of both a wall static probe and a waveguide probe with the far-field spectra from an atmospheric pressure annular combustor test. The wall static probe was installed through a borescope port in the outer liner. This port was approximately halfway between the fuel nozzles and the combustor exit. The end of this probe was flush with the inside of the outer liner. (These tests were performed under Contract DOT-FA72 WA-3023.) The levels from this probe were found to be in agreement with the farfield levels at the higher fuel-air ratios. However, at the lower fuel-air ratios, the wall static probe indicated higher levels than the corresponding farfield level. Also, the spectral shape from the wall static probe was flatter than the farfield spectra. These differences in level and spectra have been attributed to the turbulent aerodynamic pressure in the boundary layer in that region.

A waveguide probe was placed at the liner exit plane, pointing upstream into the combustor. The sound pressure levels from this probe followed the same trends as the farfield microphones over the entire operating range. There was also agreement in the spectrum shapes. It was therefore decided that wave guide probes would be used to measure combustor noise.

Two waveguide probes were chosen for the test. The upstream probe had an outside diameter of 0.635 cm with a 0.0711-cm wall thickness. The length from the sensing holes to the transducer was 50 cm. The downstream probe had the same internal dimensions; however, it was fully water-jacketed. This probe was designed for the combustor environment where temperatures can go above 1600° K. The design, Figure 2, incorporated impingement cooling on the copper tip. A photograph illustrating the water connectors can be seen in Figure 3.

3.2 PROBE CALIBRATION

The two waveguide probes were calibrated in a 2.54-cm diameter tube (Figure 4). A B&K-type 4134 microphone was used to measure the probe signals. A small (1.27-mm) reference kulite was mounted on the probe tip next to the static sensing holes. This reference kulite had a flat response from 20 to over 10,000 Hz. It was connected to a feedback compressor circuit to keep the sound pressure levels at a constant value at the probe sensing holes. The signals from both the kulite and the microphone were filtered with a 20-Hz constant bandwidth filter and the levels of each were compared. The difference between the two levels is the probe loss. The

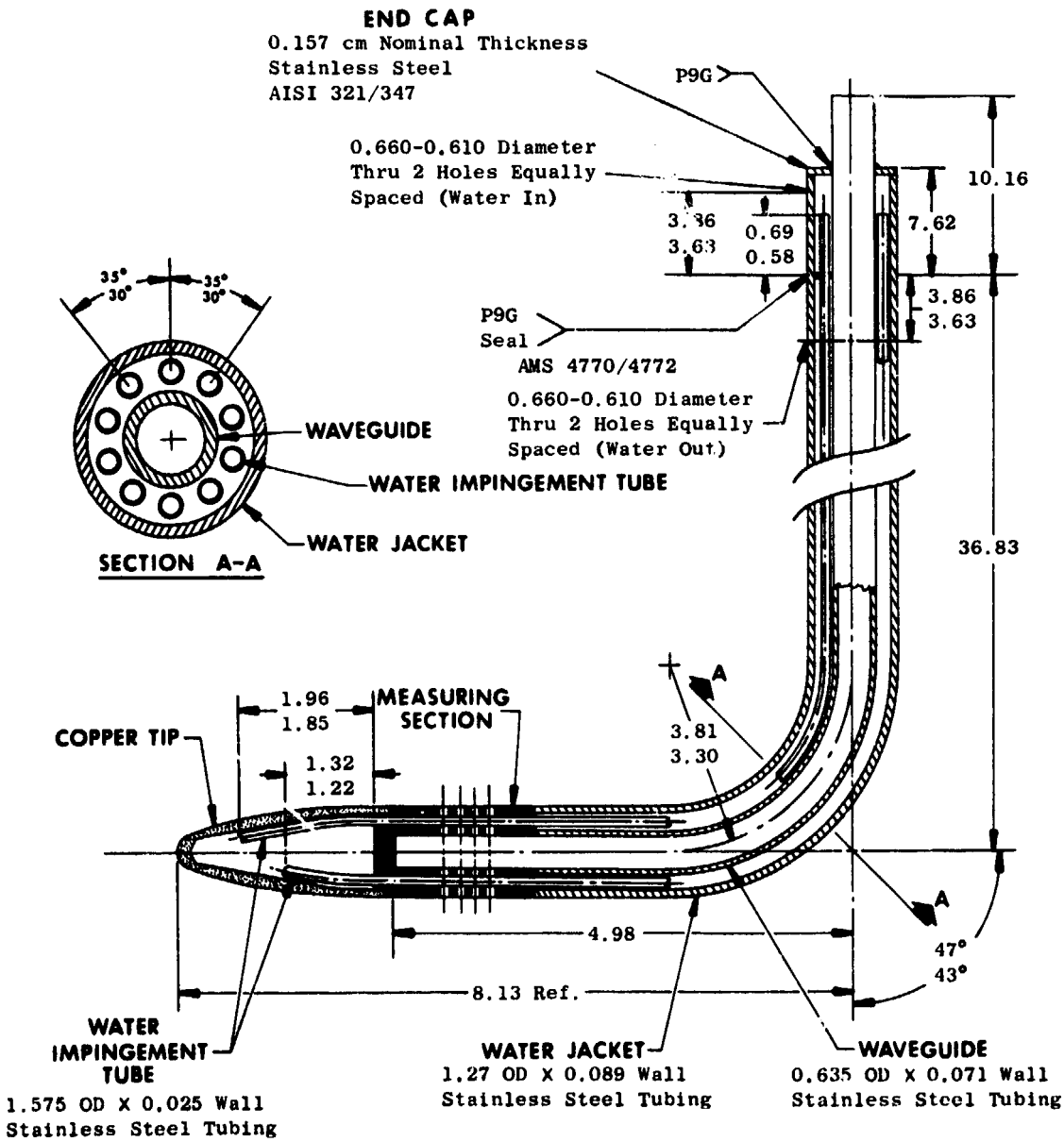

Figure 2. Water Cooled Acoustic Waveguide Probe Drawing.

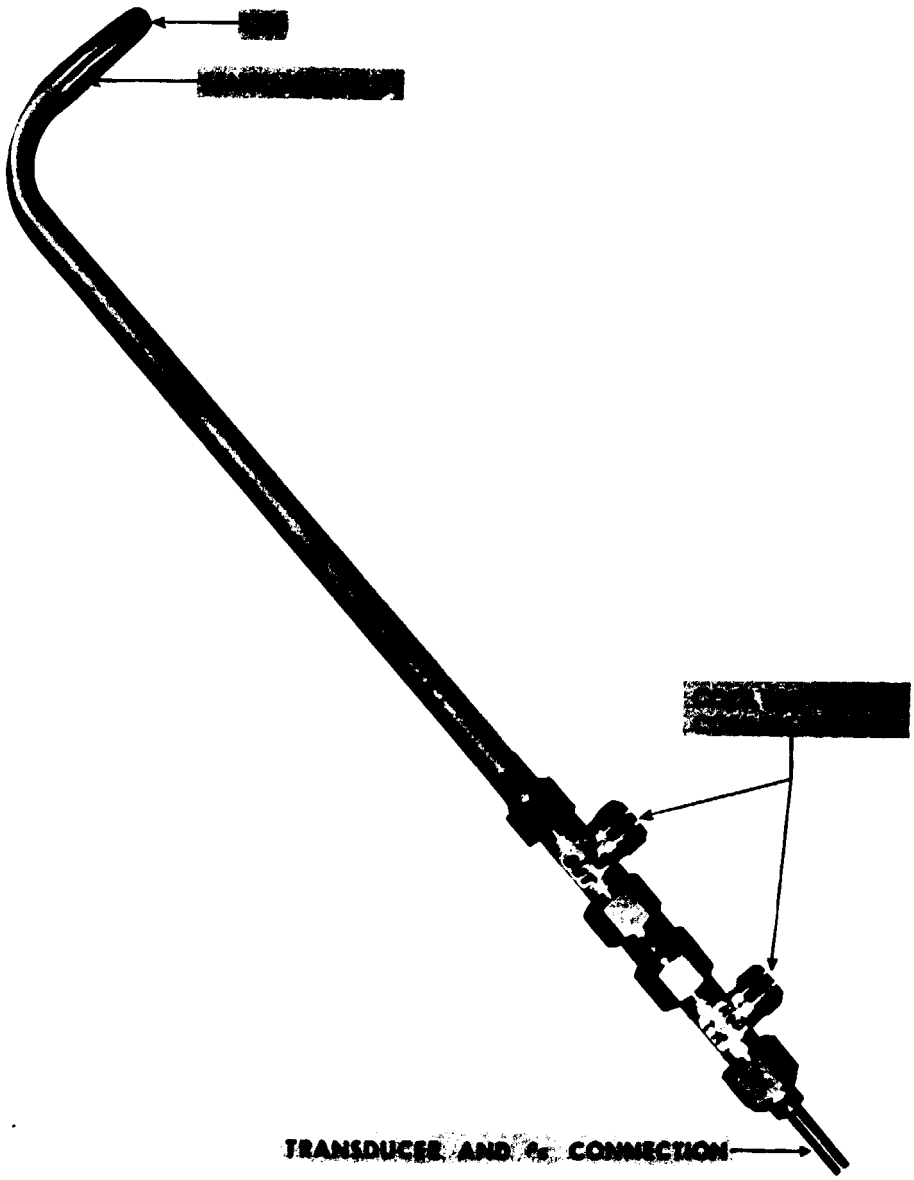

Figure 3. Water Cooled Acoustic Waveguide Probe.

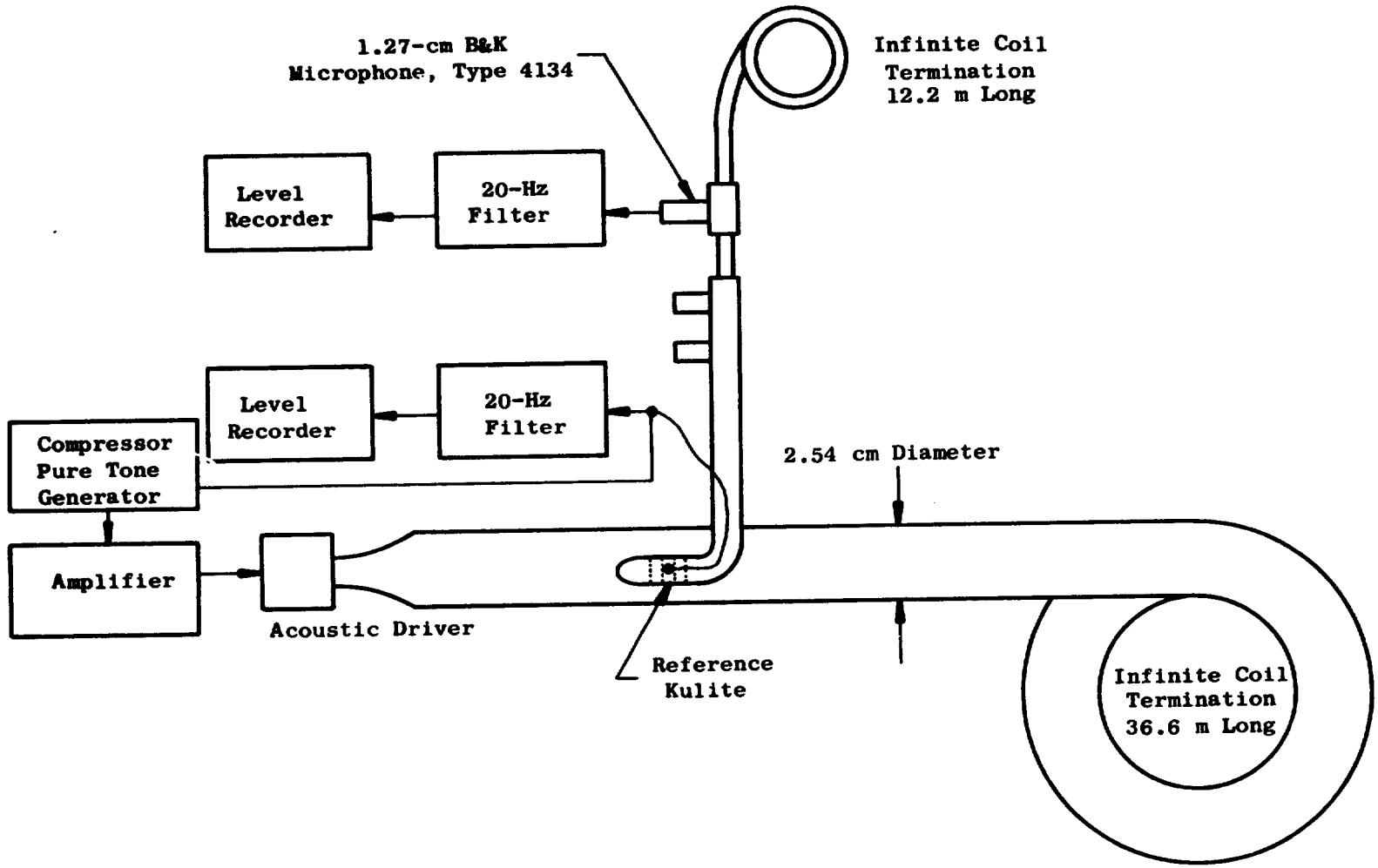

Figure 4. Waveguide Probe Calibration Schematic.

plots of the losses for each probe can be seen in Figure 5. These levels (tabulated in Table I) must be added to the levels the microphone measures in order to get the probe corrected actual sound pressure levels at the probe sensing holes.

The possible influence of the reference kulite on the sound wave entering the waveguide probe is assumed to be small. This is justified when the measured loss is within one dB of the calculated loss by the Iberall method (Reference 2). It was not possible to measure the probe loss below 100 Hz due to the limitation of the range of the acoustic driver. The attenuation below this frequency is negligible, making an exact measurement unnecessary.

3.3 EFFECT OF EXTERNAL FLOW ON PROBES

Both probes, each in turn, were mounted in a 12.7-cm by 6.1-cm duct (Figure 6). This duct height was chosen because it was similar to the annulus passage height in the combustor. The upstream piping noise was reduced in the acoustically treated plenum. Screens were used to straighten the flow in order to produce a uniform velocity profile. The flow noise was measured at 5 Mach numbers from 0.1 to 0.3 (Figures 7 and 8). The flow noise spectra peak sound pressure levels were 125 dB for the standard probe and 126 dB for the water-cooled probe. Both peaks occurred at 250 Hz. These levels were considerably lower than the combustor noise levels that were measured. This showed that the pressure levels generated by flow passing over the probe will be negligible when compared to the airborne sound pressure levels of the combustor which are higher than 135 dB.

3.4 EFFECTS OF INTERNAL FLOW

In order to determine the effect of any possible noise generated by the cooling water flow, a test was run with and without the cooling water. It was found (Figure 9) that no additional noise was generated by the cooling water. However, there is the possibility that steam could be formed in the cooling water passage. Shop air was blown through the cooling water passages to simulate the effect of steam. The only effects above the background noise that could be seen (Figure 10) were peaks at 2000 and 5000 Hz that did not exceed 65 dB. This level of signal is not significant compared to the combustor noise levels.

3.5 PROBE POSITIONS

The axial locations of the two probes in the combustor test rig are shown in Figure 11. The 6.35-mm diameter waveguide probe was placed in the center of the annulus through a rake blankoff pad at engine station 3, which is approximately 70 cm upstream of the combustor exit plane. The water-cooled downstream probe was installed just behind the combustor exit plane, which is engine station 3.9. The centers of its sensing holes were located 9.5 mm upstream of the cold liner exit plane in the center of the

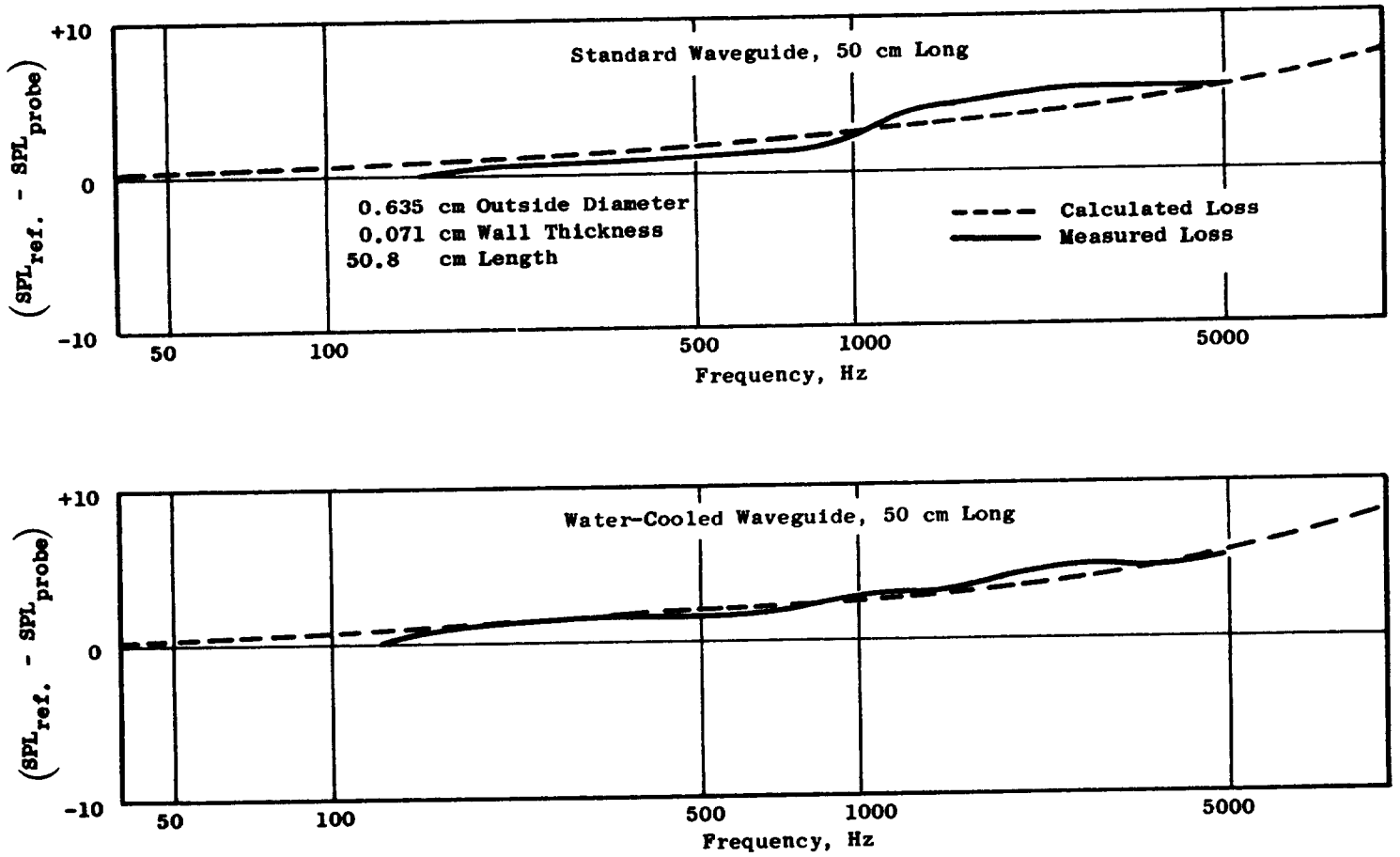

Figure 5. Measured Viscous Losses of Waveguide Probes.

Table I. Tabulation of Probe Losses.

Frequency	Upstream Waveguide Probe	Downstream Water-Cooled Waveguide Probe
31.5	0	0
40	0	0
50	0	0
63	0	0
80	0	0
100	0	0
125	0.3	0
160	0.1	0.4
200	0.2	0.7
250	0.4	1.2
315	0.5	1.0
400	0.7	1.3
500	0.8	1.4
630	1.0	1.6
800	2.0	2.0
1000	2.5	2.5
1250	3.3	2.9
1600	4.2	3.5
2000	4.9	4.0
2500	5.1	4.5
3150	5.2	4.5
4000	5.1	4.2
5000	5.0	4.0

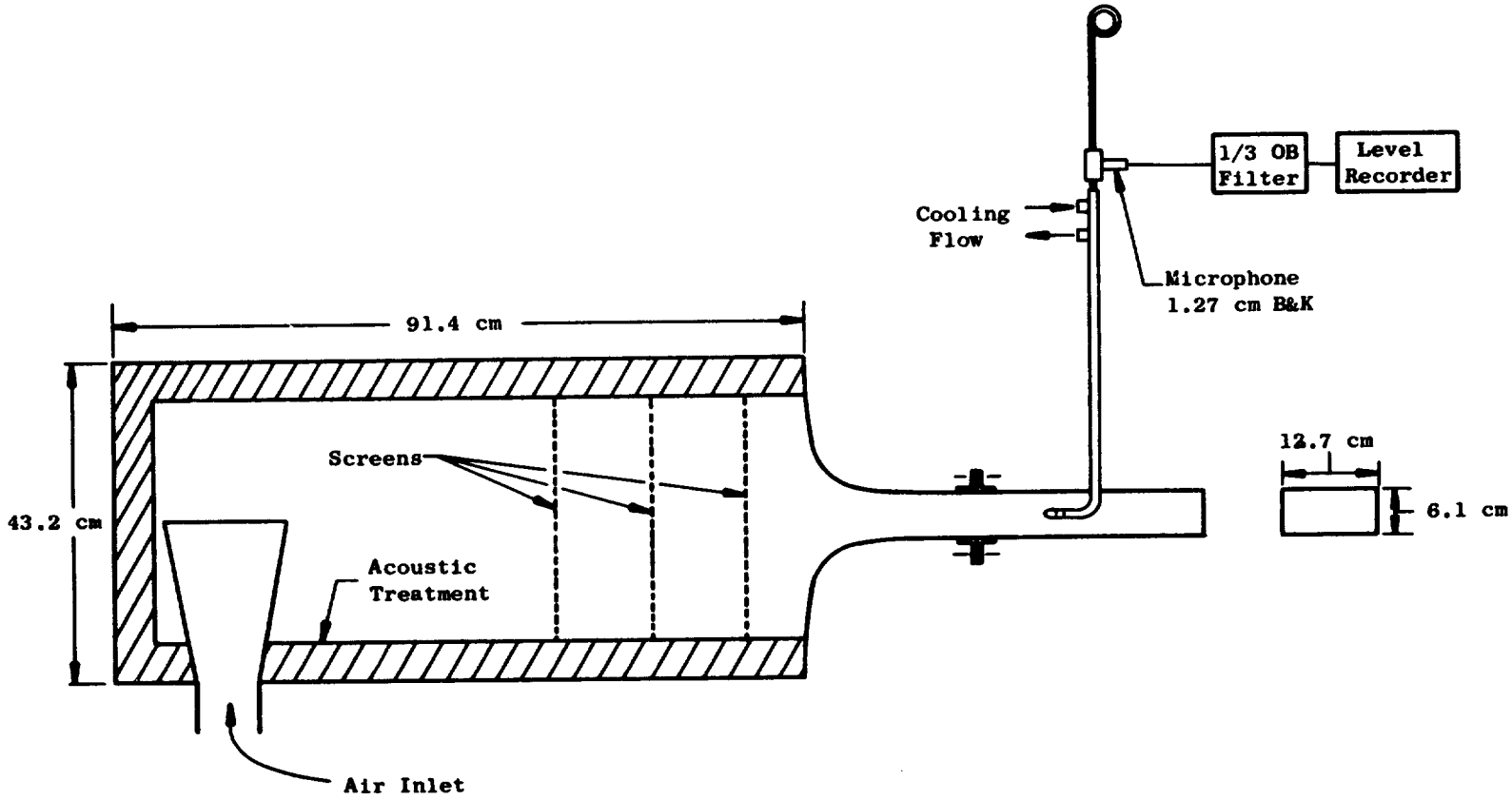

Figure 6. Acoustic Duct Facility for Probe Flow Noise Measurement.

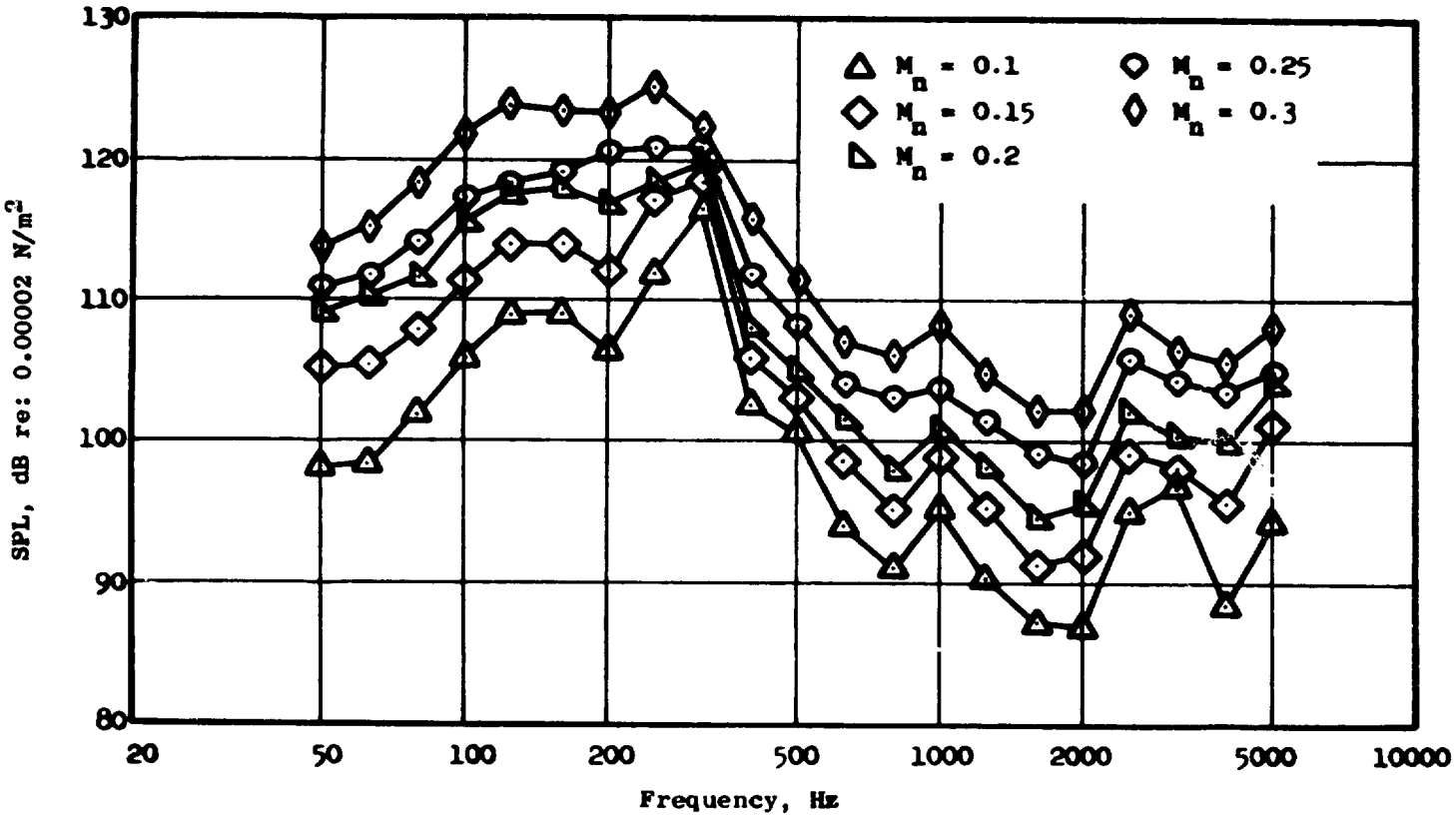

Figure 7. Corrected Probe Flow Noise, 50-cm long Waveguide.

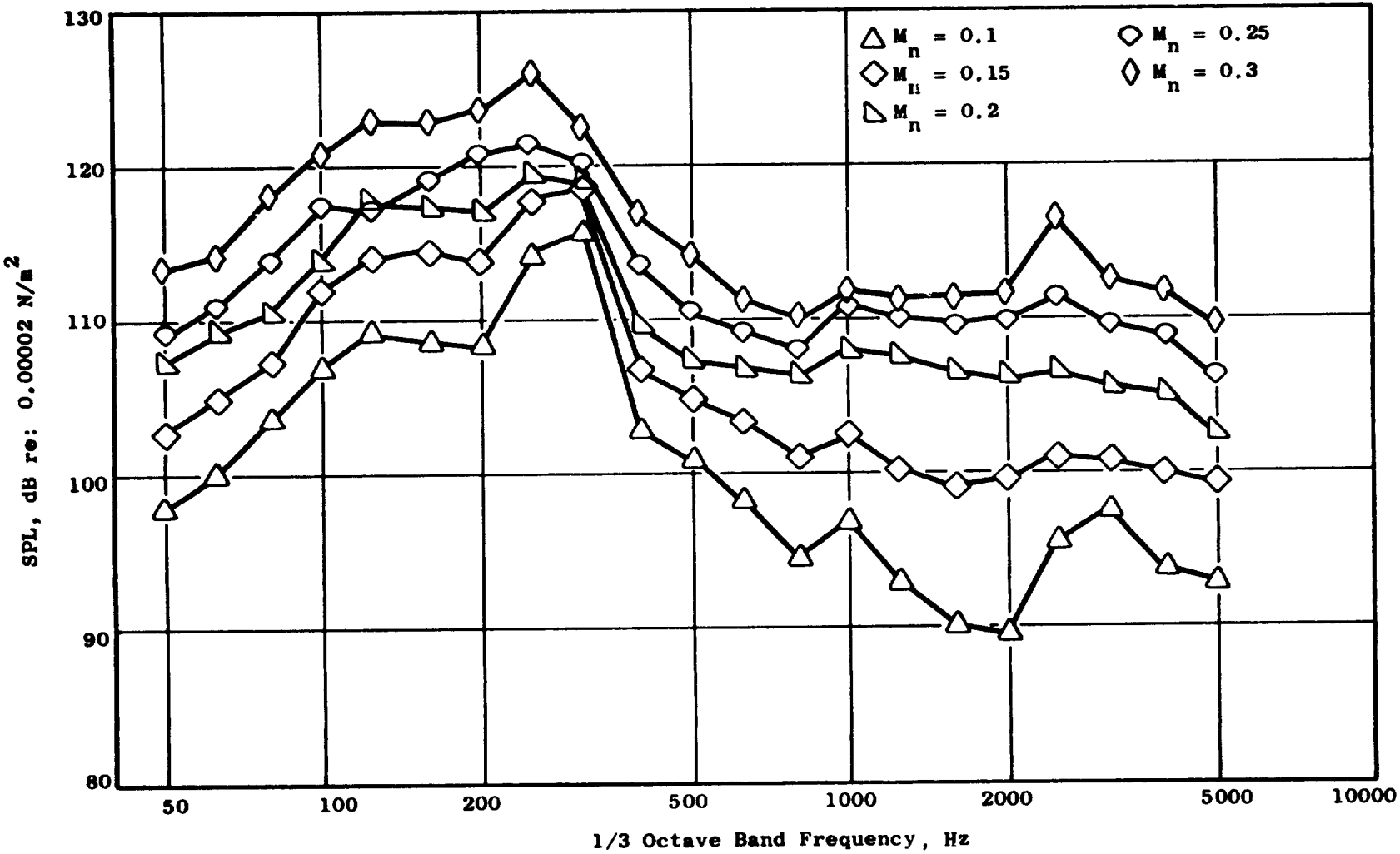

Figure 8. Corrected Probe Flow Noise, 50 cm long Waveguide with Water Jacket.

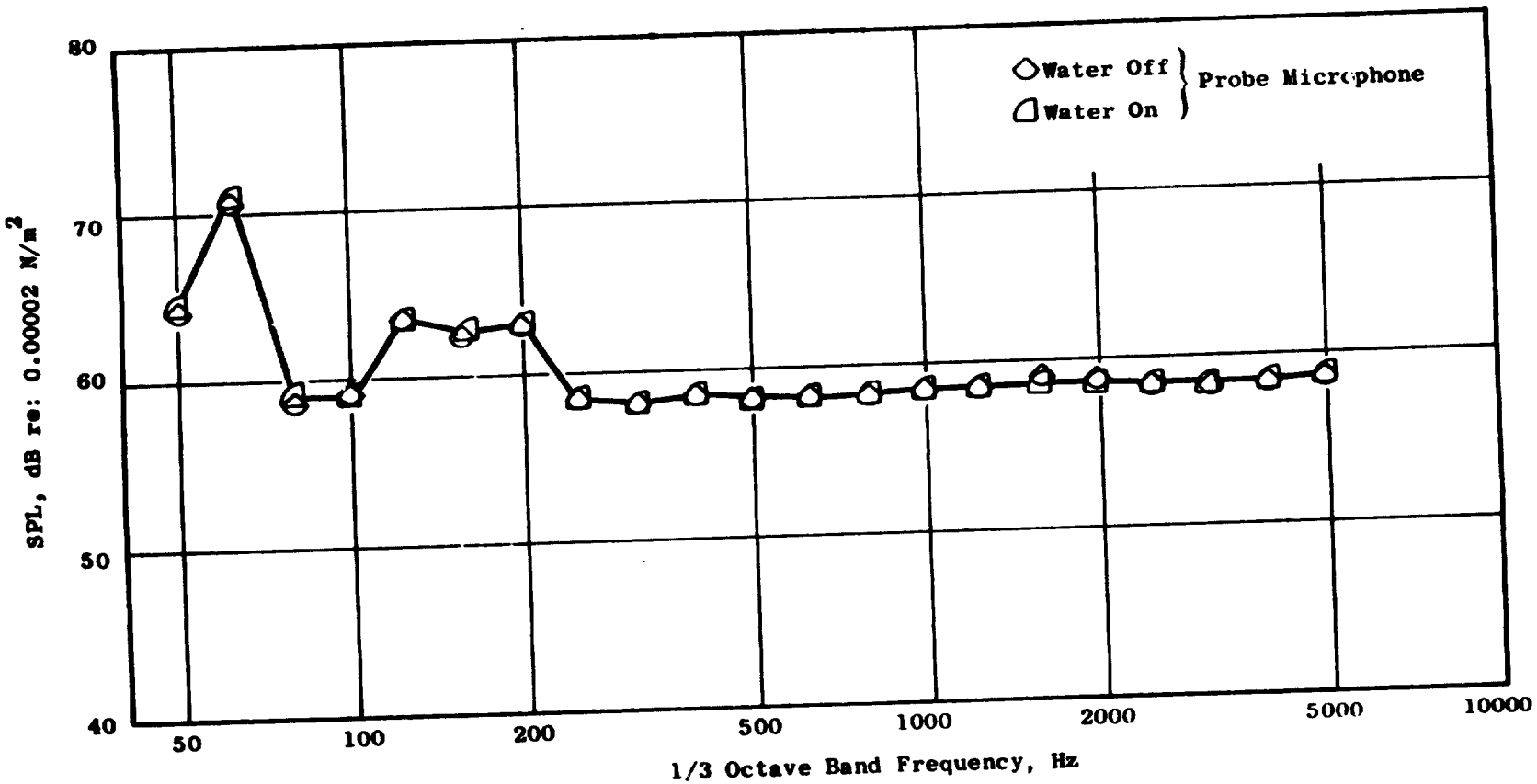

Figure 9. Effect of Cooling Water Flow Vs. Room Noise.

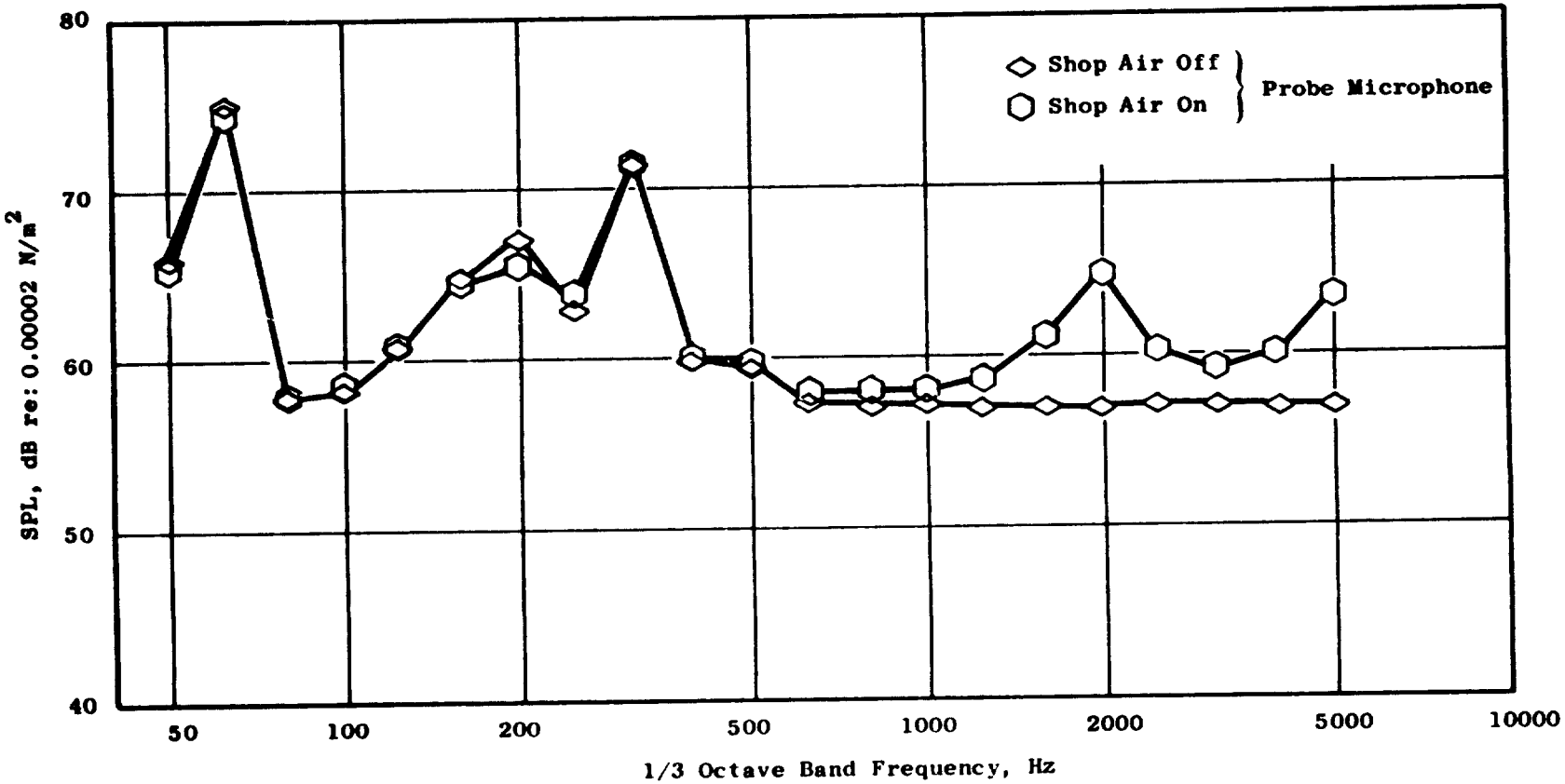

Figure 10. Effect of Shop Air Flowing Through Probe Cooling Passage Vs. Room Noise.

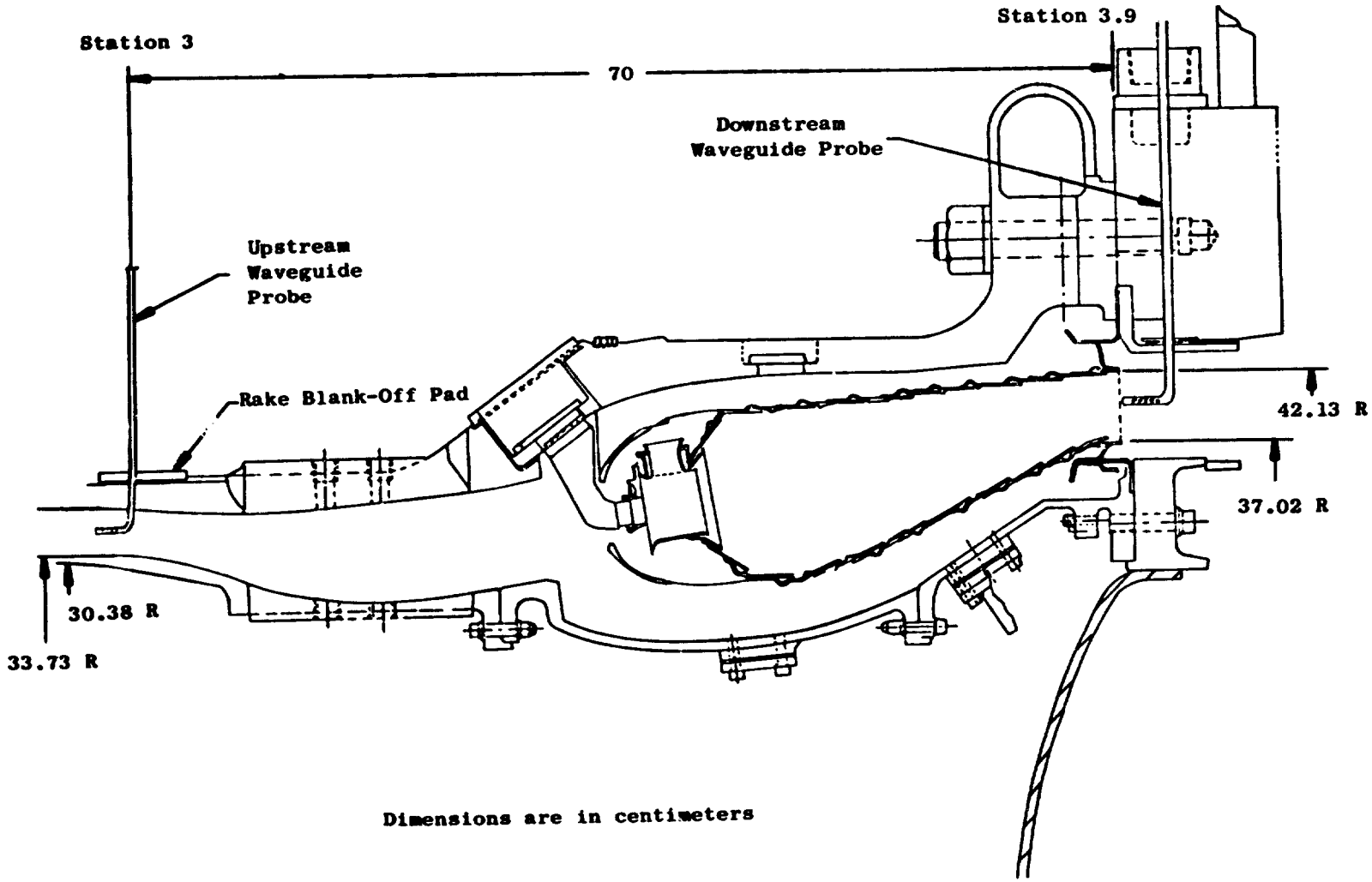

Figure 11. Top-Half Cross Section of the Experimental Clean Combustor Test Rig Showing the Acoustic Waveguide Probe Locations.

annulus. Looking downstream in the direction of the flow, the upstream probe was circumferentially located at 135 degrees and the downstream probe was at 96 degrees clockwise from the top centerline.

3.6 ELECTRICAL SYSTEM

The electrical system (Figure 12) consisted of kulites connected to low noise Princeton Applied Research amplifiers which fed into a Lockheed wide-band FM tape recorder. The kulites were Model XCEL-31-13-100D which have a flat frequency response from 20 to over 10,000 Hz.

An attempt was made to use B&K microphones on the initial tests. It was found that with the microphones connected to the probes it was difficult to obtain steady signals while the combustor was operating at high pressure. The probable cause was the seal in the microphone block apparently could not withstand the pressure during the test thus permitting gas to escape. During the tests it was not possible to determine the exact cause or location of the air leak; however, the leak allowed water vapor from the test environment to condense on the microphone diaphragm causing the erratic signals. A switch was made to kulite sensors that were presealed and had a damped static pressure balance across the sensing diaphragm.

3.7 BACKFLOW PURGE

During the initial testing fuel and water were getting into the waveguide probes during a startup. The liquid in the probes altered the response of the microphone diaphragms. In order to prevent the liquid or condensing vapors from entering the probes, a backflow purge system (Figure 13) was used as an additional precaution. Air from a higher pressure source flowed through a vapor trap, a flow restrictor and into the end of the probe terminating coil, then out through the probe tip. A test was performed (Figure 14) to determine the effect of this internal flow on the microphone signal. A peak level of 107.5 dB (Figure 15) was found on the downstream probe when a pressure differential of 0.902 atm was applied across the system. This pressure differential was higher than the pressure anticipated with the backflow purge system connected to a static pressure tap in the plenum upstream of the combustor rig. The level of sound generated by this internal flow is significantly below the levels being measured in the combustor. Cooling water coils (Figure 13) were added to reduce the temperature of the air coming from the plenum and to reduce heat conduction from the rig to the sensor in the upstream probe. Since the airflow rates in the backflow purge system were so low, it was assumed that the airflow had no effect on the calibration of the probes. After examination of the test data, there is no reason to believe that this was not a valid assumption.

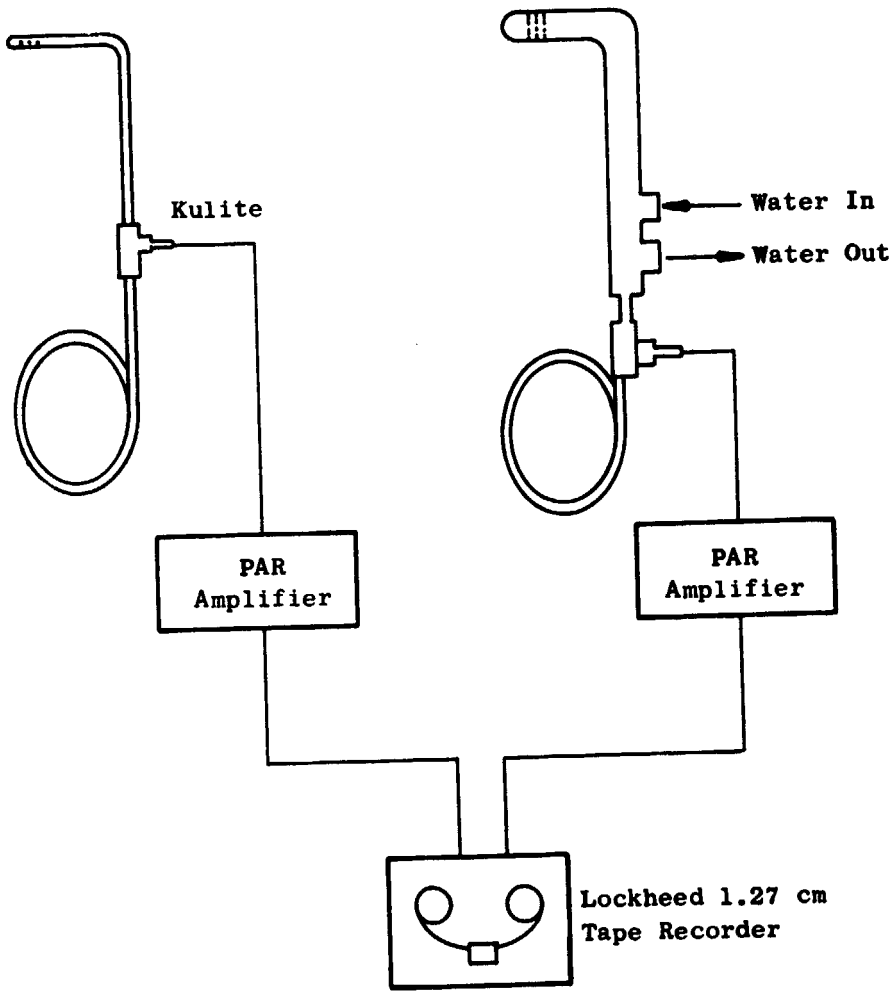

Figure 12. Electrical Schematic.

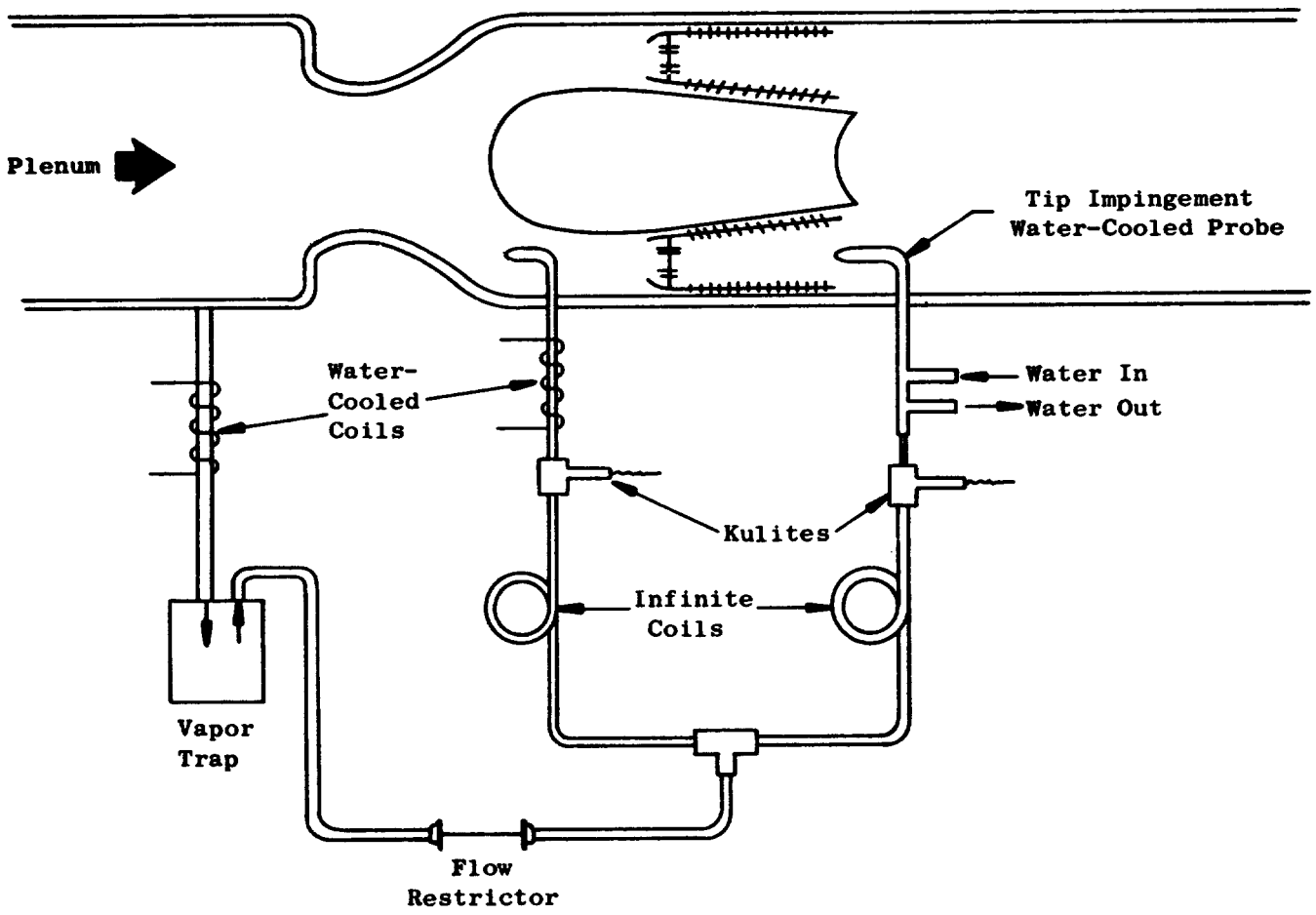

Figure 13. Backflow Purge System for Acoustic Probes.

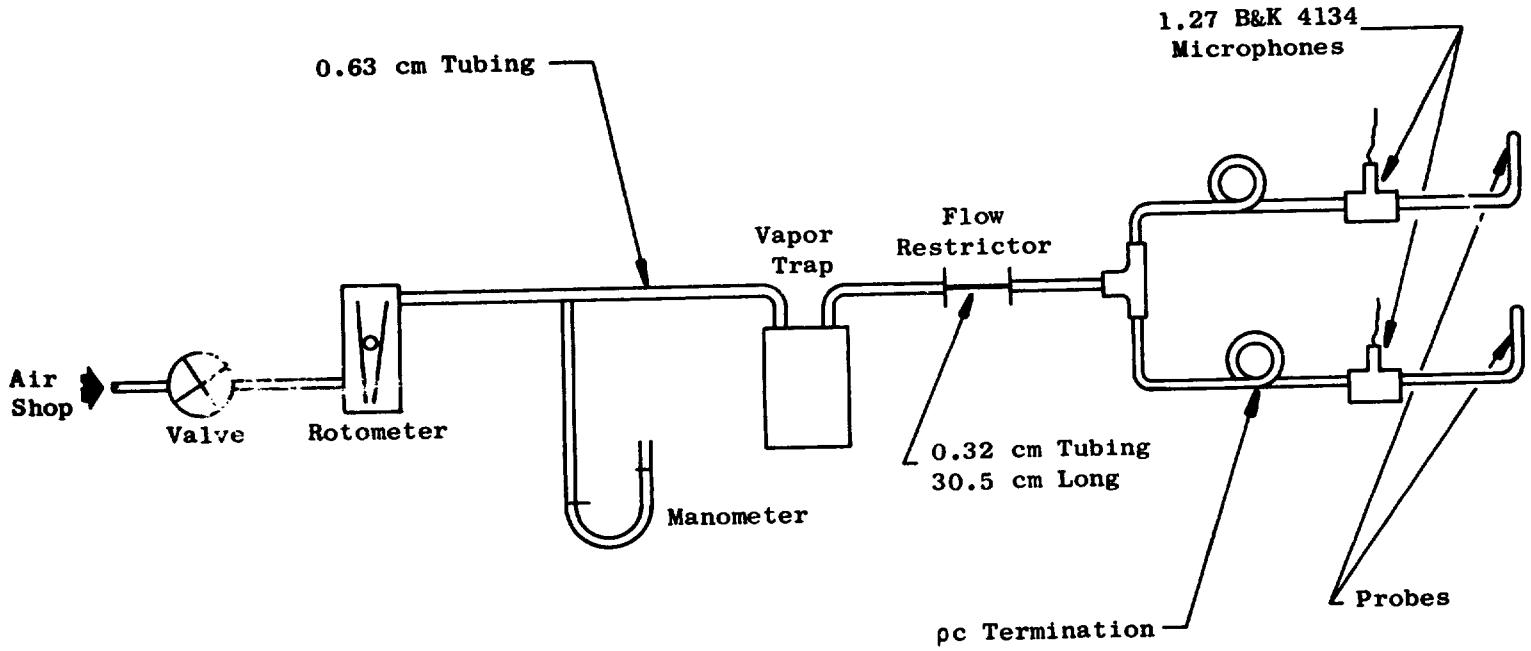

Figure 14. Probe Backflow Purge Test.

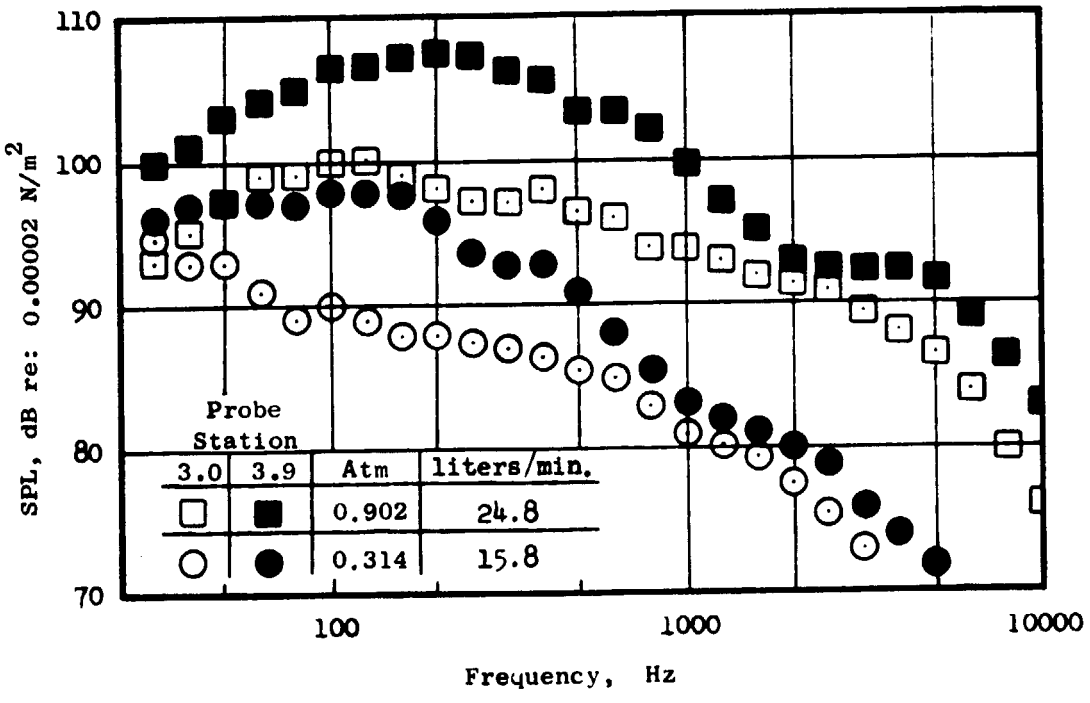

Figure 15. Back Flow Purge Internal Flow Noise Spectrum.

SECTION 4.0

EXPERIMENTAL COMBUSTOR DESIGNS

4.1 INTRODUCTION

The combustors that were tested were full-scale annular combustors. They were designed so that each would meet the design requirements that would permit these combustors to be installed in a CF6-50 dual-rotor turbofan engine. Some of the more important parameters for the CF6-50 combustor are listed in Table II. Within the imposed restraints, there were three basic design philosophies that were tested during Phase I. Any one individual configuration consisted of some unique variation of one of the basic designs. The three basic designs were called the Swirl-Can (Figure 16), Double Annular (Figure 17) and Radial/Axial (Figure 18) Combustors. Noise measurements were obtained on four versions of the first and one each of the latter two designs. The individual names and configuration numbers of the particular combustors that were measured are listed in Table III. The details of the three basic designs and the unique character of the individual combustors are described in this section.

4.2 SWIRL-CAN COMBUSTOR CONFIGURATIONS

4.2.1 Background

The Program Element I combustor configurations consisted of various versions of Swirl-Can-Modular Combustors, all sized for use in the CF6-50 engine. The Swirl-Can-Modular Combustor design concept was developed at the NASA-Lewis Research Center for application in advanced turbojet engines. This combustor design consisted of a modular array of carbureting swirl cans, each with an axial air swirler and a flame-stabilizing plate. Each module contained features to premix the fuel with air in the carburetor, swirl the fuel-air mixture, stabilize combustion in the swirl-can wake and provide interfacial mixing areas between the bypass air through the swirl-can array and the hot gases in the wake of the swirl-can modules. In such Swirl-Can-Modular Combustor designs, a large number of swirl cans, arranged in several annuli within the dome, were utilized.

The various Program Element I designs were intended to build upon the NASA Swirl-Can-Modular Combustor experience and to identify design features capable of providing further reduced CO, HC and NO_x emissions levels for this combustor design approach. They were, however, constrained to fit within the current CF6-50 engine flowpath envelope and to use the production CF6-50 combustor cooling liners. The Program Element I Swirl-Can-Modular Combustors were, of course, designed for different engine applications and different cycles than those of the previously conducted NASA investigations. Therefore,

Table II. CF6-50 Combustor Design Parameters.

Combustor Airflow (W_c)	103.42 kg/s
Compressor Exit Mach Number	0.27
Overall System Length	75.95 cm
Burning Length (L_B)	34.8 cm
Dome Height (H_D)	11.43 cm
L_B/H_D	3.0
Reference Velocity	25.9 m/s
Space Rate	2.2×10^{11} J/hr-m^3-atm
$\Delta P_T/P_{T_3}$	4.3% (Total)
Number of Fuel Nozzles	30
Fuel Nozzle Spacing (B)	6.91 cm
L_B/B	5.0
B/H_D	0.60
Design Flow Splits (Outer-Center-Inner)	33-32-35% of W_c
Liner Cooling Flow	30% of W_c

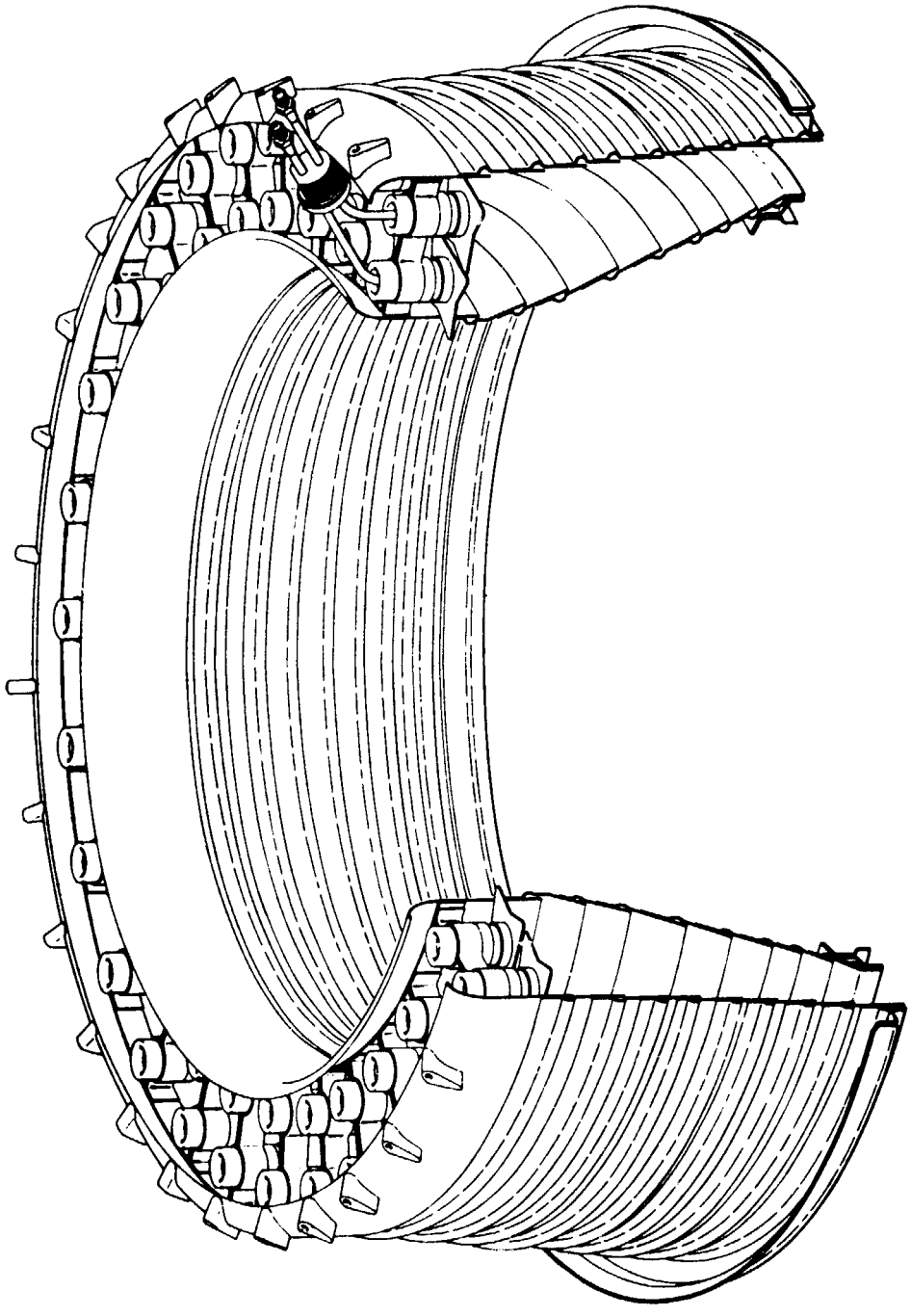

Figure 16. Swirl-Can Combustor.

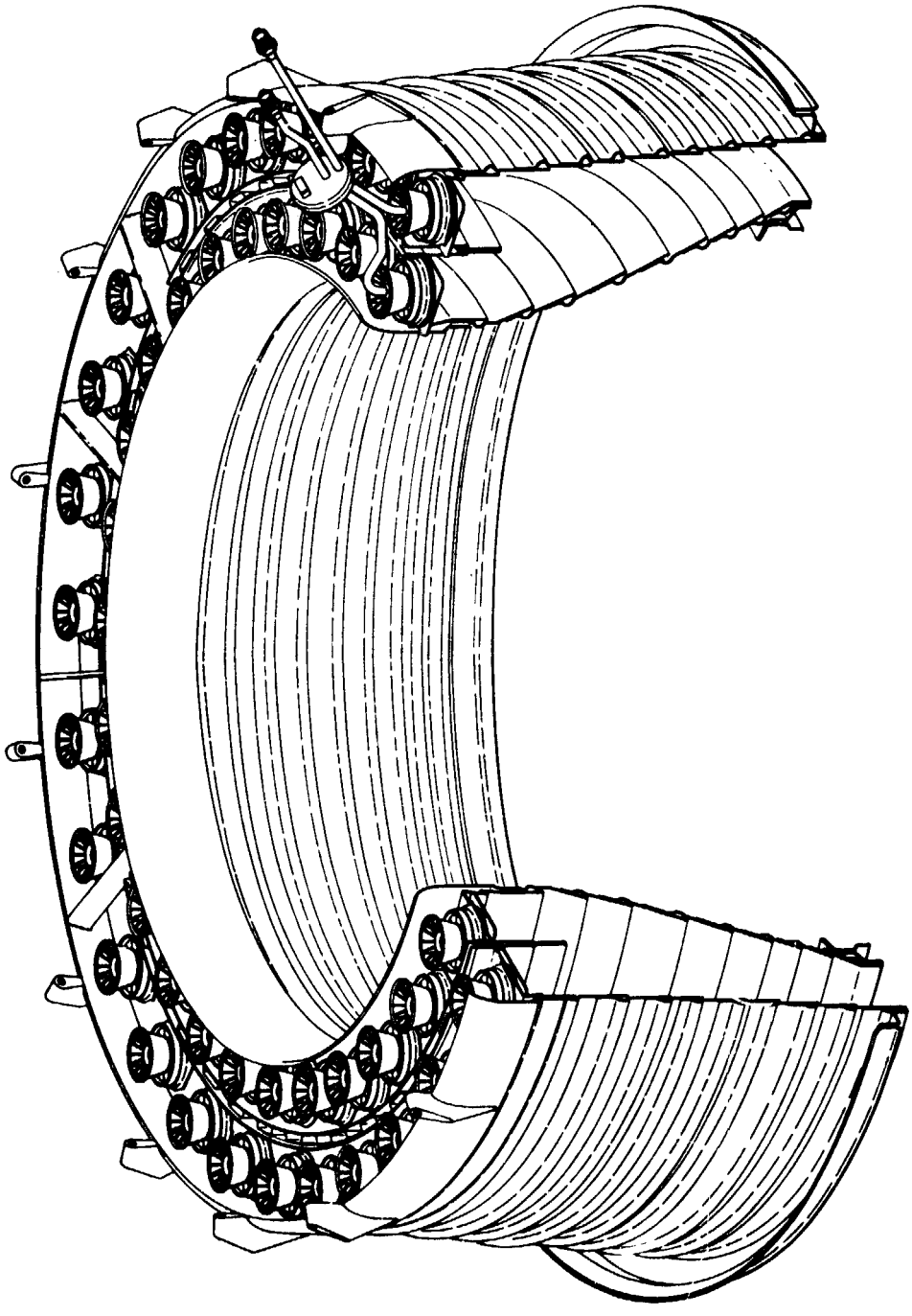

Figure 17. Double Annular Combustor.

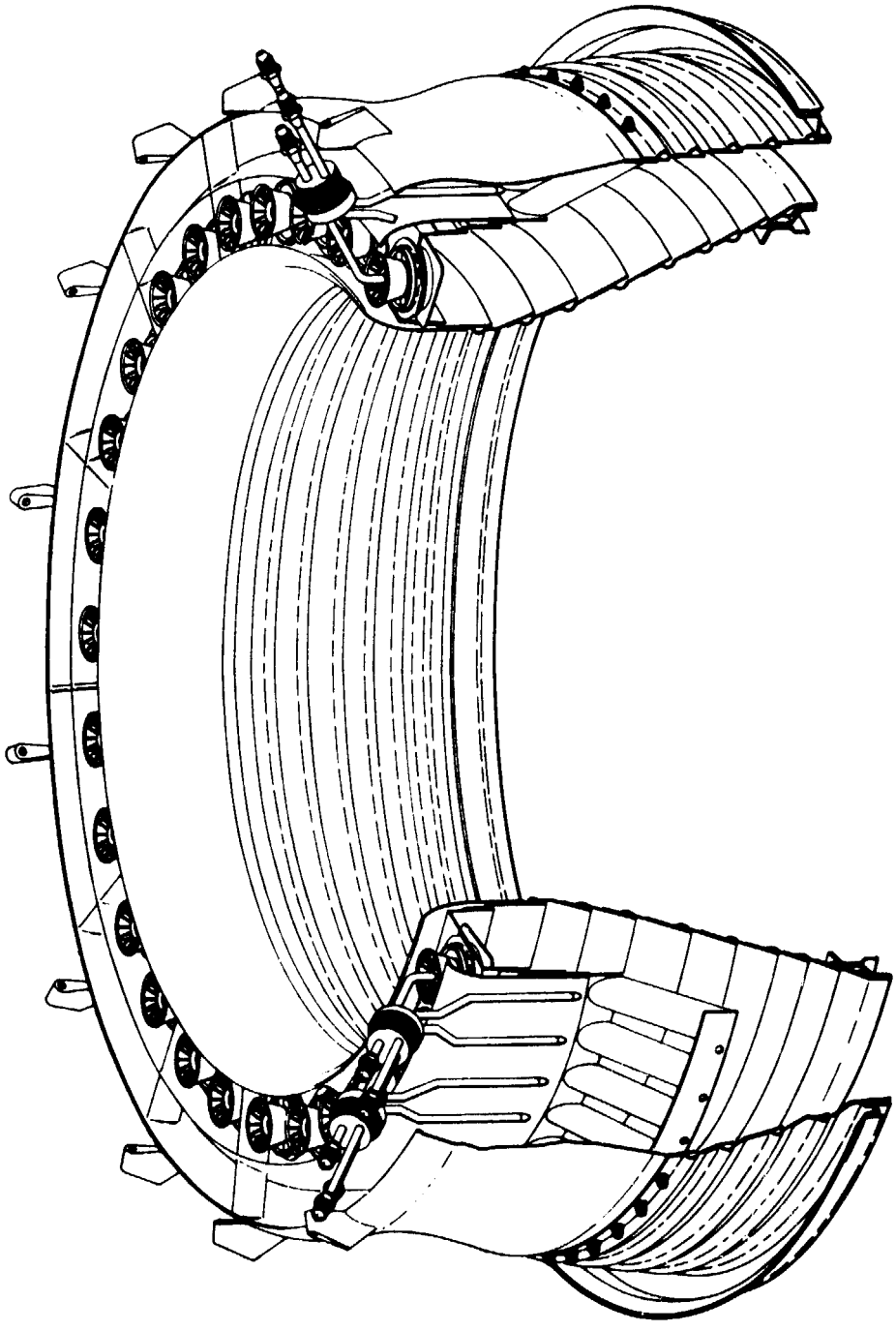

Figure 18. Radial/Axial Staged Combustor.

Table III. Combustor Configurations Tested for Noise.

Combustor Type	Configuration Number	Combustor Description
90-Swirl-Can/Sheltered Flameholder	I-12	Outer Liner Dilution
90-Swirl-Can/Flat Flameholder	I-14	Verification
60-Swirl-Can/Flat Flameholder	III-1	Extended Perimeter, AST Design
72-Swirl-Can/Counterswirl Flameholder	I-16	Atomizer, Hi^{3}. Swirl-Can Airflow
Double Annular Combustors	II-11	Biased Airflow, Flush Holes @ L/H=1.7
Radial/Axial Staged Combustors	II-12	Reduced Pilot Airflow

some differences in design were necessary. A comparison of several key design features of the CF6-50 size designs with those of typical NASA designs is shown in Table IV.

The most significant differences in the two designs were in the number of dome annuli, the size of the swirl cans, and the module air loading. The use of a two-row dome design in the CF6-50 combustor configuration (rather than three or four rows, as in the earlier NASA designs) was dictated by the geometric constraints of the CF6-50 engine flowpath and the diameters of the combustor cooling liners. To obtain an approximately square array of fuel sources, an array in which each swirl-can flameholder was approximately square in shape, the baseline CF6-50 Swirl-Can-Modular Combustor design incorporated 72 swirl cans, 36 in each row. This provided a radial spacing of 5.87 cm, and a circumferential spacing of 5.38 cm on the inner annulus and 6.40 cm on the outer annulus.

The size of the swirl can (3.18-cm diameter) was chosen to be common to all three combustor designs (60, 72, 90 cans). The limiting case was the 90-can combustor, where the swirl-can spacing was only 4.31 cm in the inner annulus. This precluded the use of a larger sized can, as was used in the earlier NASA investigations, since there would have been insufficient circumferential space for the flameholder. In addition, some of the 72-swirl-can combustor configurations were designed to accommodate a counterrotating air swirler around the swirl cans, and the 3.18-cm diameter can was the largest that could be used with this counterrotating air swirler. In addition to being a smaller diameter, the Program Element I swirl cans were also longer than the NASA cans to provide further protection against fuel escapement upstream of the swirl cans.

The various Program Element I swirl-can combustor designs were intended to permit investigations of the effects of the various design parameters on the emissions and performance characteristics of this combustor concept. Design parameters such as number of swirl cans, flameholder geometry, fuel injection technique, swirl-can airflow and combustor pressure loss were extensively varied during the test series. Since the combustors were of modular construction, most of the hardware was interchangeable among the various designs. A description of the combustor hardware common to all swirl-can combustor configurations tested in this program is presented in the following section.

4.2.2 Common Design Features

The baseline combustor configuration design featured flat flame-stabilizing plates, axial air swirlers, and low pressure fuel injection devices. Modified CF6-50 production combustor cooling liners and newly designed inner and outer cowls completed the combustor assembly. A schematic illustration of the baseline Swirl-Can-Modular Combustor, with the key dimensions indicated, is shown in Figure 19. Some of its important geometric parameters are listed in Table V.

Table IV. Comparison of GE Swirl-Can Combustors with Typical NASA Designs.

	NASA	GE	Basis
Number of Dome Annuli	3 or 4	2	Use of CF6-50 production cooling liners
Number of Swirl Can per Annulus	Varied	Equal	Fuel injection system complexity
Diameter of Swirl Cans, cm	3.81	3.81	Common diameter for all GE Swirl-Can Combustors. Largest diameter to accommodate 45 cans on inner annulus. Largest diameter to accommodate counterswirl on 72-Swirl-Can Combustor.
Length of Swirl Cans, cm	3.81	6.35	Additional margin for fuel containment (per NASA suggestion)
Flame Stabilizer Shape	Flat, Hex, Star Conical	Flat, Star Conical	Required dome blockage, extended flame-holder perimeter
Swirl Can Air Loading, kg/s-atm-can	0.094	0.056	CF6-50 cycle requirements
Fuel Injector Source Spacing	Approximately Square	Approximately Square	GE and NASA experience
Type Air Swirler	Axial, Windmill	Axial, Windmill	GE and NASA experience, ease of fabrication
Fuel Injection Technique	Tangential Low Pressure	Axial Low Pressure	Installation considerations

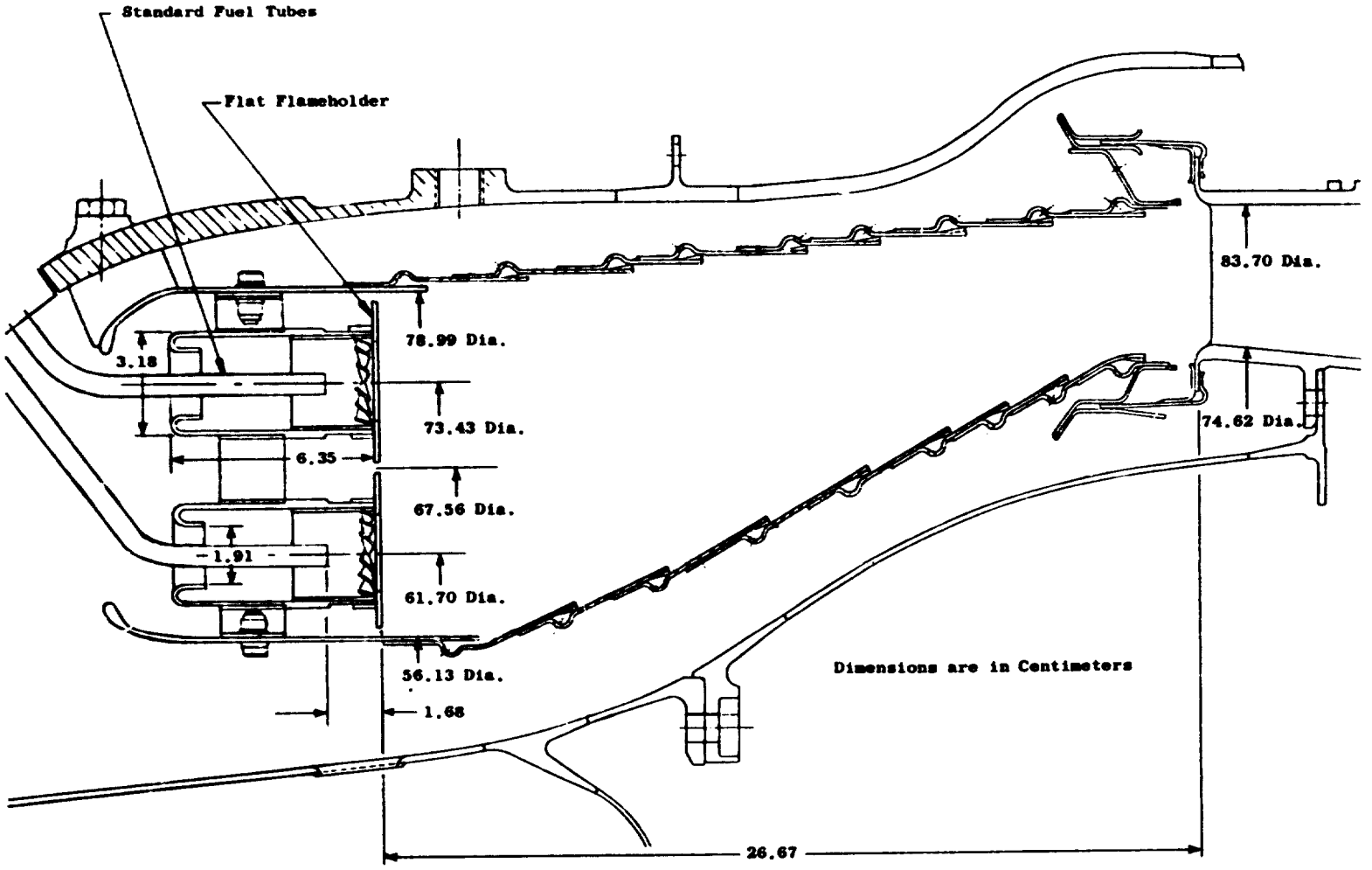

Figure 19. General Arrangement, Swirl-Can Combustor.

Table V. Geometric Design Variables, Swirl-Can Combustors.

	Inner Annulus	Outer Annulus	Overall
Dome Height[(1)], cm	5.715	5.715	11.43
Burning Length, cm	-	-	26.67
Fuel Injector Spacing, cm			
60 can	6.46	7.69	-
72 can	5.38	6.41	-
90 can	4.31	5.13	-
Area, cm^2	-	-	2426
Volume, cm^3	-	-	47,183

(1) At plane of flameholders

The basic dome support structure consisted of a network of sheet metal "spectacles" welded to an inner and an outer ring. The swirl-can assemblies were tack-welded to this dome mounting bracket, and the resulting dome assembly was bolted to the inner and outer cowls. To determine the effects of varying the number of swirl cans on emissions and performance levels, three dome mounting brackets were designed to accommodate 60, 72, or 90 swirl cans.

The swirl-can assembly which was common to all Program Element I configurations consisted of a cast cylindrical can and a sheet metal swirler and flameholder. These components were tack-welded together to allow for easy removal of any of the pieces.

The flat flameholder designs were designed in three sizes for the 60, 72 and 90-swirl-can dome arrays. These flameholders were designed with equal amounts of air on all sides of the flameholders. The flameholder extended over the front of the swirl can and served as a fuel trip ring to help provide a more uniform fuel distribution. A variation of the flat flameholder design, with a multitude of radial slots cut into each flameholder to increase the flameholder wetted perimeter, was also designed for the 60-swirl-can dome array as part of the AST combustor (Configuration III-1) evaluation.

The counterswirl flameholders were designed only for the 72-swirl-can dome array (Configuration I-16) because the counterswirler was too large for the 90-swirl-can dome. The sheltered flameholders were designed only for the 90-swirl-can dome array. All of these flameholders were intended to provide the high blockage necessary to maintain the combustor pressure drop at the CF6-50 design level. Three types of the Program Element I combustor configurations were tested: the flat flameholders, the counterswirl flameholders, and the sheltered flameholders. A description of the various configurations for each flameholder design is contained in succeeding sections.

The amount of airflow passing through the swirl cans was controlled by using different sized air swirlers. Three sizes were designed with different flow areas obtained by changing the pitch angle of the swirler vanes. The swirler was brazed to a sheet metal sleeve to allow the axial position of the swirler in the swirl can to be easily changed.

The standard fuel injectors were open-ended 0.46-cm inside diameter stainless steel tubes, with fuel metering accomplished external to the combustor (using fixed fuel metering orifices). To accommodate 60, 72 or 90 fuel tubes from the fueling ports on the existing CF6-50 combustor test rig, a variety of fuel tube configurations was required. Alternate two-tube cluster designs, as well as four-tube cluster designs, were required to provide for the various combustor configurations. The 90-swirl-can dome array required 1 2-tube cluster design and 1 4-tube design, and the 60-swirl-can dome array required 1 2-tube design. During the test incorporating the counterswirl flameholders, alternate fuel-injection devices were investigated.

4.2.3 Flat Flameholder Configurations

Two combustor configurations, which utilized the flat flameholder design, were tested for noise. A summary of the key geometric features of each configuration is shown in Table VI. Test Configurations I-14 and III-1 utilized 90 and 72-swirl-can dome arrays, respectively, and were intended to investigate the effects of the number of swirl cans. Configuration III-1 was designed and tested as part of the AST Addendum program. It provided a large increase (about a factor of 3) in the wetted perimeter of the flat flameholders. The flat flameholders can be seen in Figure 19.

4.2.4 Counterswirl Flameholder Configuration

The counterswirl flameholder combustor configuration featured the use of a counterrotating air swirler mounted around a swirl can in order to improve the fuel and air mixing within the flameholder wakes. However, the main design parameter investigated with the counterswirl series of test configurations was the fuel injection technique. Noise data which were taken on Configuration I-16 incorporated small, pressure-atomizing simplex spray nozzles (Figure 20) to provide very good fuel atomization and distribution at all test conditions. Also, for this configuration the air swirlers inside the swirl cans were removed in order to obtain the highest airflow possible through the swirl cans. The test configuration consisted of the 72-swirl-can dome array. A summary of the key geometric design features is shown in Table VII.

4.2.5 Sheltered Flameholder Configuration

Configuration I-12 featured the use of sheltered flameholders. This flameholder device was designed with the axial dimension of the flameholder extended 1.27 cm downstream from the plane of the swirl cans (Figure 21). This created a "sheltered" region in the wake of the cans and was intended to provide more time for the swirl-can air and fuel to mix before entering the primary combustion zone. This configuration used the 90-swirl-can dome. The key geometric features of each configuration are shown in Table VIII.

For Configuration I-12, dilution holes were added to the second cooling panel of the outer liner in line with and between each swirl can, in an effort to direct that portion of the dome airflow passing between the flameholders and the outer cowl into the primary combustion zone. It was felt that a large amount of available combustion air was being allowed to escape the combustion zone along the outer liner.

4.3 DOUBLE ANNULAR COMBUSTOR CONFIGURATION

The general arrangement of the Double Annular Combustor design approach is shown in Figure 22 and its geometric parameters are tabulated in Table IX.

The combustor assembly consisted of a dome assembly, a cowl and modified CF6-50 production cooling liners. The dome assembly consisted of two annular

Table VI. Swirl-Can/Flat Flameholder Combustor Configurations I-14 and III-1.

Number of Swirl Cans	Total Pressure Loss @SLTO %	Airflow Distribution, % W_c (1)				Flameholder Wetted Perimeter cm	Fuel Injector	Configuration
		Swirl Can	Flameholder	Around Flameholder	Dome Total			
90	4.20	13.1	-	69.3	82.4	1656	Standard	I-14
72	4.22	16.4	42.7	25.7	84.8	4361	Standard	III-1

(1) Liner Cooling 15.2 to 17.6 % W_c

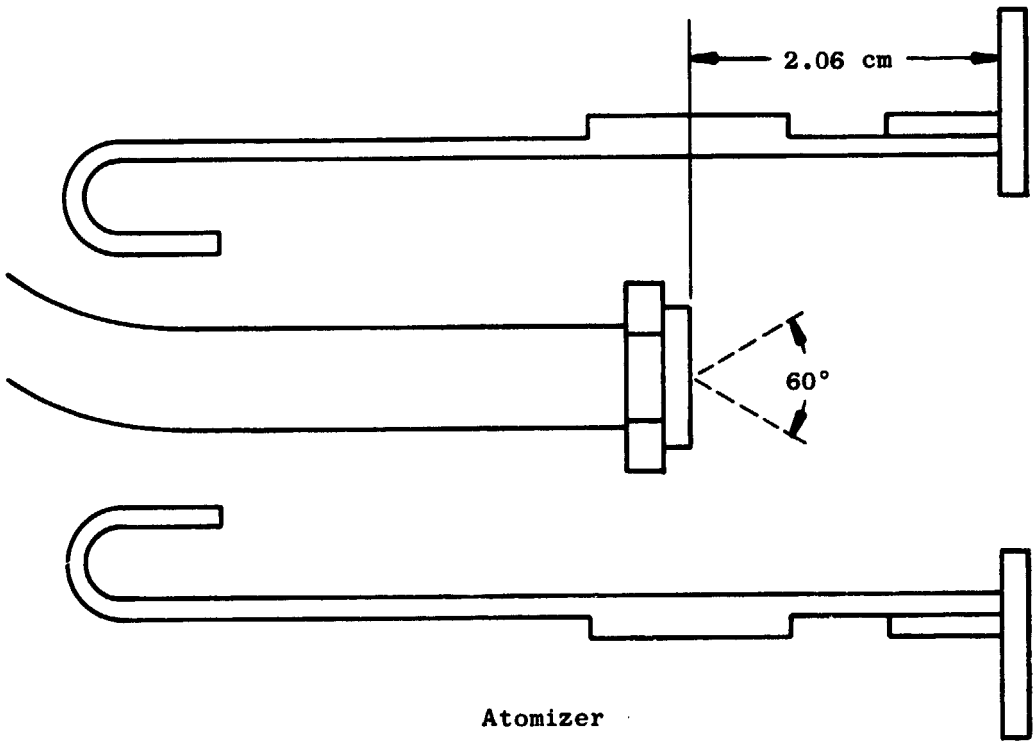

Figure 20. Fuel Injector Configuration I-16, Swirl-Can Combustor.

Table VII. 72-Swirl-Can/Counterswirl Flameholder Combustor Configuration I-16.

Number of Swirl Cans	Total Pressure Loss @SLTO %	Airflow Distribution, % W_c^*				Flameholder Wetted Perimeter cm	Fuel Injector
		Swirl Can	Outside Swirler	Around Flameholder	Dome Total		
72	3.98	30.2	14.1	40.3	84.6	1549	atomizer

* Liner Cooling 15.4 % W_c

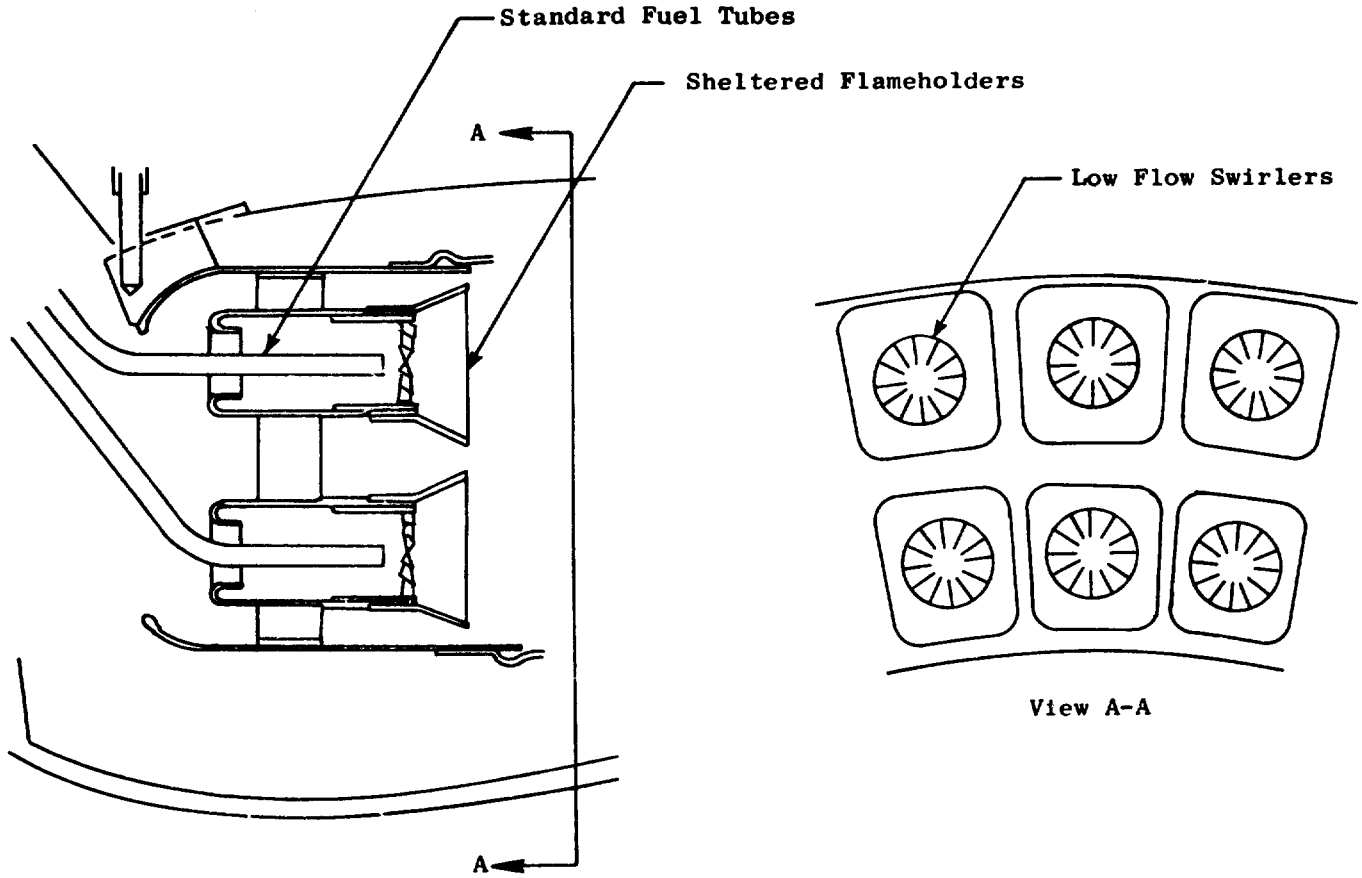

Figure 21. 90-Swirl-Can/Sheltered Flameholder Combustor Design.

Table VIII. 90-Swirl-Can/Sheltered Flameholder Combustor Configuration I-12.

Number of Swirl Cans	Total Pressure Loss @SLTO %	Airflow Distribution, % W_c^*				Flameholder Wetted Perimeter cm	Fuel Injector
		Swirl Can	Around Flameholder	Dome Total	Liner Dilution		
90	4.00	14.0	61.6	75.6	6.9	1613	Standard

* Liner Cooling 17.5 % W_c

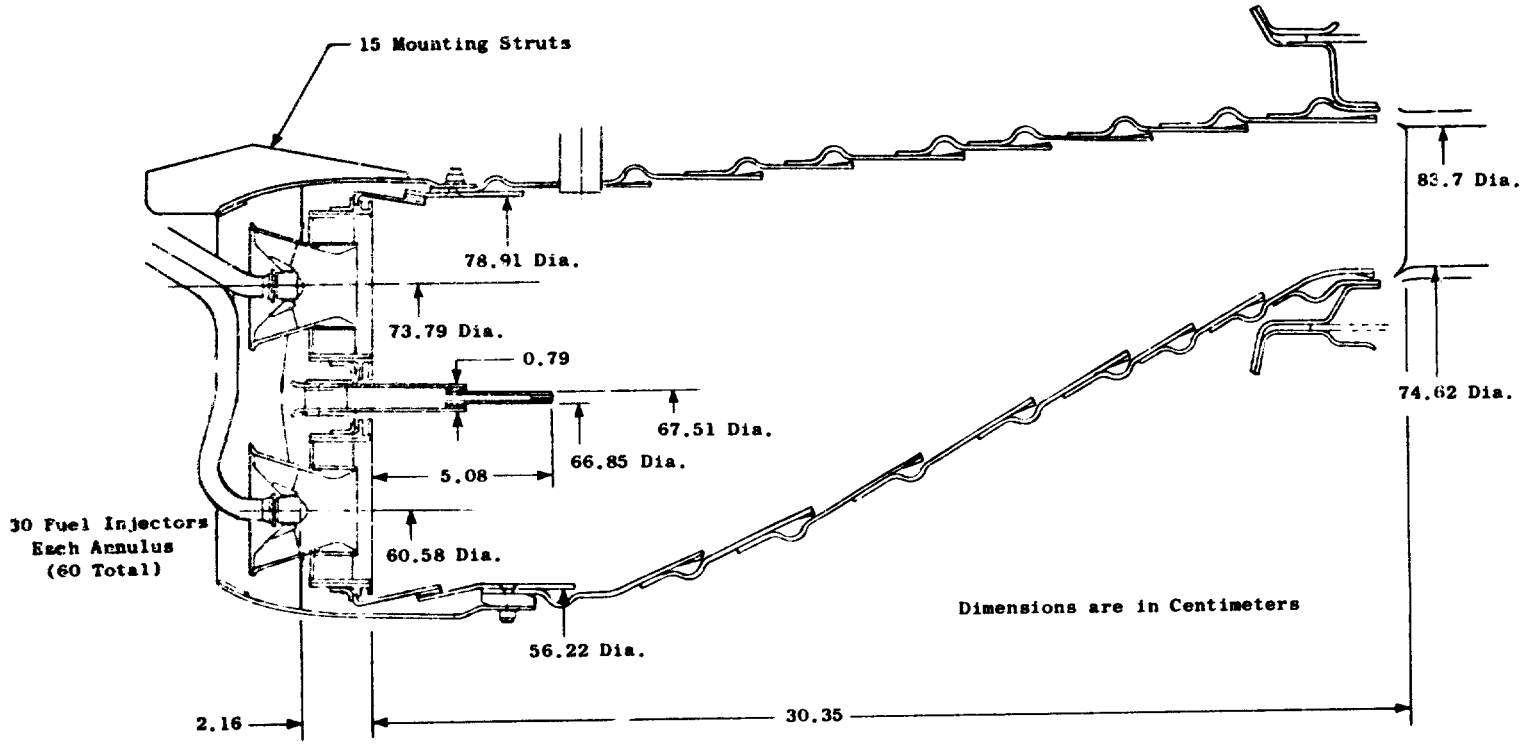

Figure 22. General Arrangement, Double Annular Combustor.

Table IX. Geometric Design Parameters, Double Annular Combustor.

	Outer Annulus	Inner Annulus	Overall
Dome Height (1), cm	5.69	5.33	11.35
Burning Length, cm	5.08(2)	5.09(2)	30.35
Fuel Injector Spacing, cm	7.73	6.34	-
Area(1), cm^2	1311	1028	2409
Volume, cm^3	6541(2)	5097(2)	54,991

(1) at trailing edge of centerbody

(2) from flameshields to trailing edge of centerbody

spectacle plates separated by a small centerbody. Assembled in the spectacle plates was an array of 60 air swirlers (30 in each annulus). The air swirler components consisted of a primary air swirler/venturi casting, a counter-rotating secondary air swirler, a flameshield and a retainer ring. The air swirler assemblies were attached to the dome spectacle plates with a radial slip joint arrangement to accommodate mechanical stackup and thermal growth between the fuel injectors and the combustor assembly. The flameshields were impingement cooled. The centerbody and dome panels were film cooled using wiggle strip construction.

The 60 fuel injectors (30 assemblies) consisted of low pressure drop devices which were inserted in the normal manner (externally) after the combustor was installed in the test rig. The fuel injector tip and counter-rotating air swirler combination used in these combustors is an airblast fuel atomization/mixing device previously developed at General Electric for use in advanced engine combustors. For this program, the fuel injector tip/primary air swirler design was used intact, but new higher airflow secondary air swirlers were designed. The key dimensions of the fuel injector/air swirler assembly are shown in Figure 23. Key design parameters are listed in Table X and Figure 24. For Configuration II-11, the airflow was highly biased to the inner annulus. The liner dilution holes were simple flush holes located in line and between each fuel injector (60 holes per liner).

4.4 RADIAL/AXIAL STAGED COMBUSTOR CONFIGURATION

The general arrangement of the Radial/Axial Staged Combustor is shown in Figure 25 and its geometric design parameters are tabulated in Table XI. The combustor assembly consisted of a pilot stage dome assembly, a main stage flameholder/chute assembly, a cowl, and modified CF6-50 production combustor cooling liners.

The pilot dome assembly consisted of an annular spectacle plate and an array of 30 air swirlers similar to those in the Double Annular Combustor configurations. The air swirler components consisted of a primary air swirler/venturi casting, a counterrotating secondary air swirler, a flameshield and a retainer ring. The air swirler assemblies were attached to the dome with a radial slip joint arrangement to accommodate mechanical stackup and thermal growth between the fuel injectors and the combustor assembly. The flameshields were impingement cooled. The dome panels were film cooled using stacked ring construction.

The main stage flameholder assembly consisted of an array of 60 sloping high blockage (about 80 percent) flameholders which were semicircular in cross section. The flameholder width is constant from base to tip so the main stage air admission gap or "chute" width varies slightly from the inner to outer diameter (Figure 26). In this design approach, the base of the flameholders is open to permit the pilot combustion products to flow radially outward in the flameholder wakes and pilot the main stage combustion process. An array of cooling air holes at the tip of the flameholders was used to cool

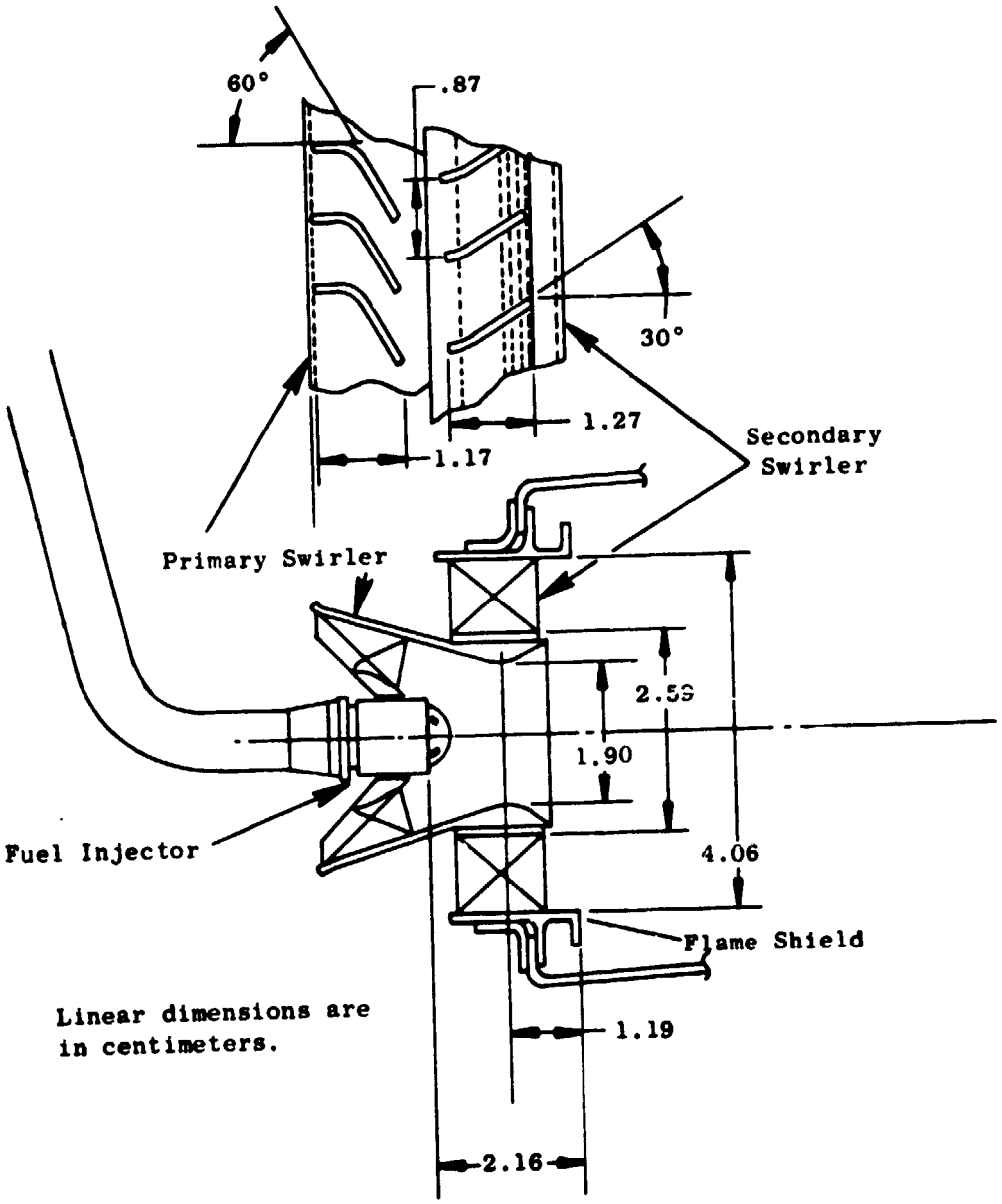

Figure 23. Fuel Injector/Air Swirler Details, Double Annular Dome Combustor.

Table X. Double Annular Combustor Configuration II-11.

Total Pressure Loss @ SLTO %	Outer Annulus			Inner Annulus			Dilution Location/Type
	Swirler	Dilution	Total	Swirler	Dilution	Total	
4.72	18.4	0	18.4	33.0	13.8	46.8	1st Panel/Flush Hole

Total Dome Cooling 7.9 % W_c

Centerbody Cooling 3.3 % W_c

Liner Cooling 23.6 % W_c

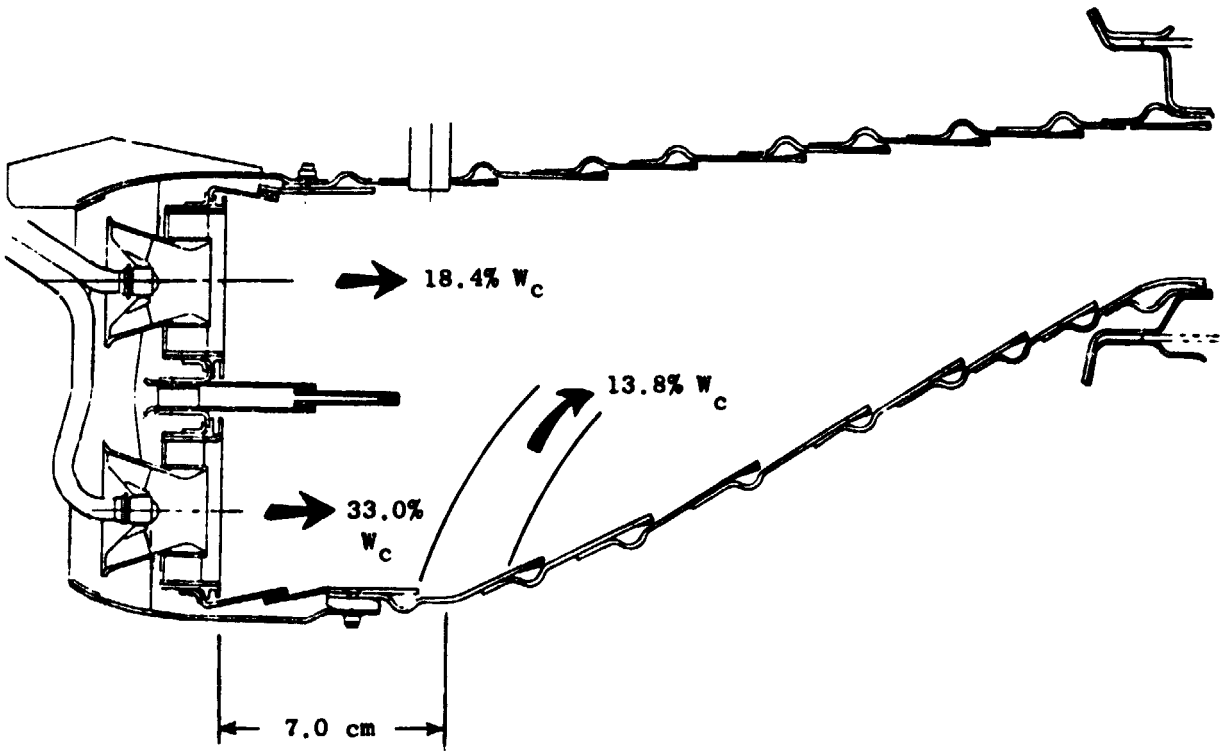

Figure 24. Design Parameters, Configuration II-11, Double Annular Combustor.

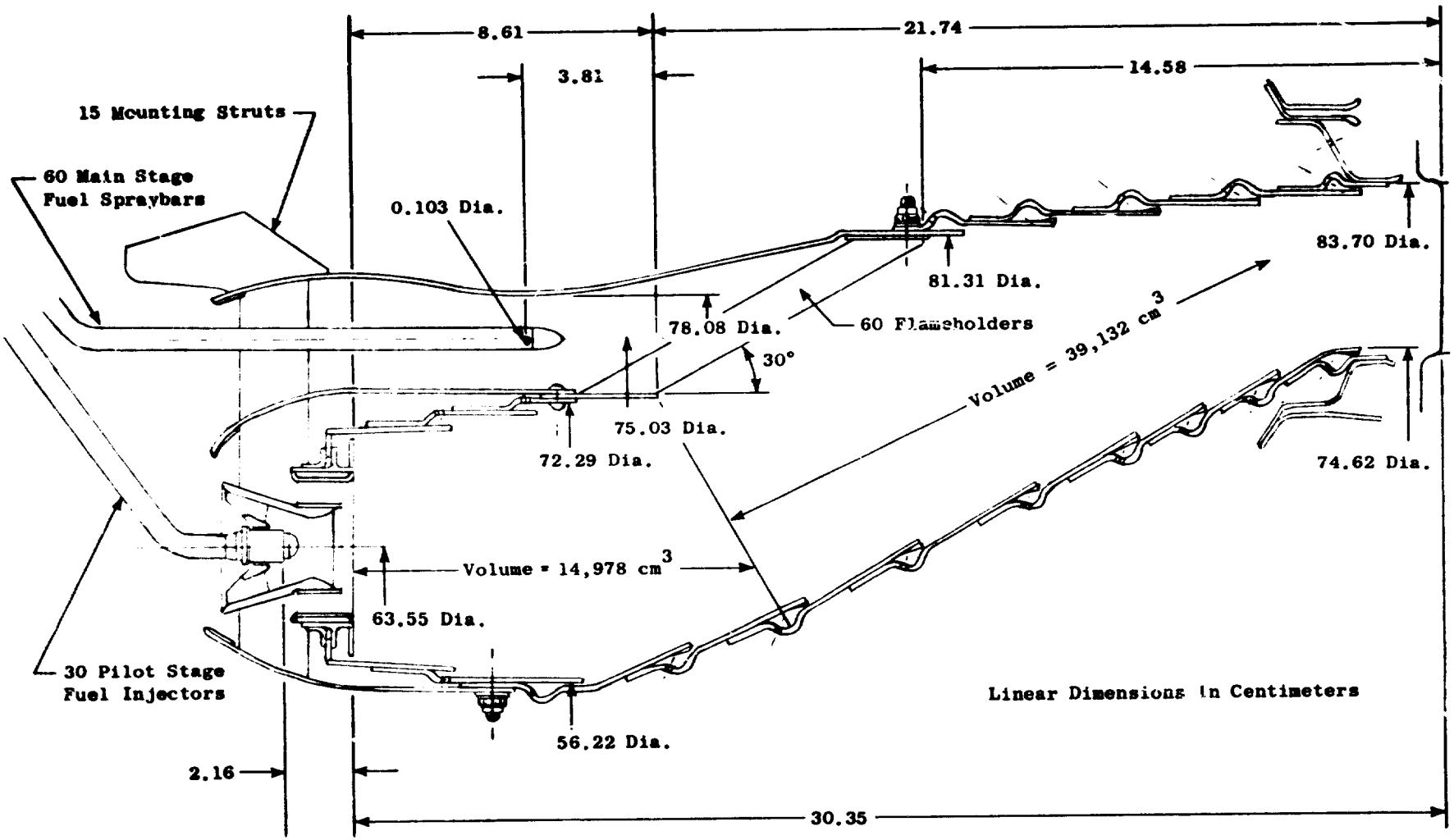

Figure 25. General Arrangement, Radial/Axial Staged Combustor.

Table XI. Geometric Design Parameters, Radial/Axial Staged Combustor.

Pilot Stage	
Dome height, cm	8.04
Burning length[(1)], cm	8.61
Fuel injector spacing, cm	6.65
Area at dome exit, cm^2	1491
Volume[(1)], cm^3	14,978
Overall	
Burning length, cm	30.35
Volume, cm^3	54,110

(1) from dome flameshields to main stage flameholders (Figure 25).

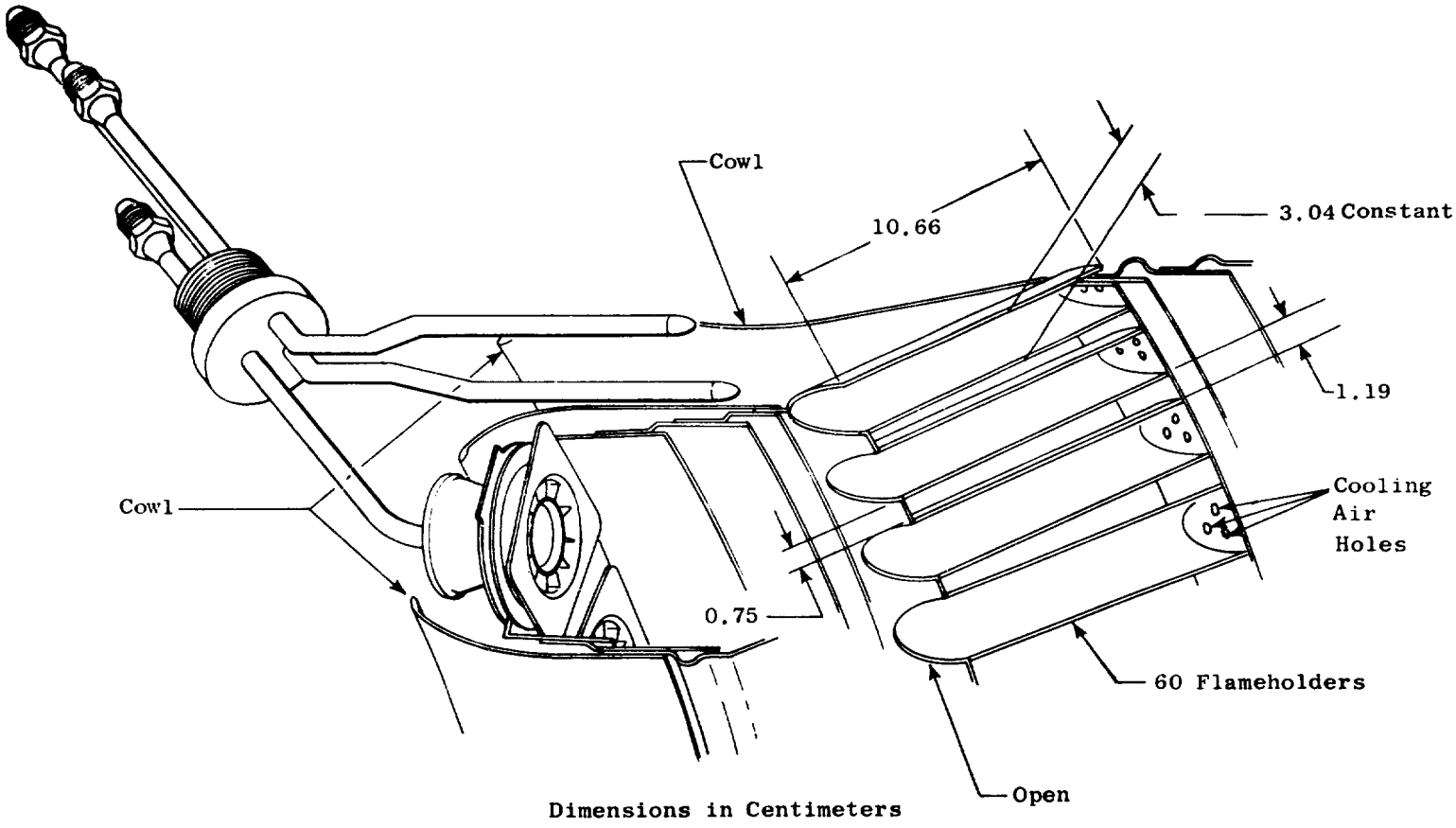

Figure 26. Flameholder Details, Radial/Axial Staged Combustor.

the outer flameholder/cowl/liner joint which was followed immediately by a film cooling slot in the outer liner.

The cowl contained a flow splitter to: (1) form a smooth flowpath for the main stage air; and, (2) isolate the main stage fuel-air mixture from the pilot outer film cooling air. The main stage flowpath was designed to smoothly accelerate the main stage air from about 46 m/s at the inlet to about 91 m/s at the fuel injection station and to about 137 m/s at the chute exit surface.

The pilot stage fuel injector/air swirler combination consisted of an airblast fuel atomization/mixing device, as was previously described. The main stage fuel injectors consisted of 60 simple low pressure drop spraybars, each having a pair of opposed circumferentially-directed orifices (0.103-cm diameter). The fuel injector assemblies were installed in the rig from the inside before the combustor was installed. This design was selected for screening tests so that the main stage fuel injector location and/or configuration could be changed readily. In actual engine application, these injectors might be mounted radially from new pads in the outer casing. Key design parameter variations are shown in Table XII and Figure 27.

Table XII. Radial/Axial Staged Combustor Configuration II-12.

Total Pressure Loss @SLTO %	Airflow Distribution* % W_c		Main Stage Fuel Injector Configuration	Other Features
	Pilot Stage Swirler	Main Stage (Chutes)		
5.15	10.8	60.4	Splash Plates	-

* Pilot Cooling 12.0 % W_c

Liner Cooling 15.4 % W_c

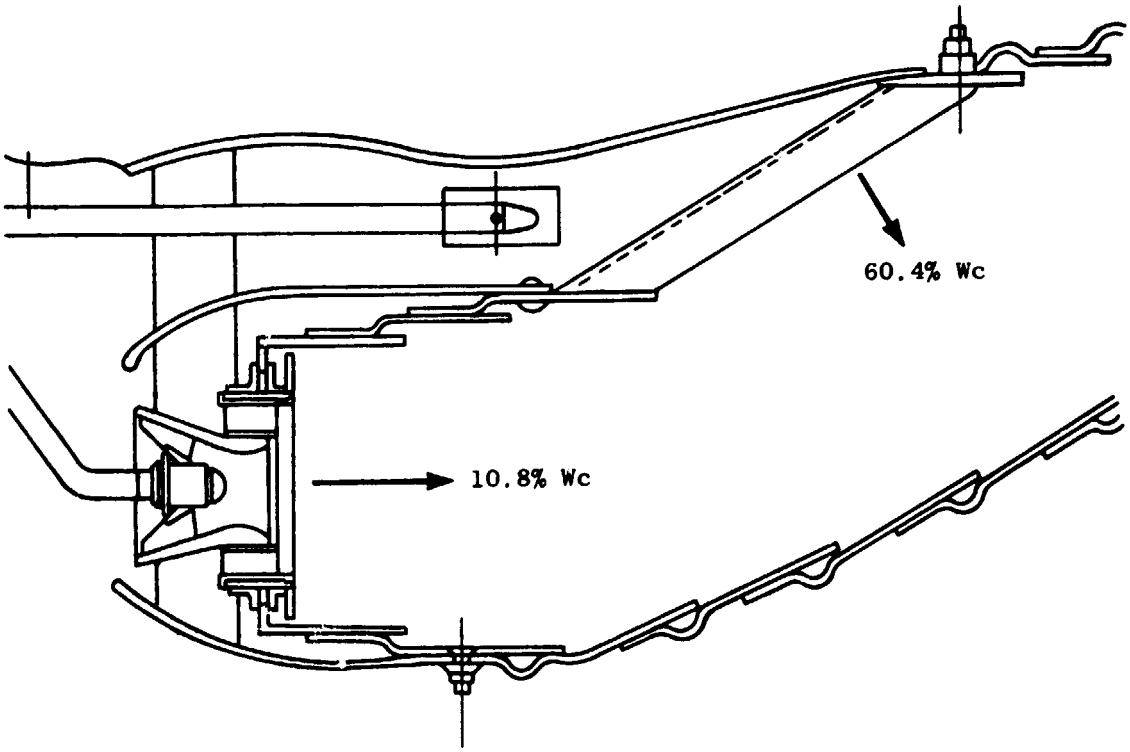

Figure 27. Radial/Axial-Staged Combustor, Configuration II-12.

SECTION 5.0

EXPERIMENTAL RESULTS

5.1 AERODYNAMIC DATA

The steady-state aerodynamic parameters were recorded for all configurations tested in the Experimental Clean Combustor Program as part of the original program plan. However, the steady-state aerodynamic data tabulated in this section pertain only to those test reading numbers for which acoustic data were taken. The data are tabulated in chronological order; i.e., successive reading numbers are listed in Tables XIII to XVIII. The parameters tabulated are the total fuel-air ratio, airflow rate, fuel flow rate, inlet and exit total temperatures, fuel temperature, inlet and exit static pressure and exit total pressure.

5.2 ACOUSTIC DATA

For each of the combustor configurations acoustic data were taken at both sea level takeoff and approach inlet conditions. At each combustor inlet condition, four fuel-air ratios were tested. One of these four consisted of the baseline dry loss or flame out condition. Configuration I-16 is the one exception. The data for this configuration do not include the takeoff inlet conditions nor the baselines for either takeoff or approach due to a premature shutdown; however, data were taken at cruise and AST inlet conditions. A total of 48 noise data measurements were obtained.

The one-third octave band sound pressure levels corrected for probe viscous losses are plotted on Figures 28 through 40 for the six configurations. The values of these same corrected sound pressure levels are listed in Tables XIX to XXIV. The upstream (U/S) and downstream (D/S) levels can be found in adjacent columns for each test reading. For each spectrum, the measured overall sound pressure level was calculated and listed across the bottom line.

During some of the tests an intermittent 60 Hz electrical pure tone appeared in the spectra. When these spikes occurred, the true broadband one-third third octave band levels were obtained from the examination of the 10 Hz narrowband levels, which are given in Appendix A. The extracted broadband levels from the narrowband spectra were adjusted for the bandwidth and used as the one-third octave band levels.

Table XIII. Summary of Aerodynamic Parameters for Acoustic Data, Configuration II-11, Double Annular Combustor.

Rdg. No.	458	459	461	463	464	467	477	478
Total f/a	0.0062	0.0175	0.0238	0.0118	0.0177	0.0241	0	0
W_c (kgm/s)	15.4	15.3	15.5	16.5	16.7	16.5	17.0	15.7
W_f (kgm/hr)	344	966	1328	725	1061	1432	0	0
T_{T3} (° K)	664	664	664	908	909	913	855	677
$T_{T3.9}$ (° K)	945	1292	1511	1369	1582	1790	855	677
T_{fuel} (° K)	300	303	301	302	302	301	295	294
P_{S_3} (atm)	3.38	3.40	3.72	4.61	4.60	4.65	4.57	3.72
$P_{S3.9}$ (atm)	3.27	3.27	3.56	4.48	4.46	4.46	4.45	3.63
$P_{T3.9}$ (atm)	3.33	3.35	3.66	4.55	4.54	4.57	4.50	3.68

Table XIV. Summary of Aerodynamic Parameters for Acoustic Data, Configuration II-12, Radial/Axial Staged Combustor.

Rdg. No.	504	505	506	507	510	513	525	526
Total f/a	0.0061	0.0137	0.0233	0.0174	0.0213	0.0241	0	0
W_c (kgm/s)	15.3	15.5	15.4	16.7	16.7	16.5	16.2	15.3
W_f (kgm/hr)	334	765	1293	1046	1278	1430	0	0
T_{T3} (° K)	672	669	668	865	868	851	859	631
$T_{T3.9}$ (° K)	974	1171	1429	1453	1588	1643	859	631
T_{fuel} (° K)	301	302	305	303	301	301	301	300
P_{S_3} (atm)	3.29	3.31	3.43	4.69	4.70	4.63	4.61	3.23
$P_{S3.9}$ (atm)	3.16	3.16	3.25	4.53	4.52	4.44	4.50	3.12
$P_{T3.9}$ (atm)	3.23	3.24	3.33	4.61	4.60	4.53	4.54	3.16

Table XV. Summary of Aerodynamic Parameters for Acoustic Data, Configuration I-12, 90-Swirl-Can/Sheltered Flameholder Combustor.

Rdg. No.	533	542	543	545	549	551	558	559
Total f/a	0.0137	0.0139	0.0176	0.0239	0.0178	0.0243	0	0
W_c (kgm/s)	15.5	16.7	16.6	16.6	15.1	15.1	15.5	16.3
W_c (kgm/hr)	764	834	1050	1427	969	1321	0	0
T_{T3} (° K)	668	860	853	855	653	659	663	850
$T_{T3.9}$ (° K)	1155	1350	1450	1650	1280	1482	663	850
T_{fuel} (° K)	295	296	295	293	296	296	298	298
P_{S3} (atm)	3.27	4.59	4.58	4.60	3.25	3.48	3.25	4.65
$P_{S3.9}$ (atm)	3.13	4.48	4.47	4.46	3.14	3.35	3.15	4.58
$P_{T3.9}$ (atm)	3.21	4.57	4.55	4.56	3.23	3.44	3.23	4.63

Table XVI. Summary of Aerodynamic Parameters for Acoustic Data, Configuration I-14, 90-Swirl-Can/Flat Flameholder Combustor.

Rdg. No.	684	685	686	689	695	697	698	708
Total f/a	0	0.0140	0.0177	0.0246	0.0244	0.0179	0.0139	0
W_c (kgm/s)	15.3	15.2	15.1	15.1	18.0	18.1	18.1	18.0
W_f (kgm/hr)	0	765	964	1335	1577	1160	906	0
T_{T3} (° K)	664	666	665	662	788	786	785	788
$T_{T3.9}$ (° K)	664	1182	1307	1522	1621	1418	1290	788
T_{fuel} (° K)	300	301	301	301	300	301	301	299
P_{S3} (atm)	3.27	3.23	3.28	3.55	4.57	4.59	4.58	4.57
$P_{S3.9}$ (atm)	3.20	3.11	3.16	3.42	4.42	4.47	4.46	4.48
$P_{T3.9}$ (atm)	3.25	3.19	3.25	3.52	4.53	4.56	4.55	4.54

Table XVII. Summary of Aerodynamic Parameters for Acoustic Data, Configuration III-1, 60-Swirl-Can/Slotted Flameholder Combustor.

Rdg. No.	776	777	778	782	783	784	793	792
Total f/a	0.0117	0.0178	0.0244	0.0118	0.0176	0.0239	0	0
W_c (kgm/s)	15.7	15.2	15.2	16.7	16.6	16.6	14.9	16.9
W_f (kgm/hr)	663	973	1333	706	1053	1434	0	0
T_{T3} (° K)	655	664	664	864	865	863	664	859
$T_{T3.9}$ (° K)	1076	1299	1514	1289	1483	1670	664	859
T_{fuel} (° K)	303	303	302	302	301	300	297	298
P_{S3} (atm)	3.23	3.40	3.63	4.60	4.59	4.58	3.22	4.57
$P_{S3.9}$ (atm)	3.11	3.26	3.49	4.50	4.48	4.46	3.20	4.56
$P_{T3.9}$ (atm)	3.19	3.34	3.58	4.58	4.57	4.56	3.25	4.61

Table XVIII. Summary of Aerodynamic Parameters for Acoustic Data, Configuration I-16, 72-Swirl-Can/Counterswirl Flameholder Combustor.

Rdg. No.	798	799	800	801	802	803	804	806
Total f/a	0.0147	0.0177	0.0247	0.0138	0.0176	0.0245	0.0179	0.0245
W_c (kgm/s)	15.2	15.2	15.1	17.6	17.7	17.5	17.1	17.0
W_f (kgm/hr)	806	972	1343	873	1124	1539	1105	1498
T_{T3} (° K)	666	667	668	733	732	729	828	828
$T_{T3.9}$ (° K)	1039	1167	1315	1336	1325	1567	1442	1656
T_{fuel} (° K)	302	302	304	305	305	306	304	306
P_{S3} (atm)	3.29	3.29	3.42	4.58	4.57	4.55	4.56	4.56
$P_{S3.9}$ (atm)	3.18	3.18	3.30	4.46	4.46	4.41	4.44	4.42
$P_{T3.9}$ (atm)	3.25	3.26	3.38	4.54	4.54	4.51	4.53	4.53

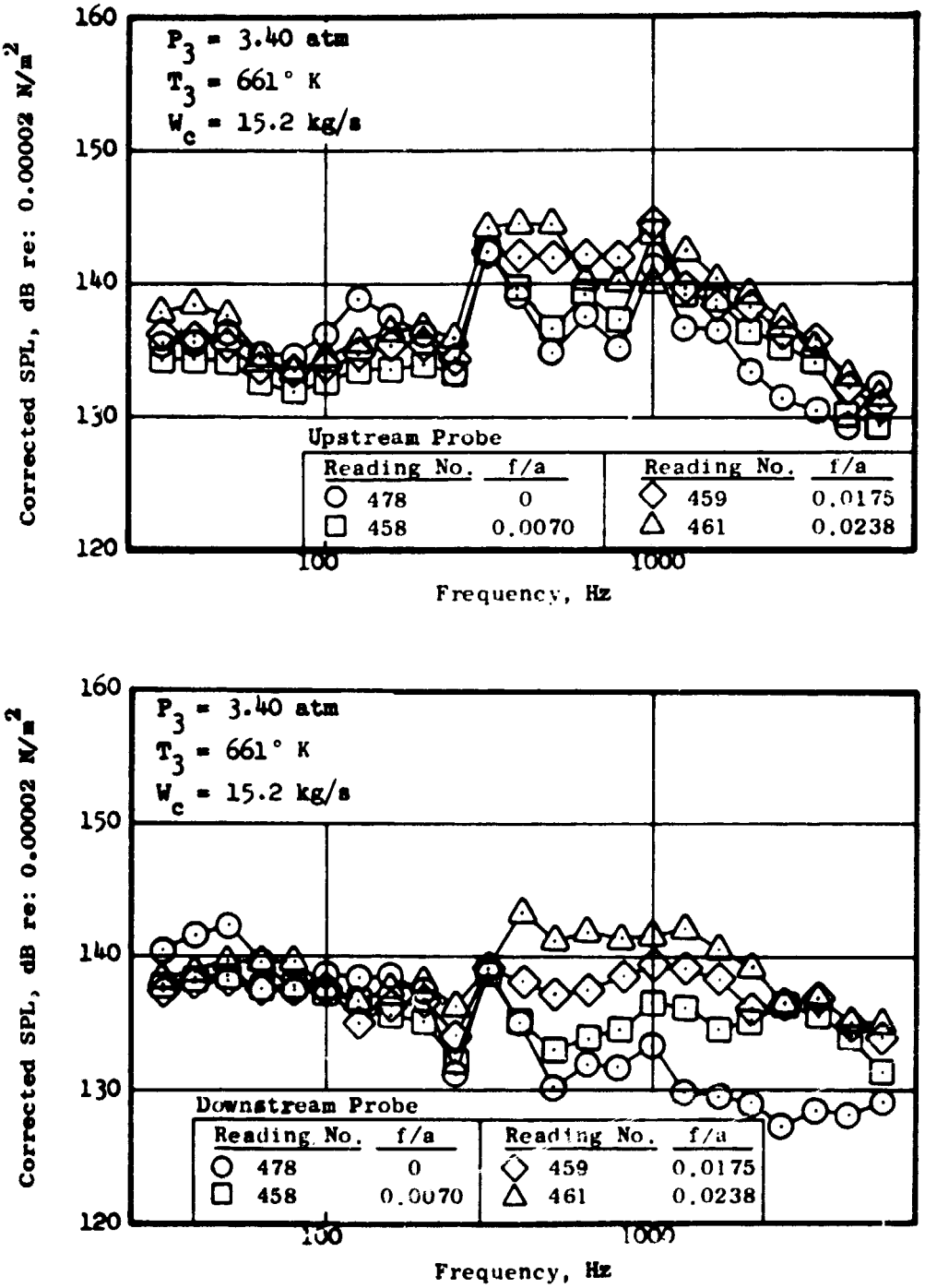

Figure 28. One-Third Octave Band Sound Pressure Levels at Approach Inlet Conditions, Double Annular Combustor, Configuration II-11.

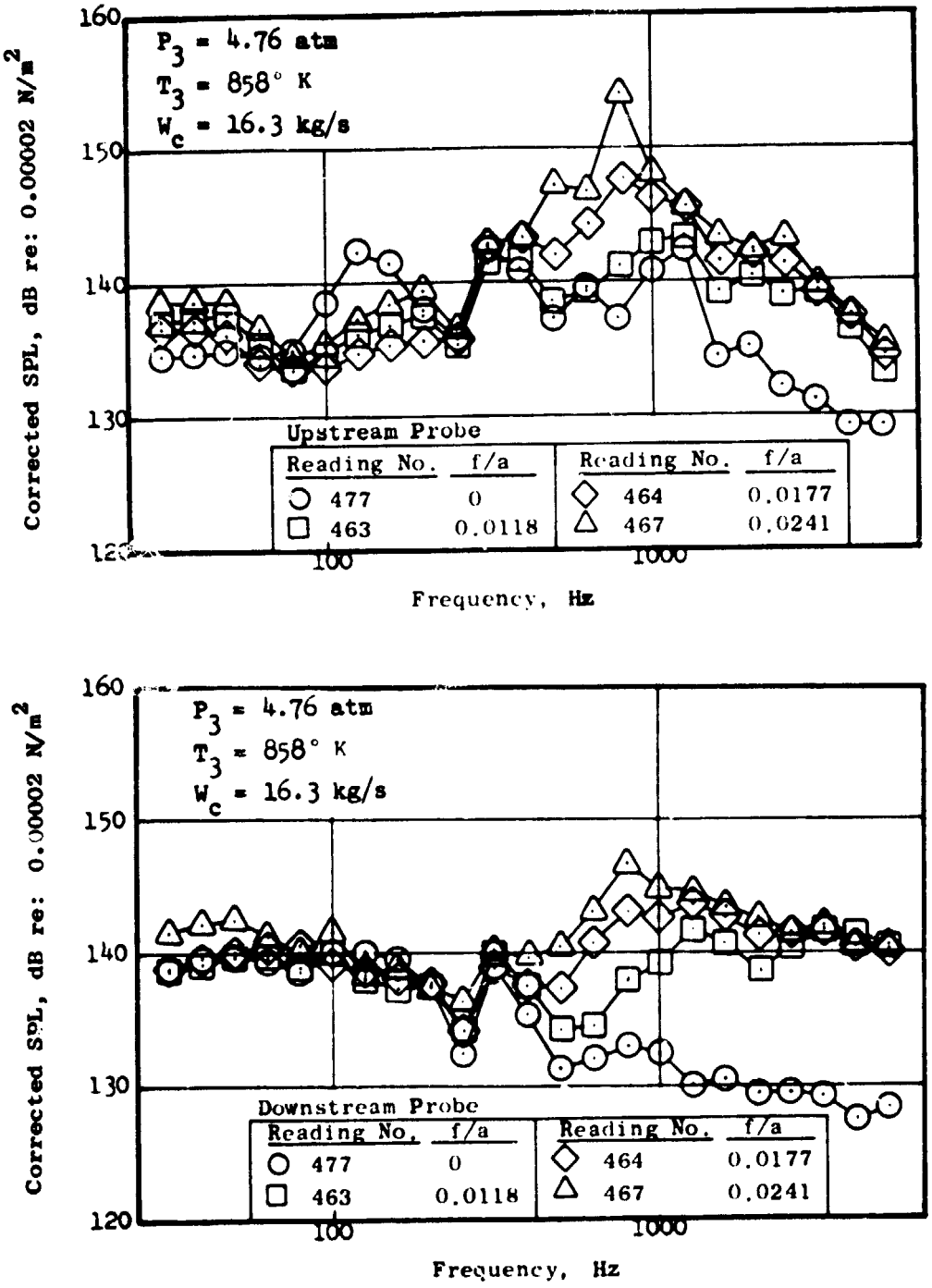

Figure 29. One-Third Octave Band Sound Pressure Levels at Takeoff Inlet Conditions, Double Annular Combustor, Configuration II-11.

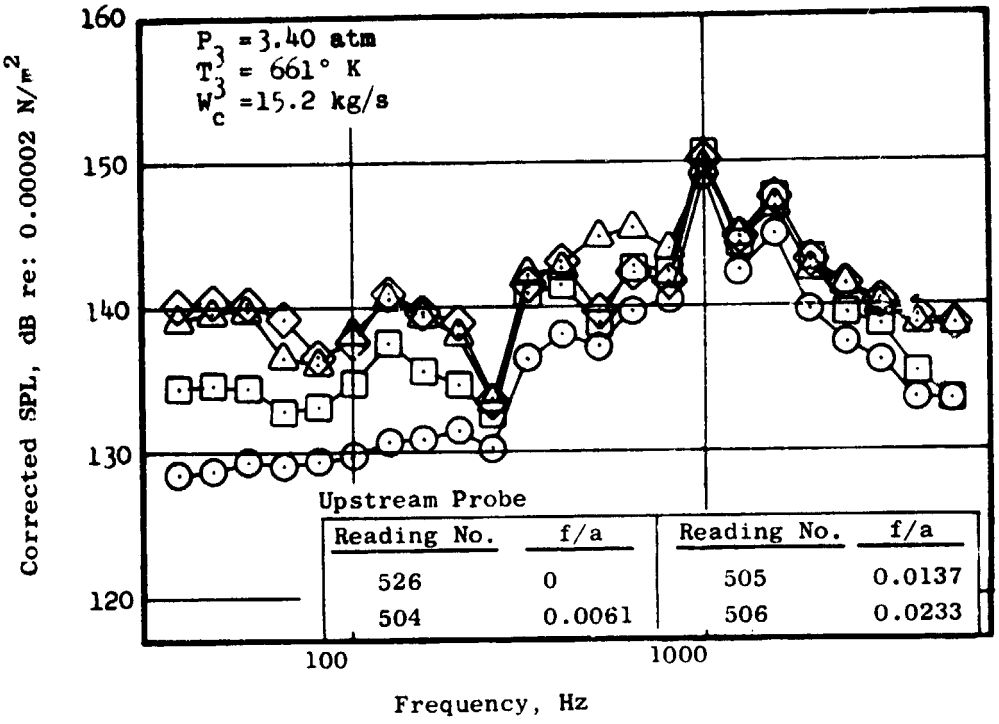

Reading No.	f/a	Reading No.	f/a
526	0	505	0.0137
504	0.0061	506	0.0233

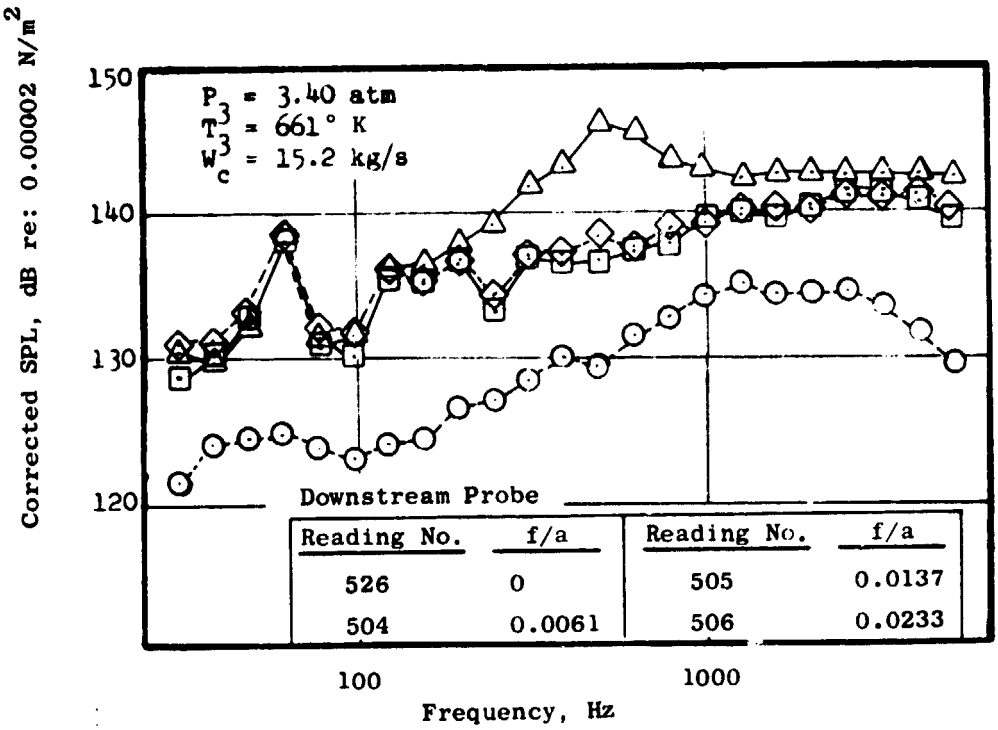

Reading No.	f/a	Reading No.	f/a
526	0	505	0.0137
504	0.0061	506	0.0233

Figure 30. One-Third Octave Band Sound Pressure Levels at Approach Inlet Conditions, Radial/Axial-Staged Combustor, Configuration II-12.

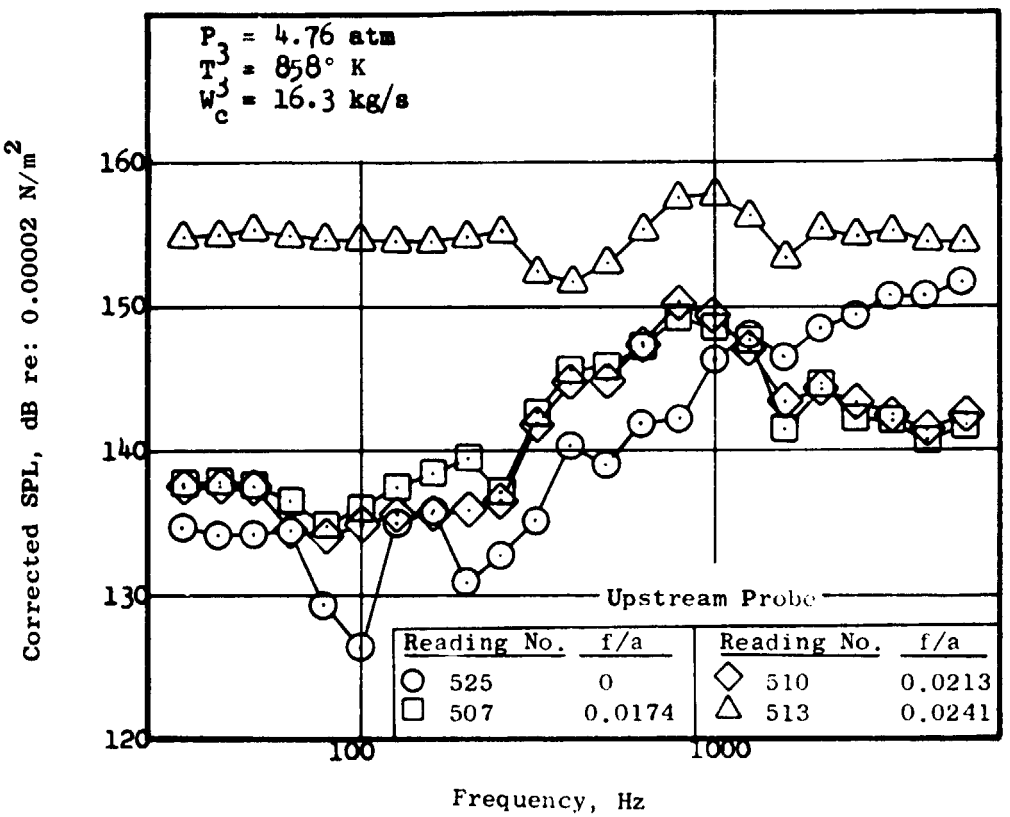

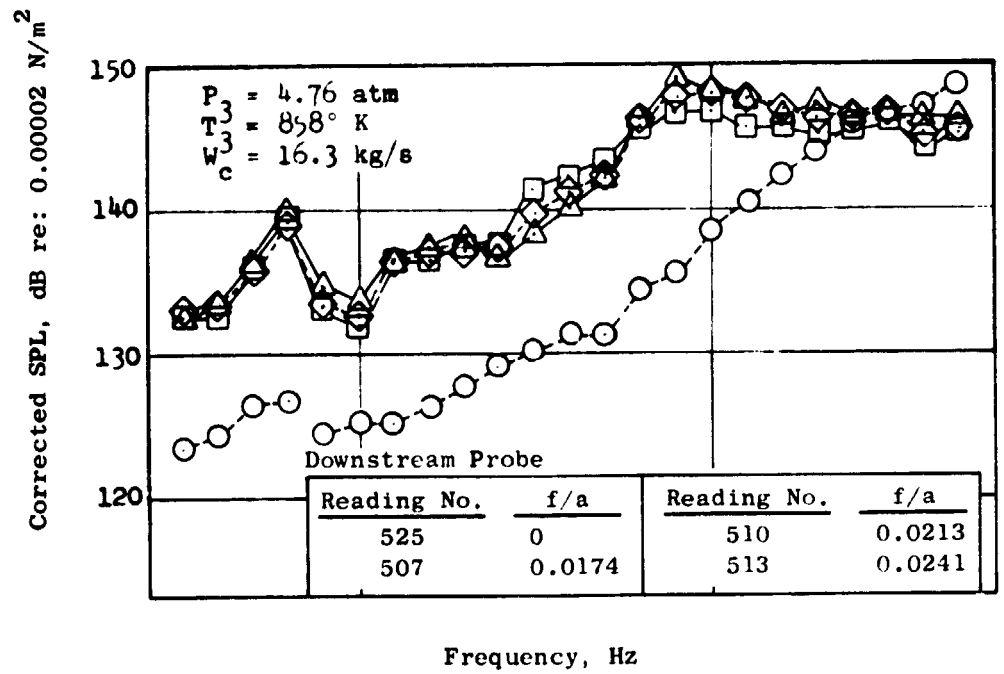

Figure 31. One-Third Octave Band Sound Pressure Levels at Take-off Inlet Conditions, Radial/Axial-Staged Combustor, Configuration II-12.

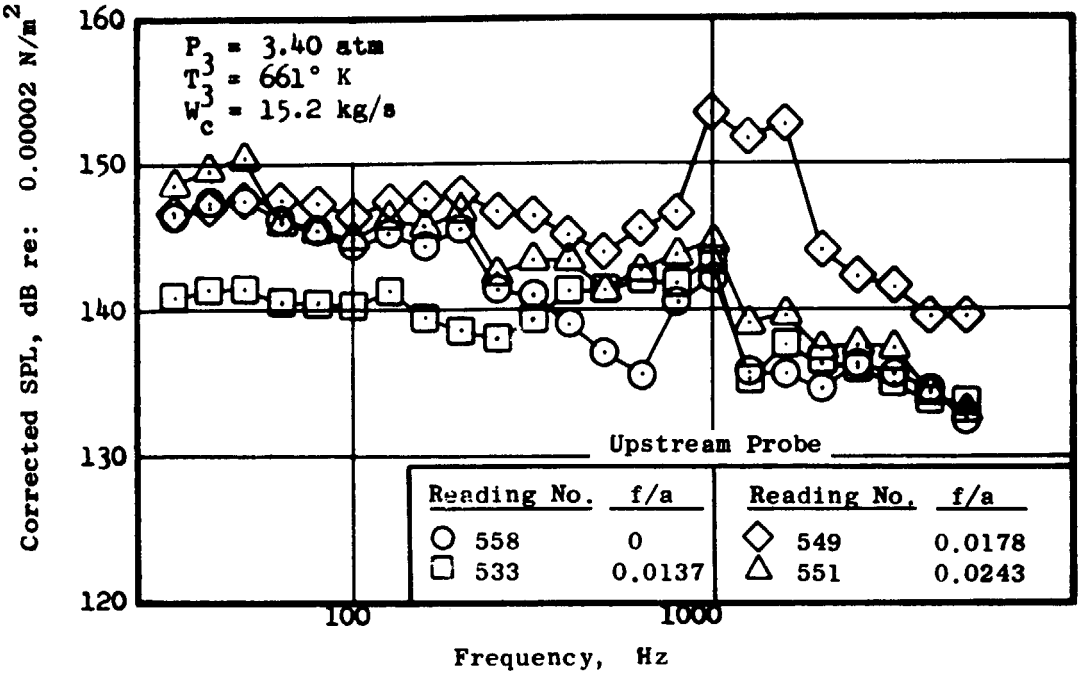

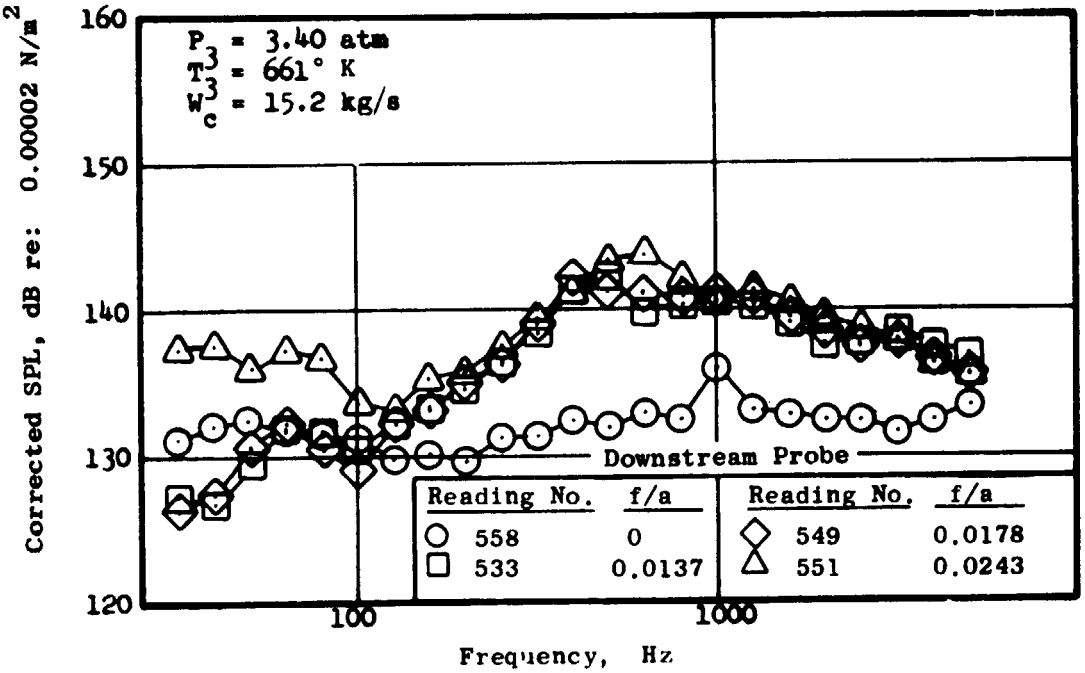

Figure 32. One-Third Octave Band Sound Pressure Levels at Approach Inlet Conditions, 90-Swirl-Can/Sheltered Flameholder Combustor, Configuration I-12.

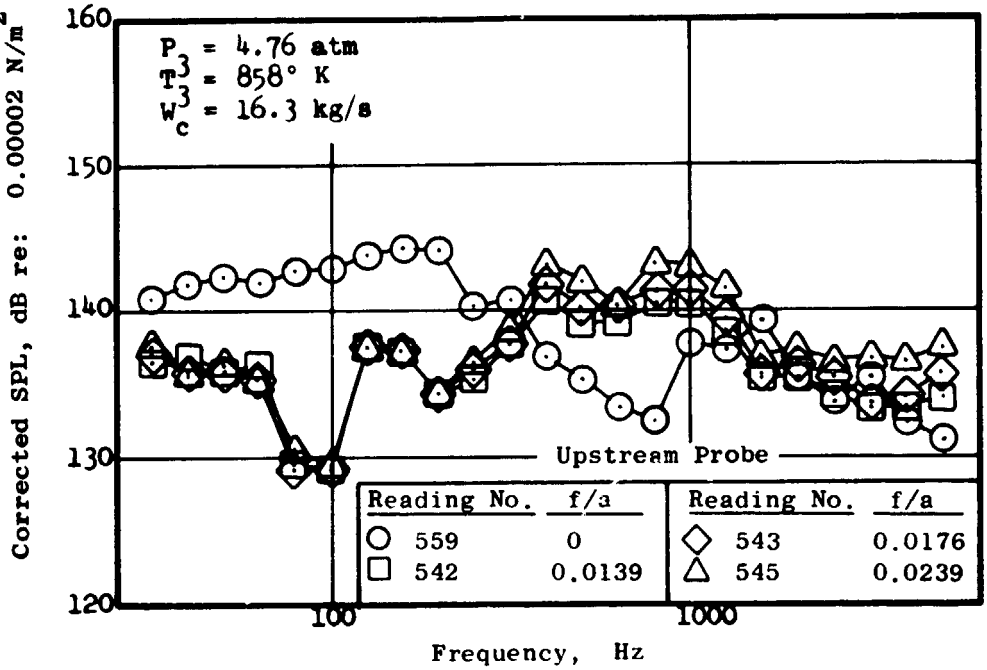

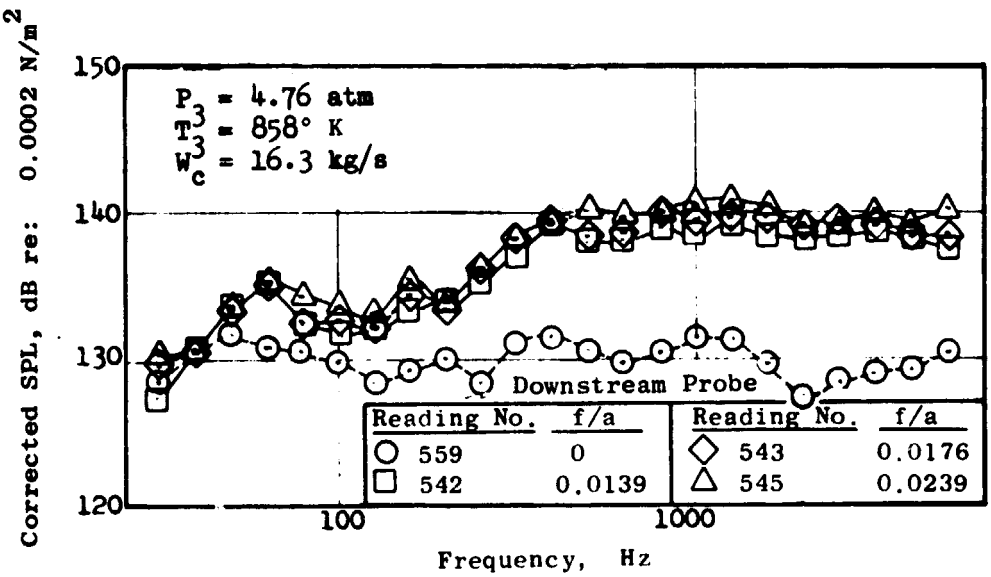

Figure 33. One-Third Octave Band Sound Pressure Levels at Takeoff Inlet Conditions, 90-Swirl-Can/Sheltered Flameholder Combustor, Configuration I-12.

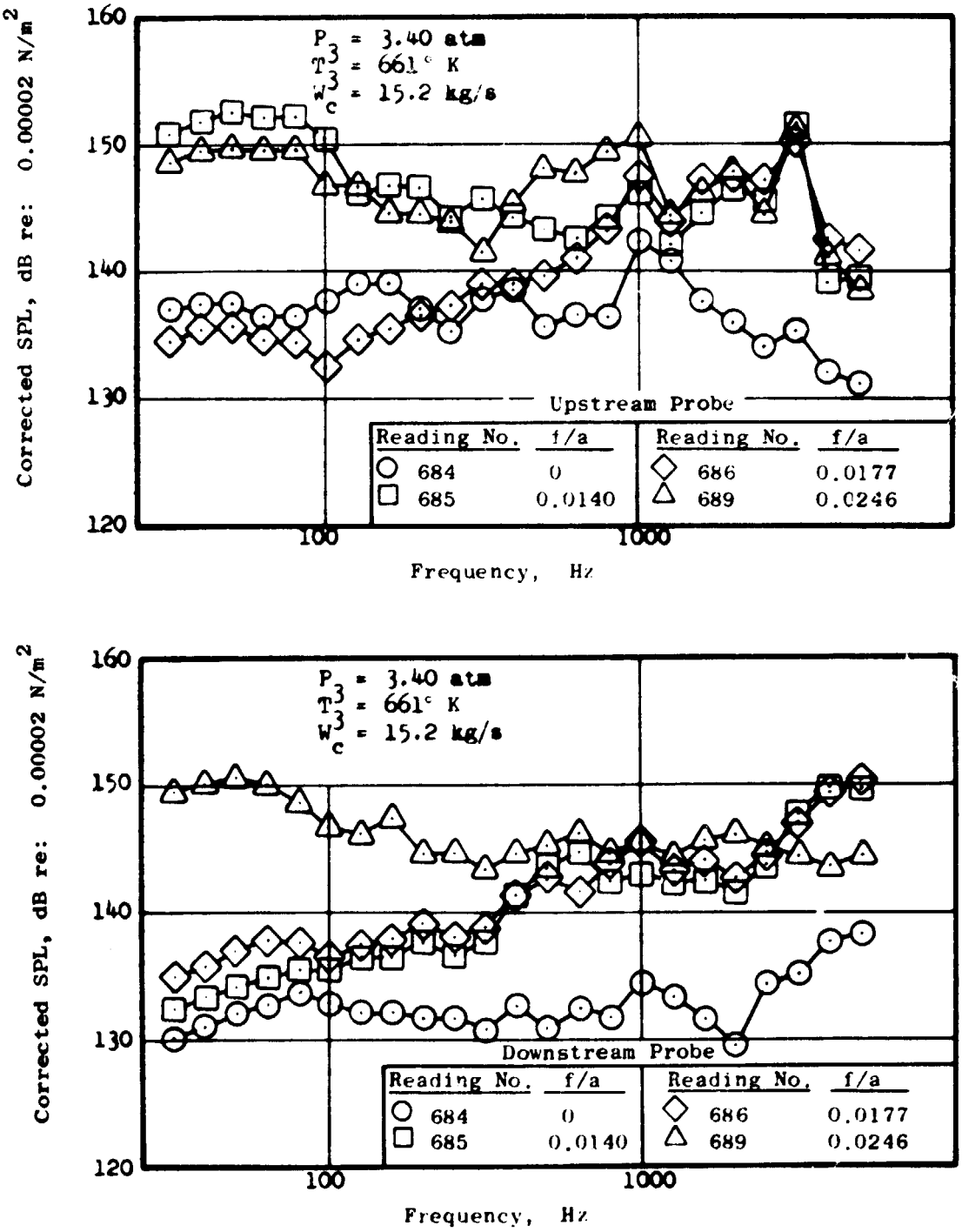

Figure 34. One-Third Octave Band Sound Pressure Levels at Approach Inlet Conditions, 90-Swirl-Can/Flat Flameholder Combustor, Configuration I-14

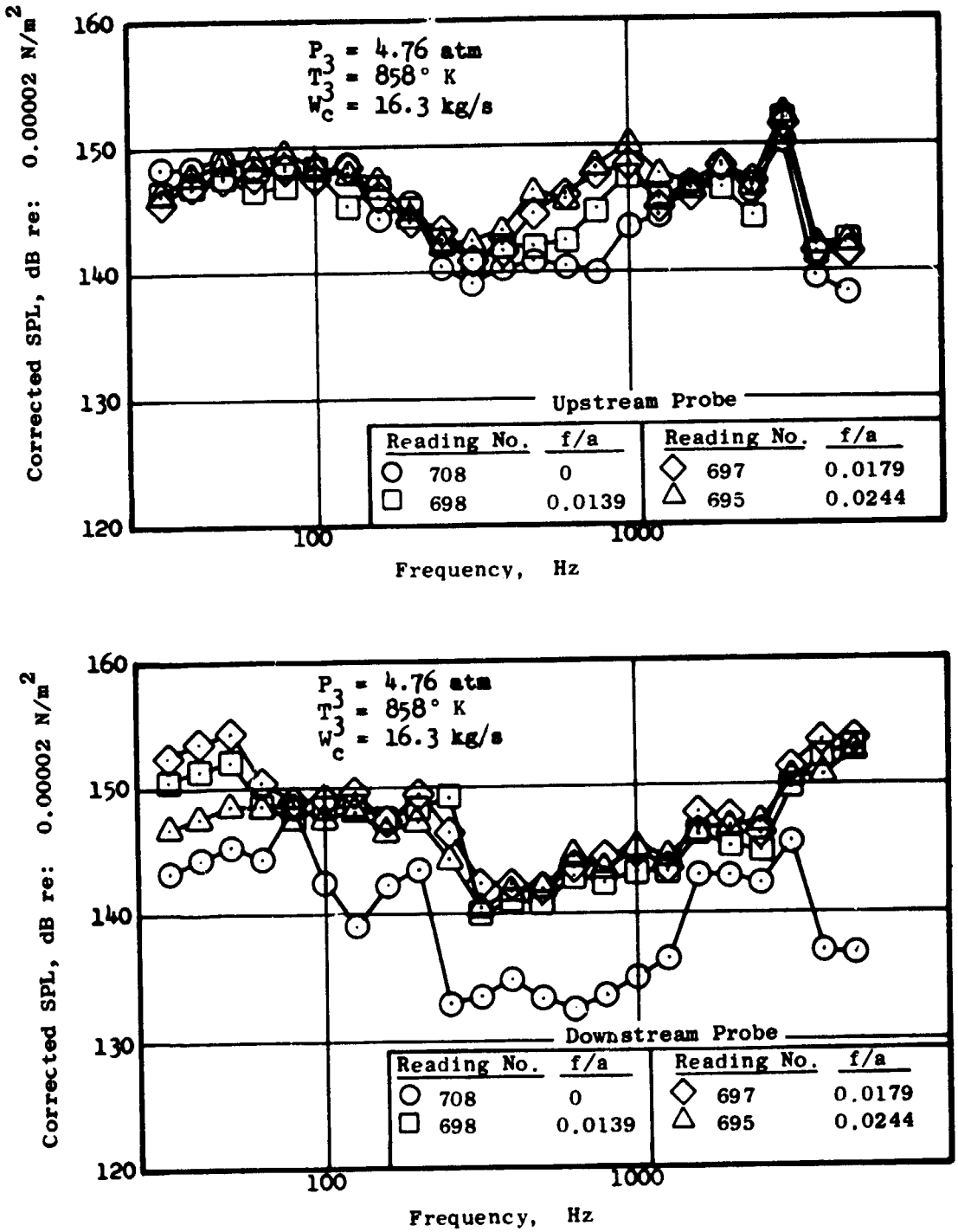

Figure 35. One-Third Octave Band Sound Pressure Levels at Takeoff Inlet Conditions, 90-Swirl-Can/Flat Flameholder Combustor, Configuration I-14.

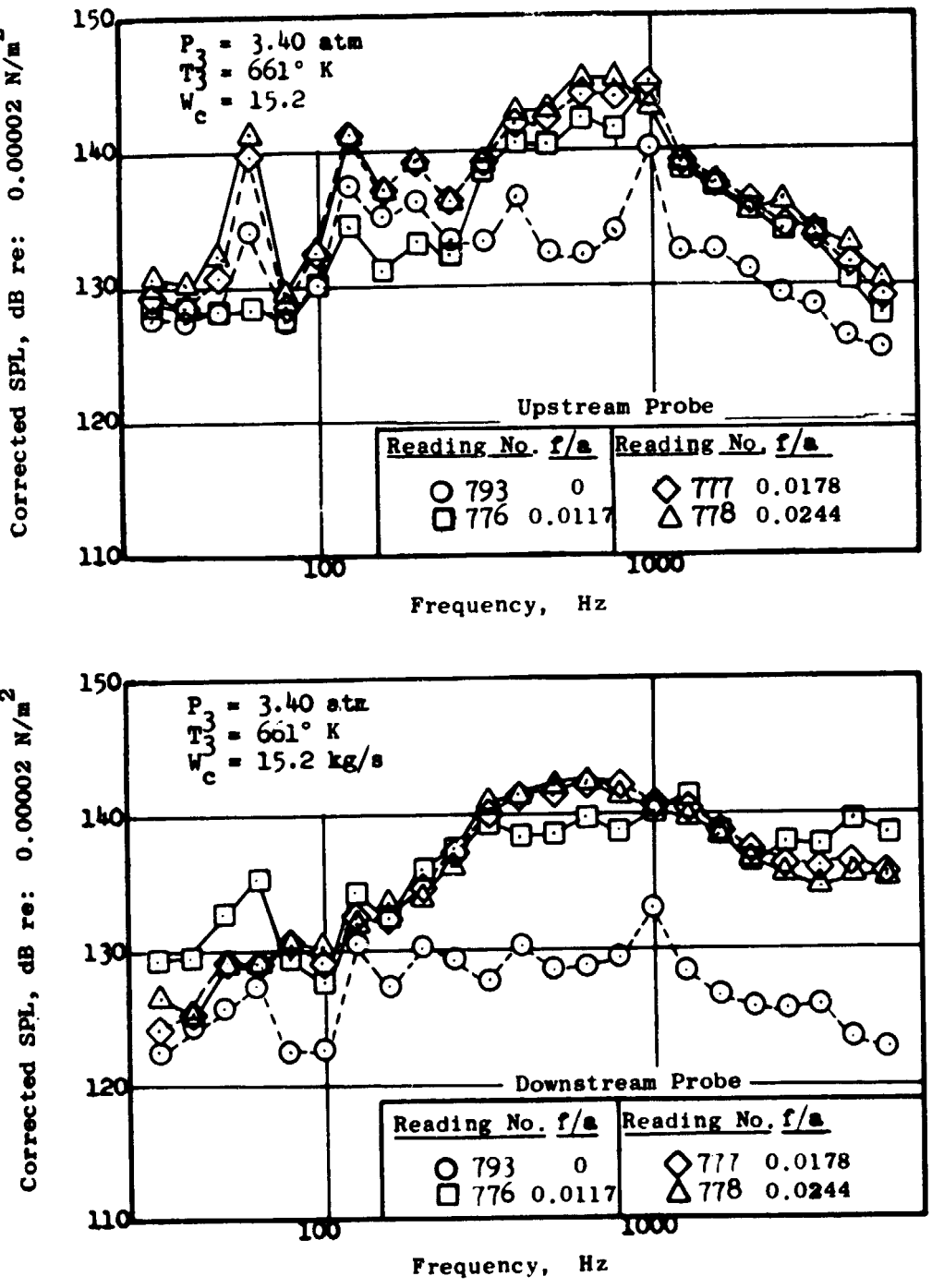

Figure 36. One Third Octave Band Sound Pressure Levels at Approach Inlet Conditions, 60 Swirl-Can/Flat Flameholder Combustor, Configuration III-1.

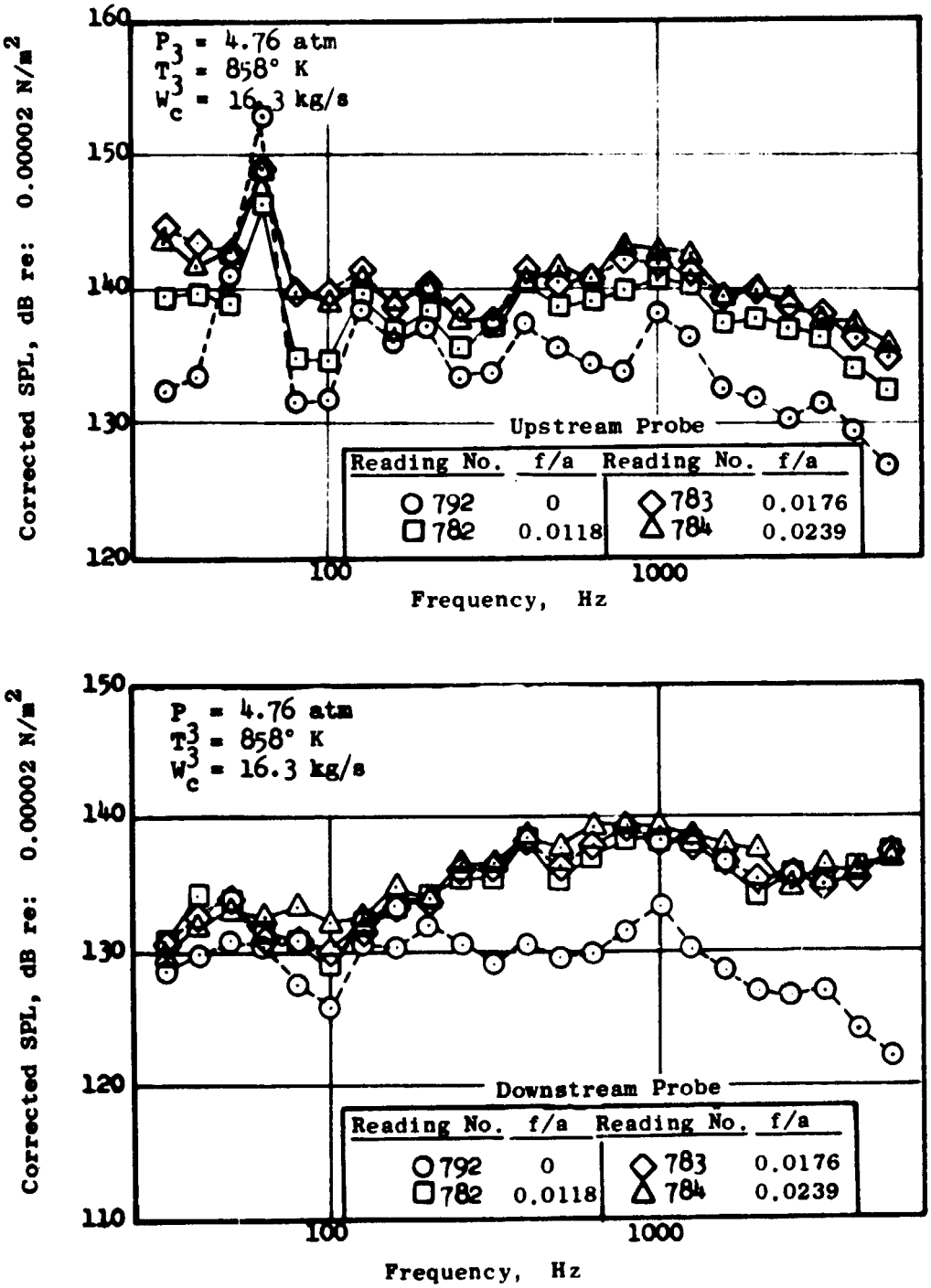

Figure 37. One Third Octave Band Sound Pressure Levels at Takeoff Inlet Conditions, 60 Swirl-Can/Flat Flameholder Combustor, Configuration III-1.

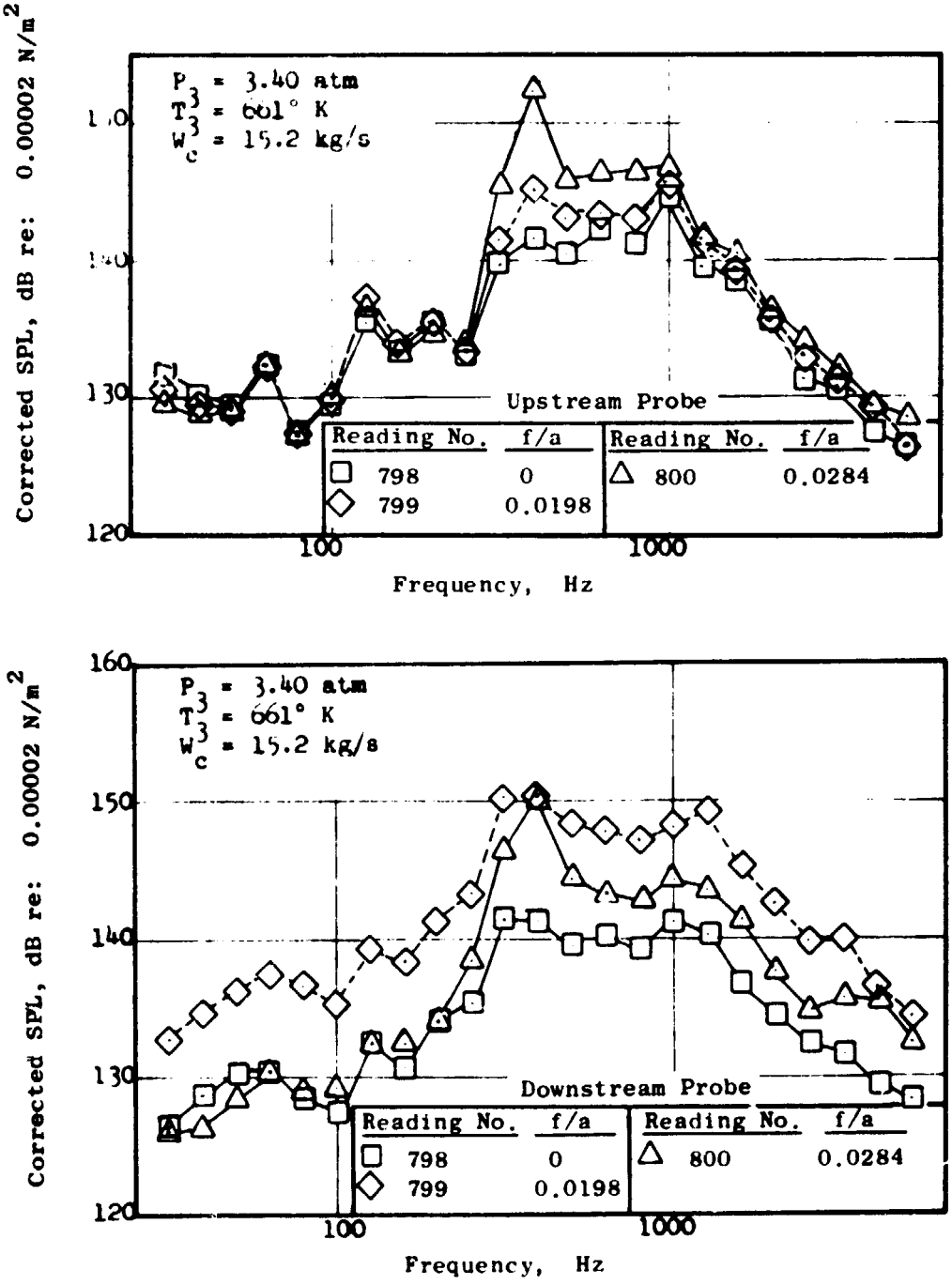

Figure 38. One-Third Octave Band Sound Pressure Levels at Approach Inlet Conditions, 72-Swirl-Can/Counter-swirl Flameholder, Configuration I-16.

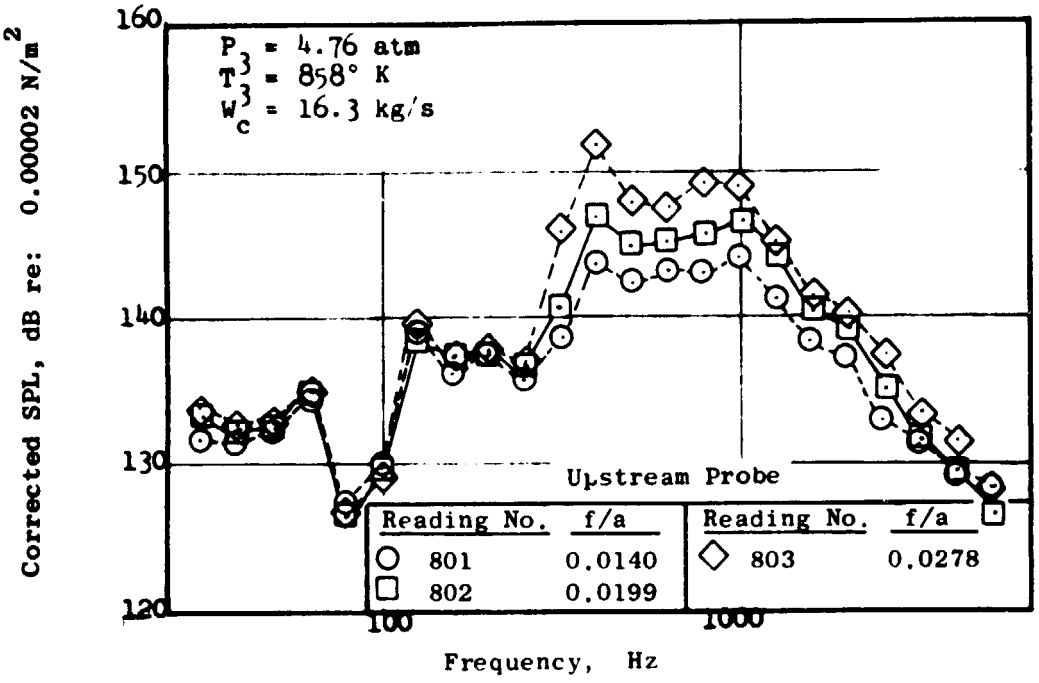

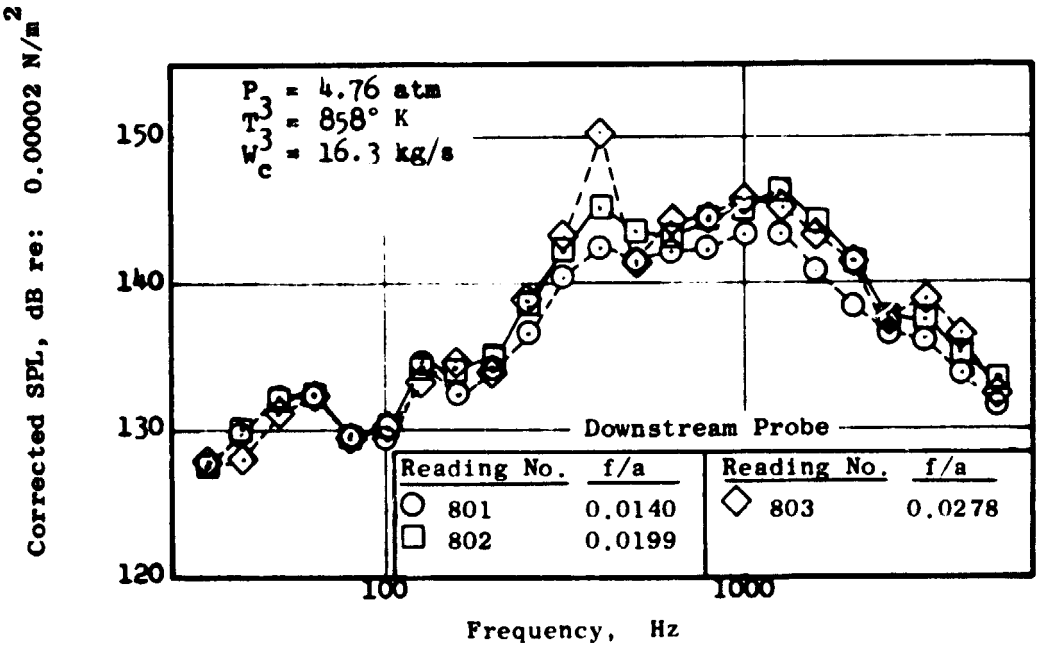

Figure 39. One-Third Octave Band Sound Pressure Levels at Takeoff Inlet Conditions, 72-Swirl-Can/Counter-swirl Flameholder, Configuration I-16.

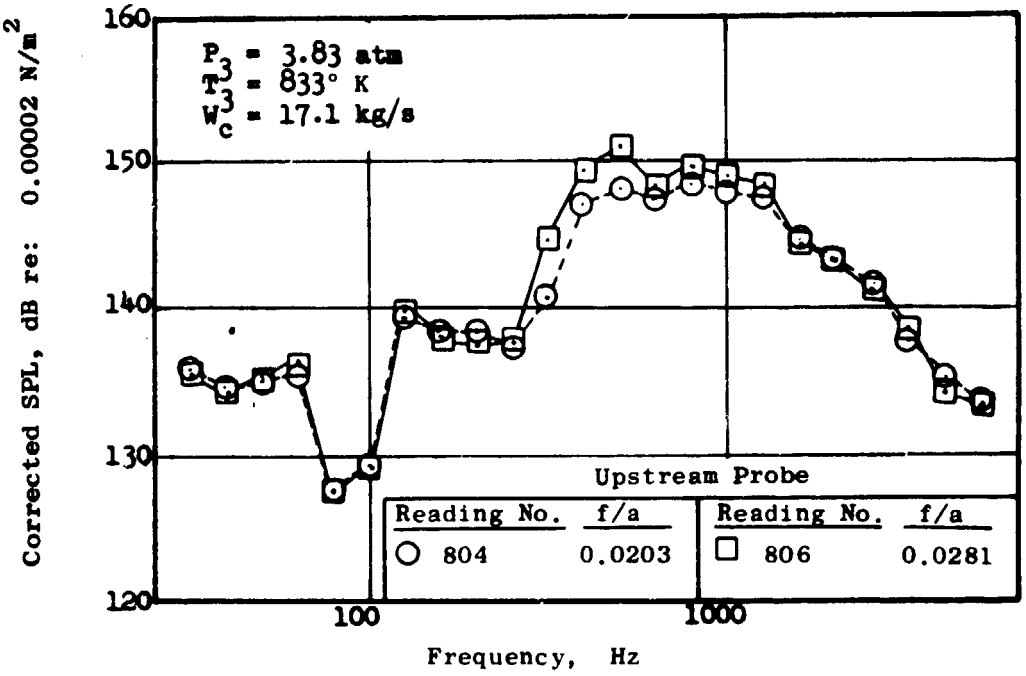

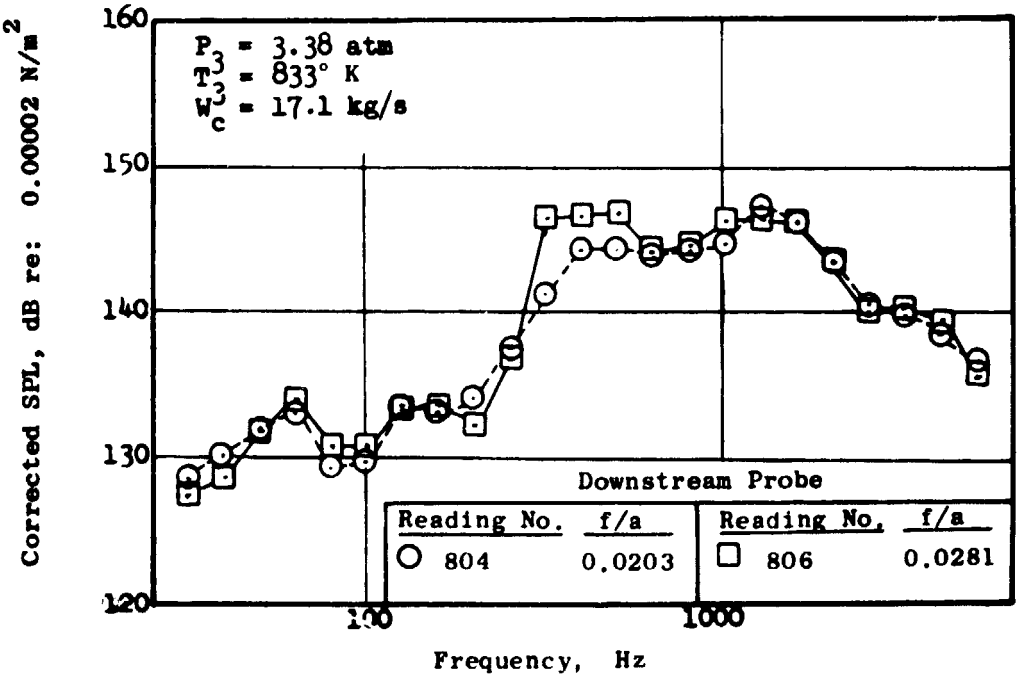

Figure 40. One-Third Octave Band Sound Pressure Levels at AST Inlet Conditions, 72-Swirl-Can/Counterswirl Flameholder, Configuration I-16.

Table XIX. One-Third Octave Band Sound Pressure Levels, Configuration II-11, Double Annular Combustor.

Rdg.	458		459		461		463		464		467		477		478	
Probe	U/S	D/S	U/S	D/S	U/S	D/S	U/S	D/S	U/S	D/S	U/S	D/S	U/S	D/S	U/S	D/S
Frequency																
31.5	134.3	137.6	136.2	137.4	137.9	138.1	137.0	138.6	136.5	138.8	138.5	141.5	134.5	138.8	135.5	140.5
40	134.3	138.2	136.0	138.0	138.4	138.8	137.1	139.0	136.5	139.4	138.6	142.1	138.6	139.4	135.7	141.6
50	134.1	138.4	135.4	138.1	137.6	139.5	137.4	139.6	136.0	139.9	138.5	142.4	134.9	139.6	136.2	142.2
63	132.6	137.5	133.7	137.5	134.4	139.5	135.3	139.7	133.9	140.3	136.5	141.2	134.6	139.3	134.8	139.5
80	131.9	137.8	133.5	137.4	133.3	139.5	133.4	138.8	133.4	140.5	134.5	140.1	134.9	138.5	134.6	137.4
100	132.5	137.1	133.8	137.6	134.5	137.6	134.7	139.9	133.6	139.1	135.2	141.4	138.4	139.9	136.1	138.5
125	133.5	136.5	134.8	135.0	135.8	136.5	136.1	137.9	134.8	138.7	137.1	138.0	142.3	140.0	138.9	138.3
159	133.6	135.6	135.4	136.3	136.3	137.6	136.8	137.1	135.3	138.0	138.3	138.8	141.4	139.4	137.6	138.4
200	133.9	135.1	135.4	136.7	136.6	138.0	137.5	137.3	135.6	137.7	139.4	137.2	137.9	137.4	136.2	137.3
250	133.7	132.4	134.6	134.2	136.1	136.4	135.6	134.2	135.8	134.2	136.6	136.2	135.8	132.5	133.7	131.4
315	142.7	139.0	142.7	139.2	144.7	140.9	141.7	139.9	142.9	139.9	142.7	140.2	142.7	138.9	142.7	139.3
400	139.9	135.4	142.0	138.4	144.9	143.5	141.8	137.2	143.1	137.4	143.7	139.5	141.0	135.4	139.1	135.3
500	136.9	133.3	142.1	137.3	144.8	141.2	138.9	134.2	142.1	137.3	147.8	141.5	137.7	130.3	135.6	130.5
630	139.7	137.1	141.7	137.9	145.5	142.0	139.8	134.7	144.5	140.5	146.8	143.0	139.8	132.1	137.8	132.2
800	137.2	134.9	142.0	138.9	145.2	141.7	141.3	137.8	147.9	143.0	154.2	146.8	137.3	133.0	135.3	131.8
1000	144.2	136.8	144.9	139.8	145.2	141.8	143.0	139.0	146.2	142.7	148.1	144.8	141.0	132.7	141.3	133.6
1250	139.5	136.2	139.8	139.2	142.8	142.2	143.5	141.9	145.8	143.8	145.8	144.9	142.6	131.0	136.8	130.0
1600	138.8	134.8	138.8	138.6	140.5	140.8	139.5	142.9	141.8	143.5	143.5	143.5	134.8	130.7	136.5	129.5
2000	136.7	135.5	138.6	136.1	139.5	139.6	140.6	138.5	142.4	141.2	142.7	142.5	135.7	129.2	133.7	129.2
2500	135.2	136.7	136.5	136.7	137.5	136.6	139.2	140.7	141.4	141.3	143.3	141.5	132.3	133.9	131.6	127.7
3150	134.7	135.8	125.9	137.0	135.7	137.0	139.8	141.8	139.6	141.7	140.0	142.0	131.7	129.1	130.7	128.8
4000	130.4	134.3	132.4	135.3	133.4	135.3	136.7	141.2	137.4	140.5	137.7	140.3	129.7	127.6	129.4	128.3
5000	129.6	131.7	130.9	134.3	131.8	135.4	133.8	140.6	134.9	140.3	135.6	140.3	129.6	128.4	133.9	129.4
OASPL	151.0	150.0	152.5	151.2	154.6	153.3	152.8	153.0	155.1	154.1	158.2	155.6	152.0	150.1	150.5	150.3

Table XX. One-Third Octave Band Sound Pressure Levels, Configuration II-11, Radial/Axial Staged Combustor.

Rdc. Probe	504		505		506		507		510		513		525		526	
	U/S	D/S	U/S	D/S	U/S	D/S	U/S	D/S	U/S	D/S	U/S	D/S	U/S	D/S	U/S	D/S
Frequency																
31.5	134.5	129.6	140.1	131.7	139.1	130.5	137.7	132.8	137.5	133.6	154.8	130.8	134.9	123.4	128.5	121.6
40	134.7	130.6	140.5	131.6	139.7	129.8	137.8	132.9	137.5	133.6	154.9	133.8	134.1	124.5	128.8	124.0
50	134.4	132.8	140.2	133.9	139.9	132.1	137.5	136.1	137.4	136.0	155.2	136.1	134.2	126.7	129.2	124.7
63	132.8	138.0	139.1	139.1	136.5	138.9	136.5	139.3	134.5	138.9	154.9	139.9	134.4	126.9	129.0	124.9
80	133.0	130.9	136.4	132.8	136.1	131.6	134.8	133.6	134.2	133.6	154.6	134.8	129.3	124.7	129.2	123.8
100	134.7	130.1	137.6	132.2	138.1	131.9	135.9	132.1	134.9	132.9	154.5	133.9	126.4	125.2	129.8	123.0
125	137.4	135.5	140.9	136.2	140.6	136.2	137.4	136.5	135.6	136.5	154.4	136.4	135.0	125.1	130.8	124.1
160	135.6	135.4	139.6	135.6	139.4	136.6	136.3	136.7	135.5	136.5	154.4	137.4	135.8	126.4	130.9	124.5
200	134.7	136.8	138.8	136.8	137.9	137.8	139.4	137.8	135.8	137.1	154.8	138.1	130.9	128.0	131.6	126.7
250	132.8	133.2	133.8	136.5	133.5	139.1	137.0	137.4	136.5	137.3	155.1	136.5	132.9	129.1	130.1	126.5
315	141.0	136.9	141.7	137.0	142.4	141.9	142.9	141.3	141.9	139.9	152.2	138.3	135.1	130.2	136.2	128.2
400	141.6	136.4	142.1	137.2	142.8	143.2	145.9	142.4	144.8	141.1	151.6	140.1	137.2	131.3	138.0	130.0
500	138.8	145.0	139.7	138.5	144.9	146.2	146.0	143.4	145.1	142.6	152.9	142.2	139.0	131.3	136.8	129.3
630	142.5	137.1	142.6	137.7	145.5	145.7	147.6	145.9	147.4	146.2	155.2	146.2	141.9	134.7	140.9	131.5
800	142.2	137.8	141.9	139.0	144.0	143.7	149.4	146.9	150.3	147.9	157.4	149.1	142.2	135.9	140.5	132.9
1000	150.1	139.8	150.3	139.7	149.1	142.9	148.6	146.9	149.1	148.0	157.6	148.0	146.4	138.6	149.3	134.4
1250	144.6	139.8	144.8	140.1	144.9	142.1	147.9	145.9	147.5	147.8	156.1	147.8	148.0	140.6	142.8	135.0
1600	147.6	139.5	147.4	140.4	146.9	142.6	143.7	145.8	143.7	146.8	153.2	146.4	146.7	142.4	145.7	134.4
2000	143.4	140.2	143.3	140.2	142.7	142.6	144.5	145.2	144.6	146.2	155.3	147.3	148.6	144.1	140.8	134.4
2500	139.3	141.7	141.5	141.4	141.6	142.4	142.4	145.4	143.3	146.7	154.9	146.3	141.4	146.2	137.5	134.6
3150	138.7	141.7	140.6	141.7	140.0	142.7	142.1	146.0	142.6	146.8	155.1	146.7	150.9	146.8	136.1	133.6
4000	135.4	140.5	139.3	141.5	138.8	142.5	140.8	144.2	141.6	145.2	154.5	145.2	150.9	147.1	133.9	131.4
5000	133.8	139.6	138.9	140.6	138.9	141.6	141.0	145.3	142.5	145.5	154.4	146.4	151.8	148.6	143.8	129.5
OASPL	155.2	152.2	156.1	152.0	156.2	155.0	157.4	156.8	157.3	157.5	168.5	157.7	158.9	154.6	153.8	144.4

Table XXI. One-Third Octave Band Sound Pressure Levels, Configuration I-12, 90-Swirl; Can/Sheltered Flameholder Combustor.

Rdg. Probe	533		542		543		545		549		551		558		559	
	U/S	D/S	U/S	D/S	U/S	D/S	U/S	D/S	U/S	D/S	U/S	D/S	U/S	D/S	U/S	D/S
Frequency																
31.5	141.0	127.7	136.6	129.7	136.9	129.7	137.6	130.6	146.7	126.5	148.6	137.4	146.4	131.2	141.0	128.7
40	141.5	126.8	136.9	130.8	135.9	130.5	135.7	130.7	147.1	127.5	149.6	137.8	147.2	132.0	142.0	130.6
50	141.5	129.9	135.9	133.9	135.9	133.5	136.2	133.8	147.5	130.8	150.5	136.0	147.4	132.5	142.5	131.8
63	140.6	132.1	136.3	135.2	135.4	135.2	135.4	135.3	147.4	132.3	146.0	137.2	146.1	131.8	142.1	130.9
80	140.5	131.8	129.7	132.5	129.0	132.8	130.0	134.6	147.2	130.3	145.5	136.8	145.5	131.5	143.0	130.6
100	140.2	130.9	129.2	131.9	129.1	132.8	129.2	133.9	146.4	129.1	145.0	133.8	144.5	131.2	143.0	129.9
125	141.3	132.3	137.6	132.2	137.6	132.4	137.6	133.4	147.3	132.3	146.2	133.4	145.3	129.9	144.0	128.4
160	139.5	133.6	137.1	133.6	137.3	134.5	137.3	135.5	147.5	133.4	145.8	135.4	144.4	130.1	144.5	129.3
200	138.6	134.9	134.4	134.1	134.7	133.6	134.6	134.0	147.9	135.0	146.8	135.9	145.5	129.8	144.5	130.0
250	138.0	136.4	135.6	135.4	135.8	136.1	136.6	136.3	146.7	136.1	142.6	137.3	141.3	131.3	140.4	128.4
315	139.2	138.3	137.9	132.0	137.9	138.3	138.9	138.3	146.3	139.1	143.4	139.3	141.0	131.4	140.9	131.1
400	141.2	141.2	140.8	139.2	141.8	139.5	143.0	139.2	145.1	142.2	143.3	142.2	139.0	132.4	136.9	131.6
500	141.3	142.2	139.1	138.0	140.0	138.5	142.0	140.2	143.9	141.2	141.3	143.4	137.0	132.0	135.3	130.5
630	142.0	139.9	134.3	138.1	140.4	138.8	141.4	139.8	145.5	141.1	142.8	143.8	135.5	132.9	133.5	129.9
800	141.9	140.2	140.5	139.0	141.2	140.1	143.4	140.0	146.6	140.9	142.9	142.0	140.6	132.5	132.6	130.3
1000	143.5	140.6	140.7	138.7	141.8	139.6	143.0	140.7	153.4	141.0	144.7	140.7	142.1	136.0	137.9	130.7
1250	135.4	140.1	138.5	139.1	139.7	139.8	141.6	140.8	151.8	140.8	139.0	141.1	135.8	133.1	137.4	131.2
1600	137.6	138.9	135.4	138.7	135.5	139.9	136.7	140.5	152.7	139.7	139.8	140.6	139.8	131.9	139.2	129.8
2000	136.3	137.6	135.2	138.2	136.2	134.0	137.2	139.4	144 1	138.4	137.2	139.2	134.7	132.5	135.5	127.4
2500	136.0	137.7	134.2	138.7	135.5	138.7	136.5	139.4	142.2	137.7	137.6	138.5	136.1	132.5	133.9	128.4
3150	135.1	138.3	133.6	138.8	133.9	139.0	136.8	140.0	141.6	137.8	137.3	137.7	135.6	131.7	135.4	129.0
4000	133.9	137.4	133.5	138.2	134.2	138.4	136.5	139.1	139.5	136.5	134.5	136.2	134.6	132.5	132.3	129.3
5000	133.7	136.8	134.3	137.5	135.8	138.5	137.5	140.2	139.5	135.5	133.2	135.5	132.4	133.3	131.2	130.6
OASPL	153.5	151.2	150.7	150.5	151.3	151.1	152.6	151.8	161.3	151.5	158.4	152.9	156.6	145.8	154.0	143.7

Table XXII. One/Third Octave Band Sound Pressure Levels, Configuration I-14, 90-Swirl-Can/Flat Flameholder Combustor.

Rdg.	684		685		686		689		695		697		698		708	
Probe	U/S	D/S	U/S	D/S	U/S	D/S	U/S	D/S	U/S	D/S	U/S	D/S	U/S	D/S	U/S	D/S
Frequency																
31.5	137.0	130.0	150.8	132.2	134.6	134.9	141.5	149.3	146.7	146.7	145.5	152.4	146.3	150.5	148.3	143.4
40	137.5	131.0	151.8	133.1	135.5	135.8	149.4	150.1	147.8	147.6	146.5	153.4	146.9	151.3	148.3	144.4
50	137.5	132.0	152.5	134.0	135.7	136.9	149.7	150.6	148.5	148.5	147.4	154.3	147.5	152.0	149.0	145.4
63	136.5	132.6	152.0	134.9	134.7	137.8	149.6	150.0	149.0	148.5	147.6	150.5	146.5	148.7	148.2	144.5
80	136.4	133.5	152.1	135.5	134.4	137.5	144.6	146.8	149.4	148.3	148.5	149.0	147.0	147.7	148.1	148.5
100	137.7	132.8	150.4	135.4	132.5	136.4	146.0	146.8	148.7	147.5	147.5	149.1	148.1	148.2	147.5	142.7
125	139.0	132.0	146.0	136.3	134.8	137.3	146.8	146.0	147.9	148.1	148.4	149.7	145.3	148.7	148.6	139.0
160	139.0	132.0	146.8	136.4	135.6	137.9	144.7	147.2	147.2	146.3	146.0	147.3	146.8	147.4	144.4	142.3
200	137.0	131.7	146.6	137.6	136.4	139.0	144.5	144.7	144.4	147.1	144.2	149.4	145.0	148.2	145.5	143.7
250	135.2	131.7	144.2	135.6	137.2	138.0	144.0	144.8	142.2	144.6	143.1	146.2	142.5	149.1	140.4	132.9
315	137.9	130.8	145.8	137.8	139.1	138.8	141.5	143.3	142.5	140.3	140.9	142.3	141.0	140.1	139.0	133.5
400	138.6	132.7	144.2	141.2	139.0	141.3	145.2	144.7	143.3	141.7	141.8	142.3	142.2	141.1	140.2	134.9
500	135.7	130.9	143.4	143.7	139.8	142.7	148.0	145.2	146.3	142.0	144.8	142.0	142.0	140.9	140.9	133.2
630	136.5	132.3	142.6	144.9	141.0	141.8	147.8	146.0	145.8	144.8	146.0	143.8	142.7	143.0	140.4	132.4
800	136.3	131.8	144.2	142.3	143.4	143.9	149.3	144.8	148.3	143.6	147.8	144.5	145.0	142.4	140.0	133.5
1000	142.3	134.5	146.0	143.0	147.3	145.5	150.5	145.5	150.1	145.1	148.5	144.9	147.6	143.2	143.7	134.9
1250	140.9	133.3	142.1	142.0	144.1	143.3	144.3	144.4	147.8	144.5	145.1	143.5	145.9	143.2	144.7	136.3
1600	137.7	131.6	144.7	142.4	147.0	144.1	146.1	145.7	146.9	146.2	146.1	147.9	146.7	146.1	146.9	143.0
2000	136.0	129.6	146.3	141.6	147.2	142.8	147.8	146.1	148.2	146.7	148.4	147.3	146.6	145.2	148.3	143.0
2500	134.1	134.5	145.5	143.8	147.0	144.4	144.6	145.1	146.7	146.9	147.0	146.1	144.5	145.2	146.2	142.3
3150	135.2	135.1	151.5	147.7	150.2	146.9	151.1	144.4	152.3	150.5	151.6	151.3	152.2	149.9	150.2	145.6
4000	132.1	137.8	139.0	149.8	142.2	149.5	141.1	143.8	143.1	150.8	141.7	153.4	141.6	152.2	139.6	136.9
5000	124.1	138.2	139.5	149.8	141.8	150.2	138.5	144.7	142.4	152.5	141.6	153.7	142.4	152.9	138.2	136.7
OASPL	151.1	146.9	161.7	156.7	156.7	157.0	160.9	160.3	161.1	161.0	160.3	163.2	159.8	162.0	159.7	155.7

Table XXIII. One-Third Octave Band Sound Pressure Levels, Configuration III-I, 60-Swirl-Can/Flat Flameholder Combustor.

Rdg. Probe	776		777		778		782		783		784		792		793	
	U/S	D/S	U/S	D/S	U/S	D/S	U/S	D/S	U/S	D/S	U/S	D/S	U/S	D/S	U/S	D/S
Frequency																
31.5	128.5	129.5	127.6	124.3	130.7	126.6	139.5	130.8	144.7	130.8	143.7	129.8	132.3	128.6	127.7	122.5
40	128.6	129.7	128.7	125.8	130.3	125.6	139.8	134.1	143.5	132.5	141.8	131.9	133.4	129.9	127.6	124.5
50	128.0	132.8	130.6	129.2	132.1	124.1	138.9	133.8	142.7	133.9	142.7	133.1	142.9	130.9	128.2	125.9
63	128.3	135.4	137.9	129.1	140.0	129.2	146.3	131.3	149.0	130.9	148.9	132.7	152.9	130.3	134.1	127.2
80	127.8	129.7	128.7	130.9	130.3	130.6	134.9	130.7	130.7	130.8	139.9	133.3	131.4	129.5	127.6	122.5
100	130.2	127.8	132.8	129.0	134.2	130.2	134.8	129.0	139.7	129.9	138.9	132.1	131.7	125.9	130.1	122.8
125	134.7	134.5	141.3	132.2	141.5	152.1	139.7	132.4	141.4	131.4	140.3	132.6	158.2	130.5	137.5	130.6
160	131.0	132.2	137.0	132.6	137.3	133.7	136.9	133.3	138.8	133.2	139.1	134.9	136.0	130.3	135.2	127.3
200	133.4	136.0	139.3	134.8	139.6	133.9	138.2	134.1	140.2	133.8	140.1	134.0	137.1	131.9	136.2	130.1
250	132.4	137.3	136.6	137.3	136.4	136.4	135.6	135.3	138.5	136.1	137.5	136.5	133.4	130.5	133.7	129.2
315	138.6	134.1	139.4	140.1	139.4	141.2	136.8	135.4	137.6	136.2	137.6	136.5	133.9	129.1	133.7	127.9
400	140.6	138.2	141.5	141.2	141.8	141.3	140.6	138.2	141.6	138.1	140.8	138.5	137.5	131.4	136.8	130.2
500	140.6	138.5	142.8	141.4	143.0	142.3	138.7	135.3	140.3	136.2	141.5	137.7	135.7	129.6	132.7	127.2
630	142.2	139.9	144.2	142.1	144.6	142.7	139.1	126.9	140.9	137.8	140.9	139.1	134.5	129.8	132.2	128.8
800	141.9	141.9	144.0	142.0	145.3	141.2	139.9	138.2	142.1	139.2	143.2	139.2	133.9	131.3	134.1	129.4
1000	144.7	140.1	145.0	140.9	143.9	140.0	140.9	138.1	141.9	138.0	142.9	139.1	138.1	133.2	140.1	133.0
1250	138.5	141.3	138.6	140.2	141.3	139.8	140.5	138.0	141.2	137.8	142.5	138.5	136.3	130.1	132.6	128.1
1600	137.6	138.8	137.5	138.9	139.4	138.5	137.4	136.6	139.3	136.8	139.4	137.9	132.5	128.5	132.5	126.6
2000	136.1	136.3	136.1	137.3	137.0	136.9	137.8	134.1	139.9	135.3	140.0	137.3	131.8	126.9	131.0	125.9
2500	134.0	137.9	135.0	136.4	139.5	135.6	137.0	135.8	138.7	135.8	139.0	134.7	130.2	126.6	129.3	125.7
3150	133.7	137.7	134.2	136.0	138.7	134.7	136.3	135.1	138.1	134.9	137.5	136.1	131.3	126.9	128.3	125.9
4000	130.3	139.3	131.9	136.2	138.2	135.5	134.0	136.2	136.2	135.5	137.3	135.9	129.3	124.1	126.0	123.1
5000	127.9	138.2	129.1	135.6	137.1	135.2	132.4	137.3	134.9	137.3	136.0	137.7	126.9	122.0	120.3	122.4
OASPL	151.1	151.2	152.9	151.4	153.8	151.3	142.8	149.1	155.1	149.3	155.2	150.0	154.4	143.2	147.1	141.4

Table XXIV. One-Third Octave Band Sound Pressure Levels, Configuration I-16, 72-Swirl-Can/Counterswirl Flameholder Combustor.

Rdg.	798		799		800		801		802		803		804		806	
Probe	U/S	D/S	U/S	D/S	U/S	D/S	U/S	D/S	U/S	D/S	U/S	D/S	U/S	D/S	U/S	D/S
Frequency																
31.5	131.8	126.6	130.7	132.9	129.9	125.1	131.9	127.6	133.6	127.7	133.9	127.9	135.9	128.8	135.7	128.6
40	130.1	128.9	129.8	134.9	128.9	125.2	131.9	129.9	132.7	130.1	132.9	128.0	134.9	130.1	134.7	128.9
50	129.3	130.2	128.9	136.2	129.1	128.4	132.2	132.2	132.8	132.2	133.0	131.1	135.1	132.0	135.1	133.5
63	132.2	130.6	132.6	137.6	132.5	130.4	134.5	132.6	135.4	132.5	135.1	132.3	135.5	133.1	136.4	134.4
80	127.7	128.7	126.9	136.7	127.6	128.9	127.5	129.8	126.7	129.6	126.7	129.9	127.6	129.4	127.7	131.8
100	129.4	127.4	130.1	135.1	130.1	129.1	130.0	129.6	130.0	130.1	129.2	130.3	129.3	129.9	129.3	131.4
125	135.7	132.5	137.2	139.4	136.8	132.6	138.8	134.8	139.6	134.6	139.8	133.4	139.6	133.8	138.0	133.5
160	133.5	130.8	134.2	138.5	133.5	132.6	136.2	132.6	137.5	134.5	137.4	134.9	138.6	133.3	138.0	133.5
200	135.3	134.1	135.7	141.3	134.8	134.2	137.6	134.4	137.6	135.1	137.8	134.0	138.4	134.1	137.5	133.9
250	133.8	135.7	133.7	143.4	134.1	138.7	135.9	136.6	136.9	138.9	137.0	138.7	137.0	137.5	137.5	136.8
315	139.9	141.5	141.5	150.3	145.7	146.6	138.9	140.4	140.8	142.3	145.8	148.1	140.8	141.3	144.9	140.4
400	141.7	141.4	145.2	150.7	152.2	150.5	143.8	142.4	147.1	145.4	152.0	150.4	147.0	144.4	149.6	147.6
500	140.7	139.7	143.1	148.3	145.8	144.7	142.7	141.7	145.0	143.7	147.9	146.3	147.9	144.3	151.0	146.8
630	142.2	140.2	143.6	147.9	146.4	143.2	143.4	142.0	145.2	142.0	147.5	143.2	147.1	143.9	148.2	145.1
800	141.1	139.2	143.1	147.1	146.2	142.8	143.1	142.2	145.9	144.4	149.3	144.4	148.5	144.1	149.9	144.5
1000	144.8	141.2	145.9	148.1	146.9	144.2	144.0	143.2	146.7	145.1	149.0	145.8	147.9	144.8	149.0	145.2
1250	139.7	140.4	141.5	149.2	141.5	143.6	141.4	143.4	144.4	146.4	145.3	145.1	147.6	147.1	148.4	146.3
1600	138.7	136.8	139.6	145.0	140.3	141.3	138.7	140.9	140.5	144.2	141.6	143.7	144.8	146.0	144.6	145.8
2000	135.6	134.6	135.6	142.7	136.3	137.7	137.3	138.3	139.2	141.4	142.4	141.5	144.2	143.3	144.4	143.5
2500	131.2	132.7	133.2	139.9	134.4	134.9	133.0	136.7	135.2	137.8	137.2	137.5	141.5	140.6	141.1	139.8
3150	130.8	131.9	131.5	140.0	132.7	135.8	131.7	136.1	131.5	137.7	133.5	139.0	137.9	139.9	138.6	140.1
4000	127.5	129.6	129.5	136.4	129.5	135.6	129.2	133.8	129.5	135.6	131.0	136.5	135.4	138.5	134.4	139.3
5000	126.7	128.4	126.7	134.7	128.8	132.7	126.7	131.9	126.5	133.8	128.4	132.7	133.7	136.5	133.5	135.5
OASPL	151.4	150.3	153.1	158.5	156.3	155.1	152.6	152.3	154.8	154.4	157.7	156.2	156.9	155.0	158.4	156.0

SECTION 6.0

DISCUSSION OF RESULTS

6.1 SOUND PRESSURE LEVEL SPECTRA

A typical comparison of the upstream to downstream probe is shown in Figure 41. For both takeoff and approach inlet conditions the upstream probe appears slightly higher (ignoring the obvious 60 cycle contamination). This might be due to the difference in cross-sectional area at the two measuring stations. If the upstream and downstream radiated power from the combustor were equal, the upstream probe would measure 2.8 dB higher due to its small flowpath area.

It is very difficult to determine from these data whether or not the downstream probe is contaminated by facility piping noise, since no wave propagation direction can be ascertained at either probe. The change in levels at both probes when inlet conditions are constant and fuel-air ratio is varied (Figures 28 through 40), however, does lend to a tentative conclusion that both are measuring combustor noise. It is also felt that noise sources downstream of the combustor had a negligible influence due to the significant damping effect of the cooling water spray downstream of the combustor. When the cooling water was turned off briefly during a test, the noise level increased significantly. The effect of damping of acoustic waves by water injection has been observed and studied in the literature (Reference 3). However, a quantitative study of this phenomenon was not performed. It can be concluded that the downstream probe signals will most accurately measure the combustor noise signature.

A comparison of the six combustors, spectra based on the downstream probe and the same fuel-air ratio can be seen in Figure 42. The broad band hump in the frequency range of 400 to 1000 Hz appears to be the most common for all the configurations. The peak levels in this frequency range and the overall sound pressure levels for the spectra are listed in Table XXV. It is difficult to say conclusively which configuration makes more noise.

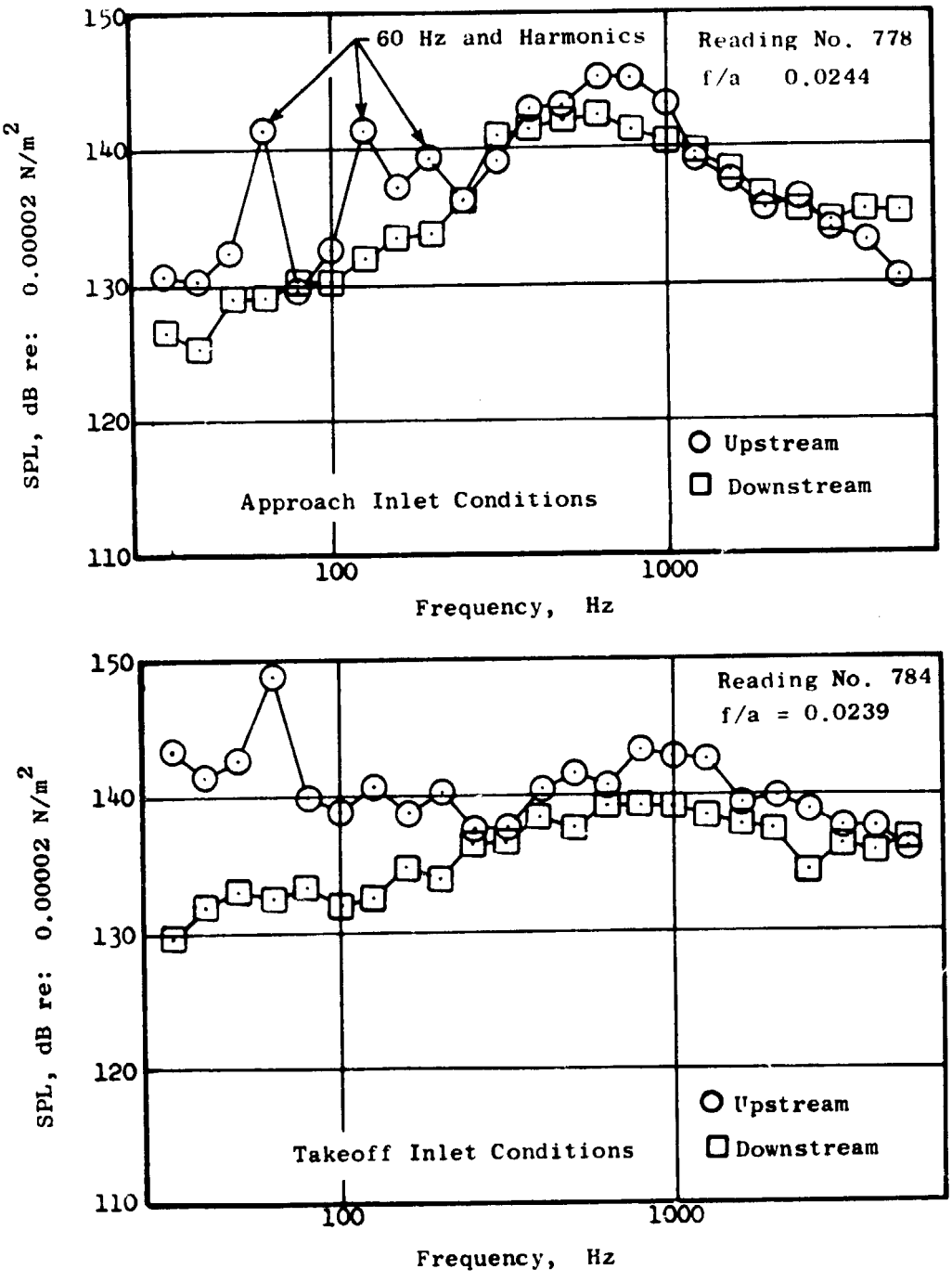

Figure 41. Comparison of Upstream to Downstream Sound Pressure Levels. 60-Swirl-Can/Flat Flameholder Combustor, Configuration III-1.

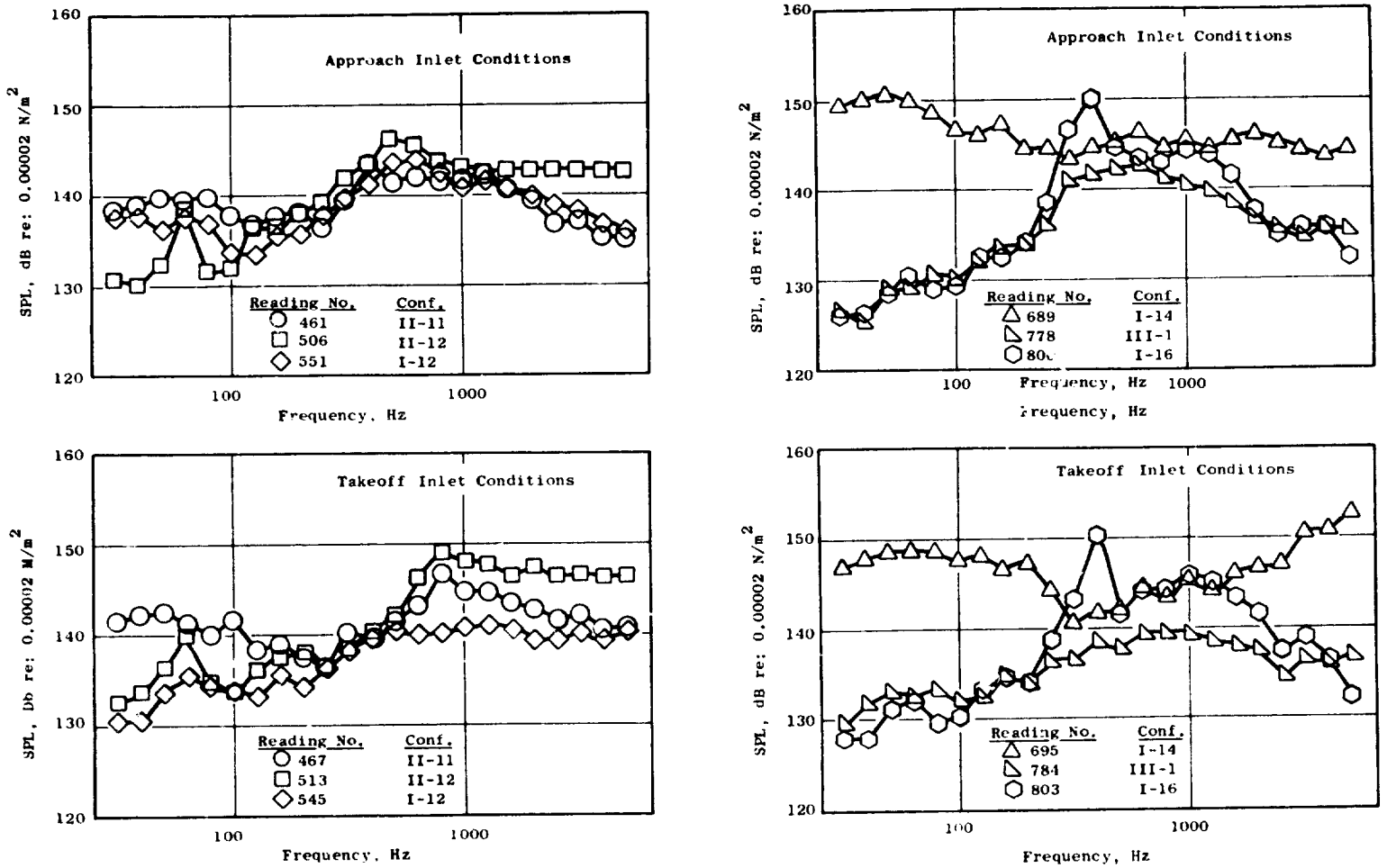

Figure 42. Comparison of Six Combustors with the Downstream Probe at a Constant Fuel-Air Ratio of 0.0245.

Table XXV. Configuration Comparison of Peak Sound Pressure Levels.

Configuration	Approach 400 to 1000 Hz Peak SPL (dB)	Approach OASPL (dB)	Takeoff 400 to 1000 Hz Peak SPL (dB)	Takeoff OASPL (dB)
II-11	143.5	153.3	146.8	155.6
II-12	146.2	155.0	149.1	157.7
I-12	143.8	152.9	140.8	151.8
I-14	146.0	160.3	145.1	161.0
III-1	142.7	151.3	139.2	150.0
I-16	150.5	155.1	150.4	156.2

6.2 ACOUSTIC POWER LEVELS

An estimate of the combustor noise power level can be made by assuming a uniform sound pressure level across the annulus area. The overall power level (OAPWL) is calculated from the overall sound pressure level (OASPL). The measured OASPL is the logarithmic sum of the measured one-third octave band levels summed over the frequency range of 31.5 to 5000 Hz. The spectra were previously corrected for probe losses. The OAPWL was calculated based on the measured OASPL corrected to standard day conditions from the local temperature, pressure and Mach number through:

$$OAPWL = OASPL + 9.9 + 10 \log_{10} A + 10 \log_{10} (1 + M_n)^2 + 1o \log_{10} \left(\frac{P_o}{P_s} \sqrt{\frac{T_s}{T_o}} \right)$$

where the area A is the annulus area (in square meters) of the airflow path in the axial plane of the sensing holes of the probe and M_n is the Mach number of the flow through that area. It is assumed in this equation that the acoustic waves strike the probe in a direction normal to the tip. This is most likely the case in the combustor environment where the wavelengths of the noise being evaluated are several times the annulus passage height dimension.

The calculated overall power levels can be compared to engine data by plotting them against a correlating parameter.

$$OAPWL = K + 10 \log_{10} \left[\dot{W} (T_4 - T_3)^2 \left(\frac{\rho_3}{\rho_o} \right)^2 \right]$$

This parameter was derived from the evaluation (Reference 4) of noise from a T64 turboshaft engine. The three lines drawn through the data (Figure 43) represent the observed (References 5,6) trend differences from the evaluation of turbojet, turboshaft, and turbofan engine types. The distance between the lines is attributed to the differing amounts of attenuation of combustor noise

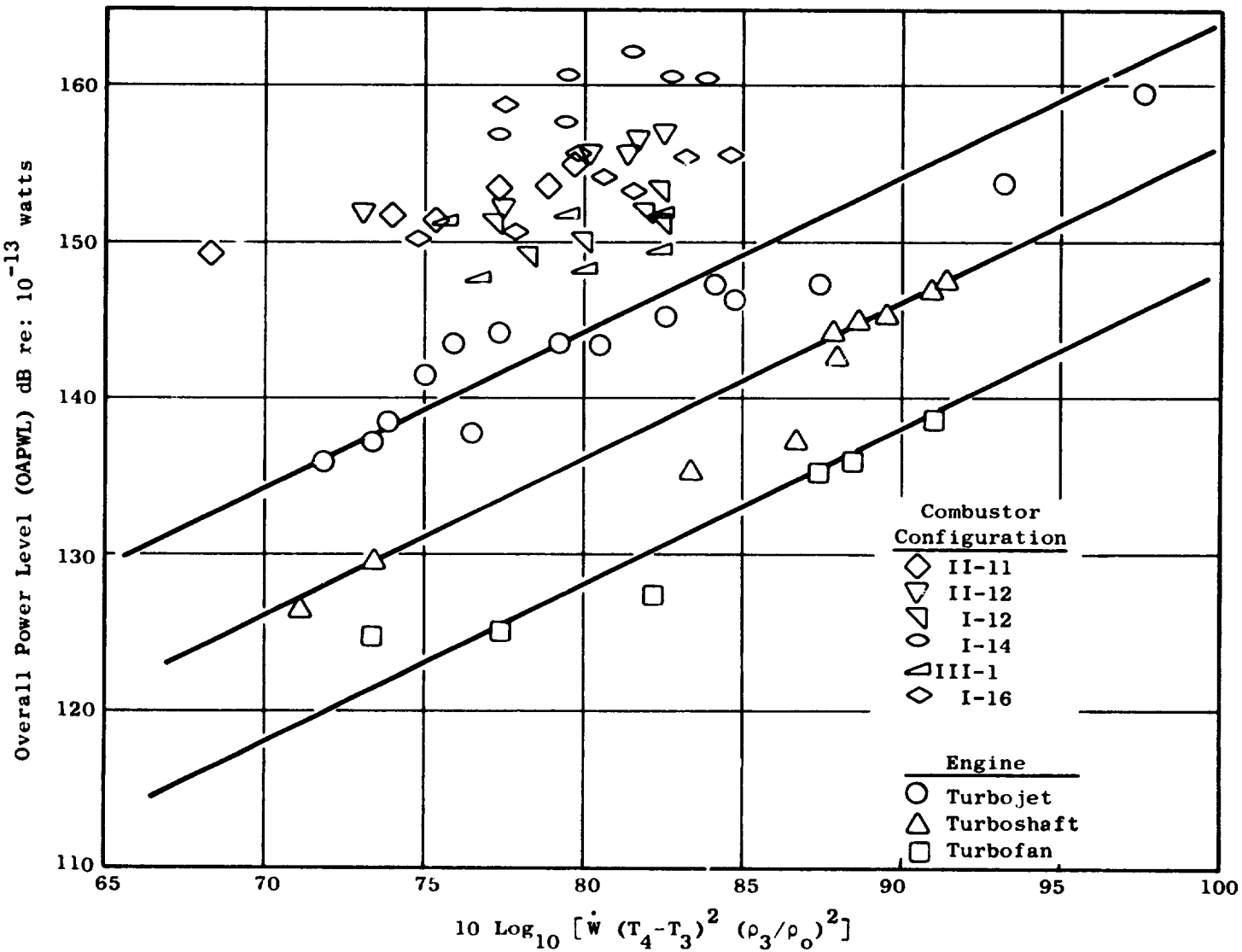

Figure 43. Engine Combustor Noise Power Level Prediction.

along the propagation path through the turbine stages, exhaust duct and nozzle to the farfield where the engine levels were measured. Therefore, three constants k, depending on the engine type being evaluated, are used in this prediction.

A significant difference (over 20 dB) can be seen in the source power levels for these CF6-50 turbofan engine type combustors when compared to the turbofan engine core noise prediction line, as is shown in Figure 43. This reinforces the argument for attenuation of noise along the propagation path through the turbine.

SECTION 7.0

CONCLUSIONS

It has been demonstrated that broadband combustion noise can be measured using waveguide probes. The measured combustor noise one-third octave band sound pressure levels were found to peak between 140 and 150 dB. This is potentially a significant noise source from an aircraft gas turbine. Differences in spectral shape and level were observed for each combustor configuration. The inlet temperature, pressure, airflow rate, and the fuel-air ratio have also been shown to affect the combustor noise signature. However, in an aircraft gas turbine this signature will be modified due to the propagation path it must take to reach the farfield.

Although it has been assumed that the unsteady pressure signal measured by the probe is an acoustic pressure only, it remains to verify this assumption.

APPENDIX A

NARROWBAND SPECTRA

Selected 10 Hz bandwidth spectrums from each configuration can be seen in Figures 44 to 67. The narrowband spectra have not been corrected for either probe loss or local temperature or pressure.

During some of the tests, there was an intermittent 60 Hz electrical signal and, at times, its harmonics occurred in the spectra. The data recorded during the testing of Configuration I-14 contained the greatest amount of 60 Hz contamination. These electrically caused spikes and their harmonics produced inaccurate one-third octave band levels when they occurred. Some of the one-third octave band data presented in this report have been corrected for these spikes. The correction involved examining the 10 Hz narrowband spectra and calculating the one-third octave band levels using a bandwidth adjustment for the broadband levels obtained by fairing out the 60 Hz signals (Figure 68). This correction was performed for all of the data from Configurations II-11 and I-14. It was also performed for Configuration II-12 (with the exception of readings 510, 525 and the downstream signal of reading 526) and for Configuration I-12 data (with the exception of readings 542, 545 and the downstream signals of readings 543, 549 and 559). This correction was not necessary for Configurations II-1 and I-16 (reading numbers 776 to 806). Special wiring was installed which minimized the problem for those configurations.

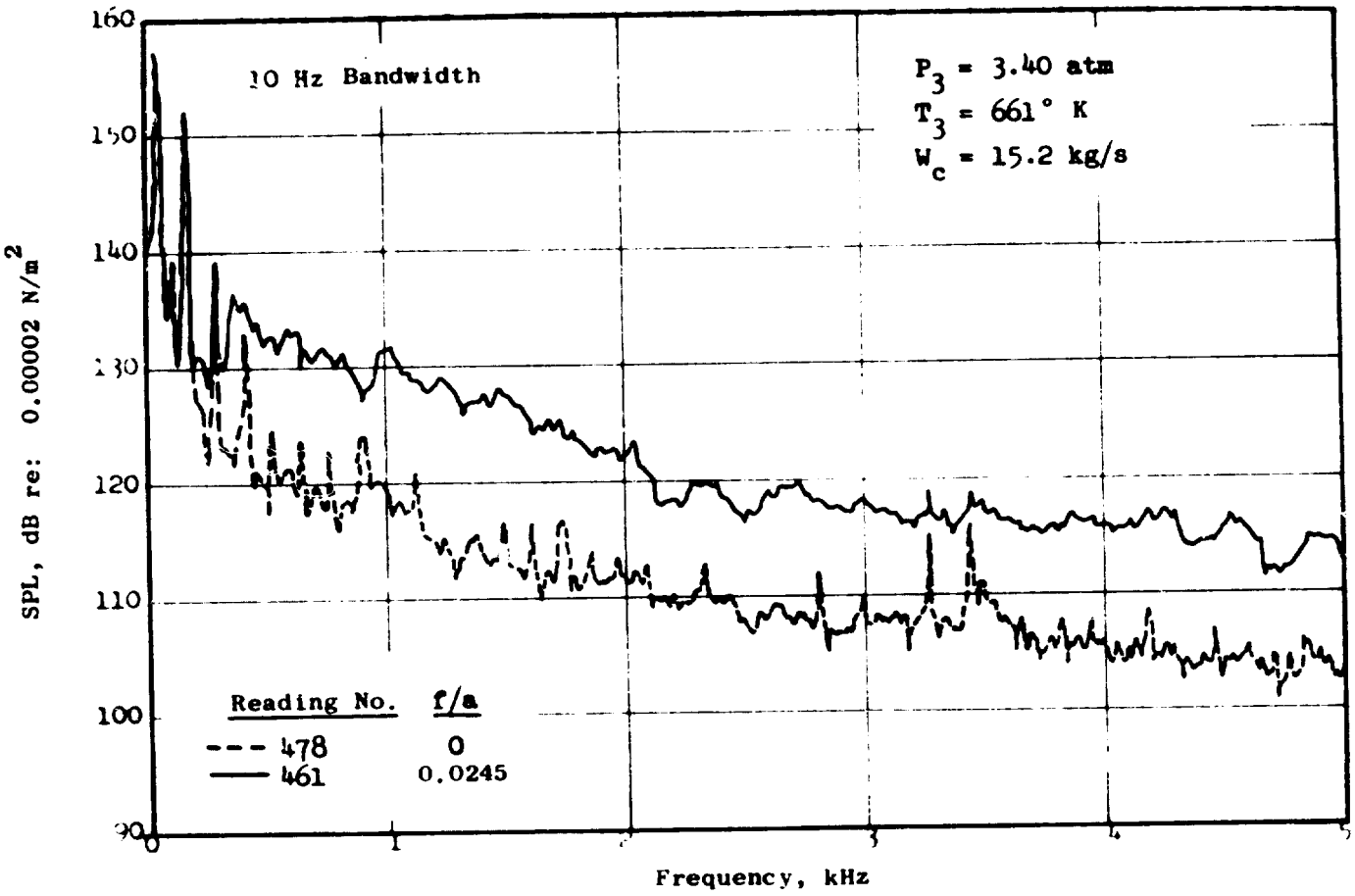

Figure 44. Comparison of Narrowband Spectra for Two Fuel-Air Ratios at Approach Inlet Conditions, Double Annular Combustor, Configuration II-11, Downstream Probe.

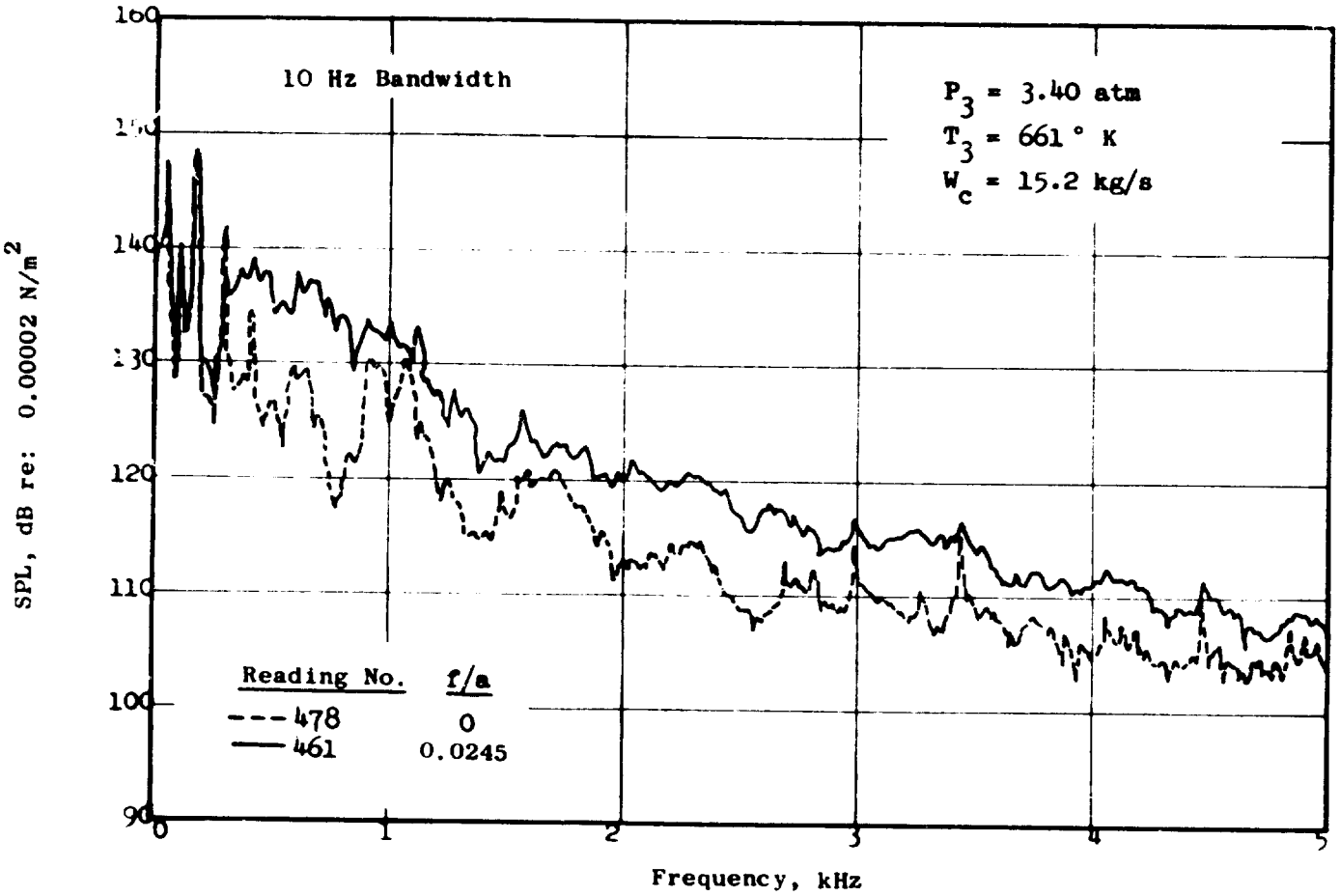

Figure 45. Comparison of Narrowband Spectra for Two Fuel-Air Ratios at Approach Inlet Conditions, Double Annular Combustor, Configuration II-11, Upstream Probe.

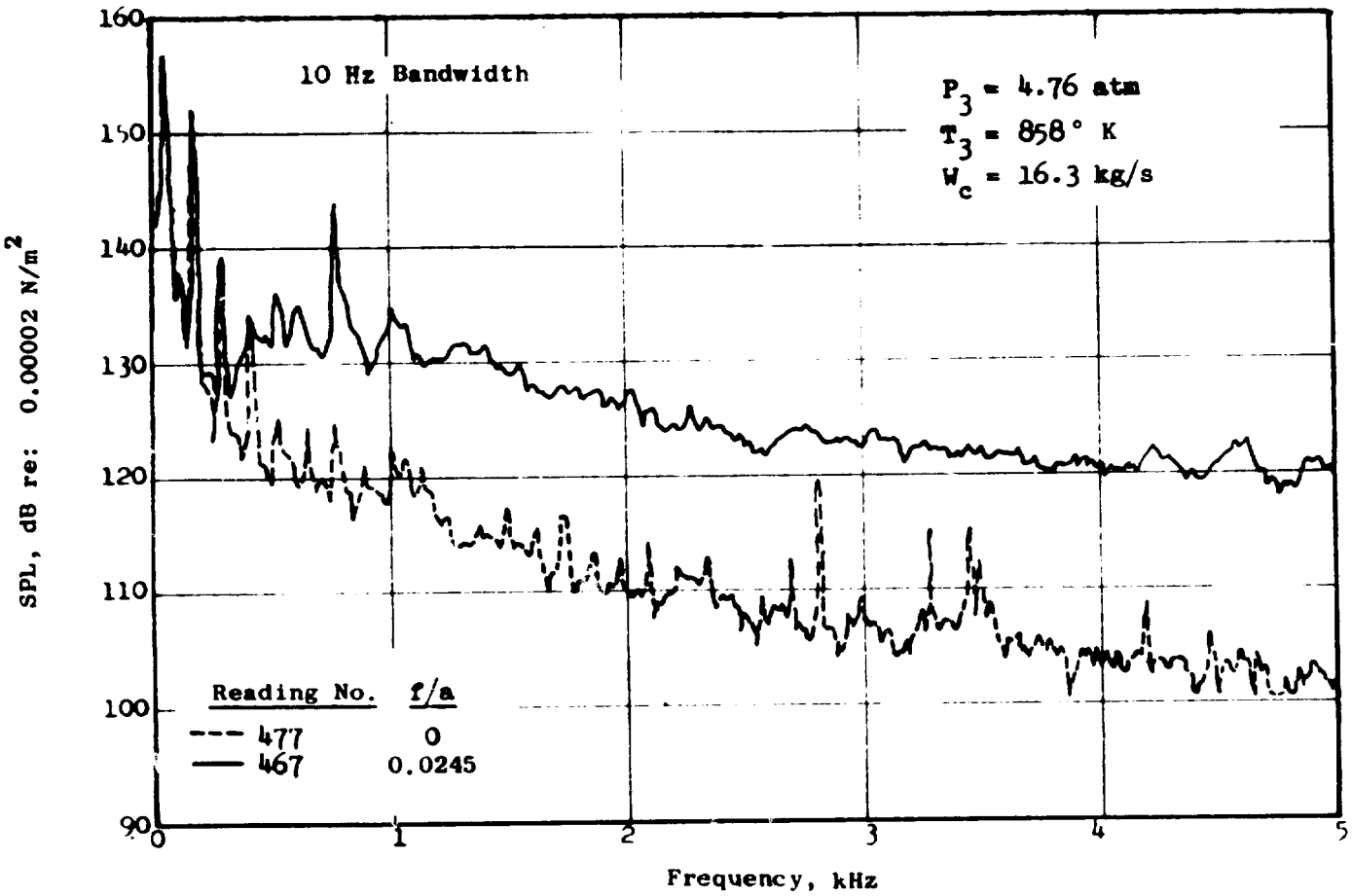

Figure 46. Comparison of Narrowband Spectra for Two Fuel-Air Ratios at Takeoff Inlet Conditions, Double Annular Combustor, Configuration II-11, Downstream Probe.

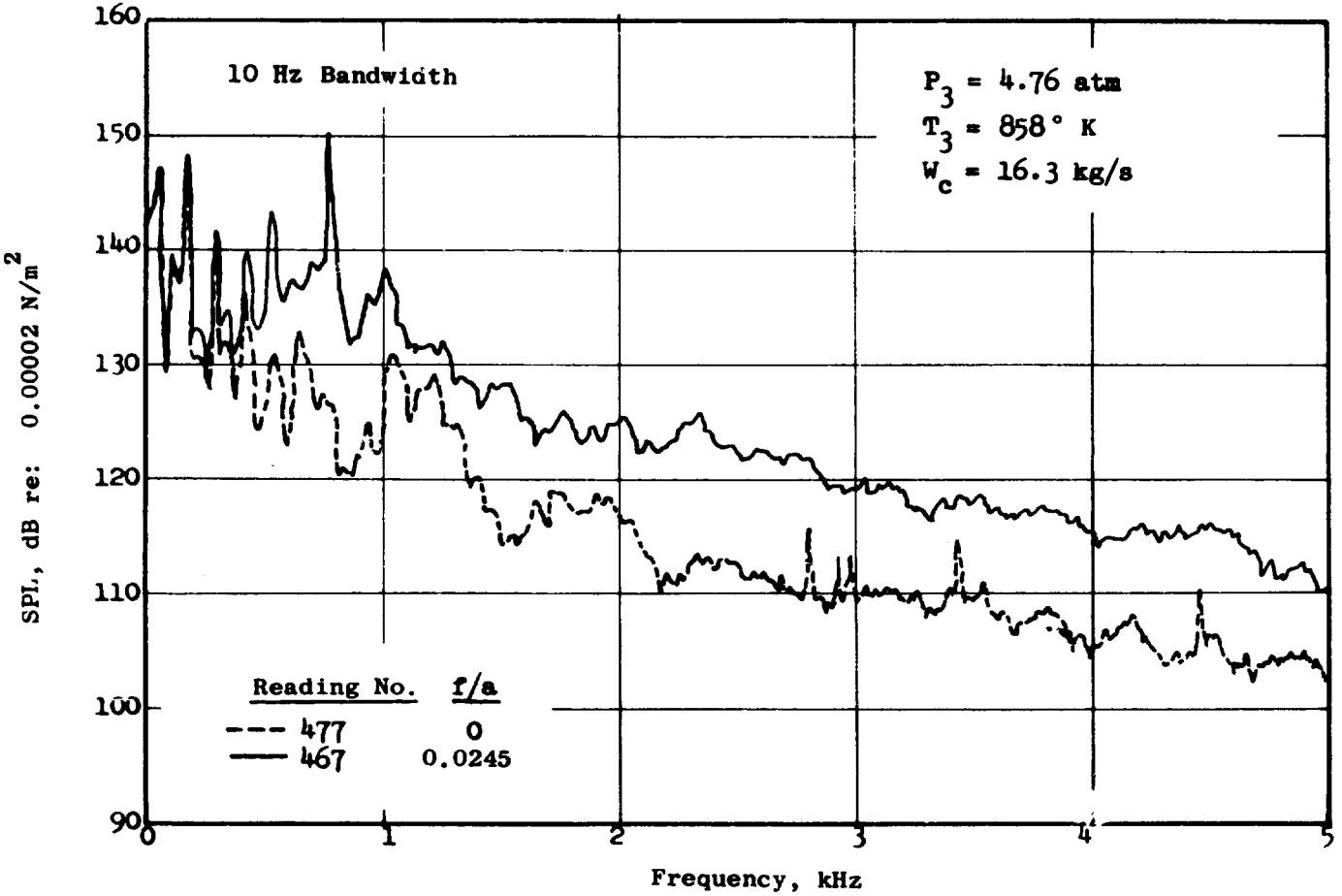

Figure 47. Comparison of Narrowband Spectra for Two Fuel-Air Ratios at Takeoff Inlet Conditions, Double Annular Combustor, Configuration II-11, Upstream Probe.

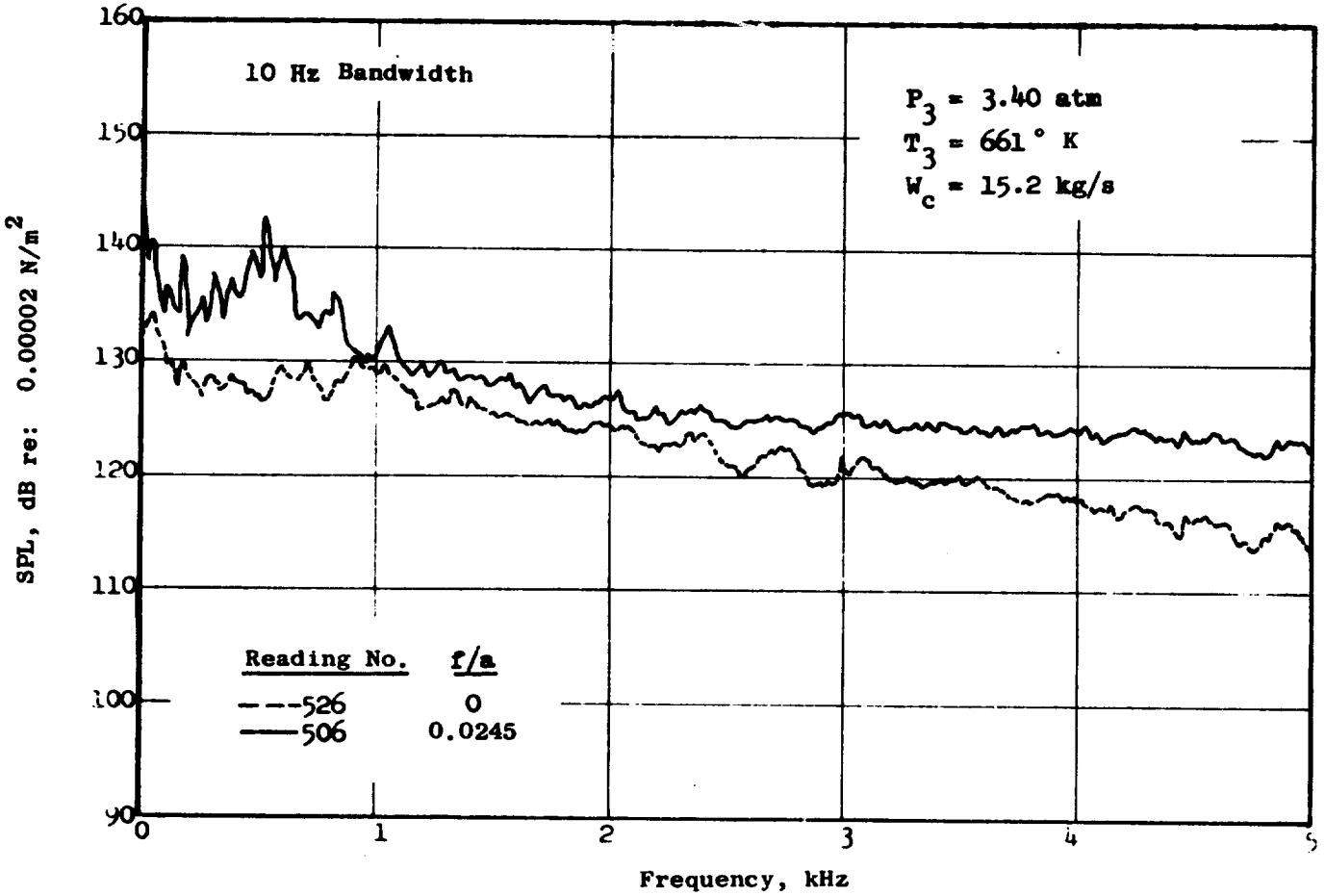

Figure 48. Comparison of Narrowband Spectra for Two Fuel-Air Ratios at Approach Inlet Conditions, Radial/Axial Staged Combustor, Configuration II-12, Downstream Probe.

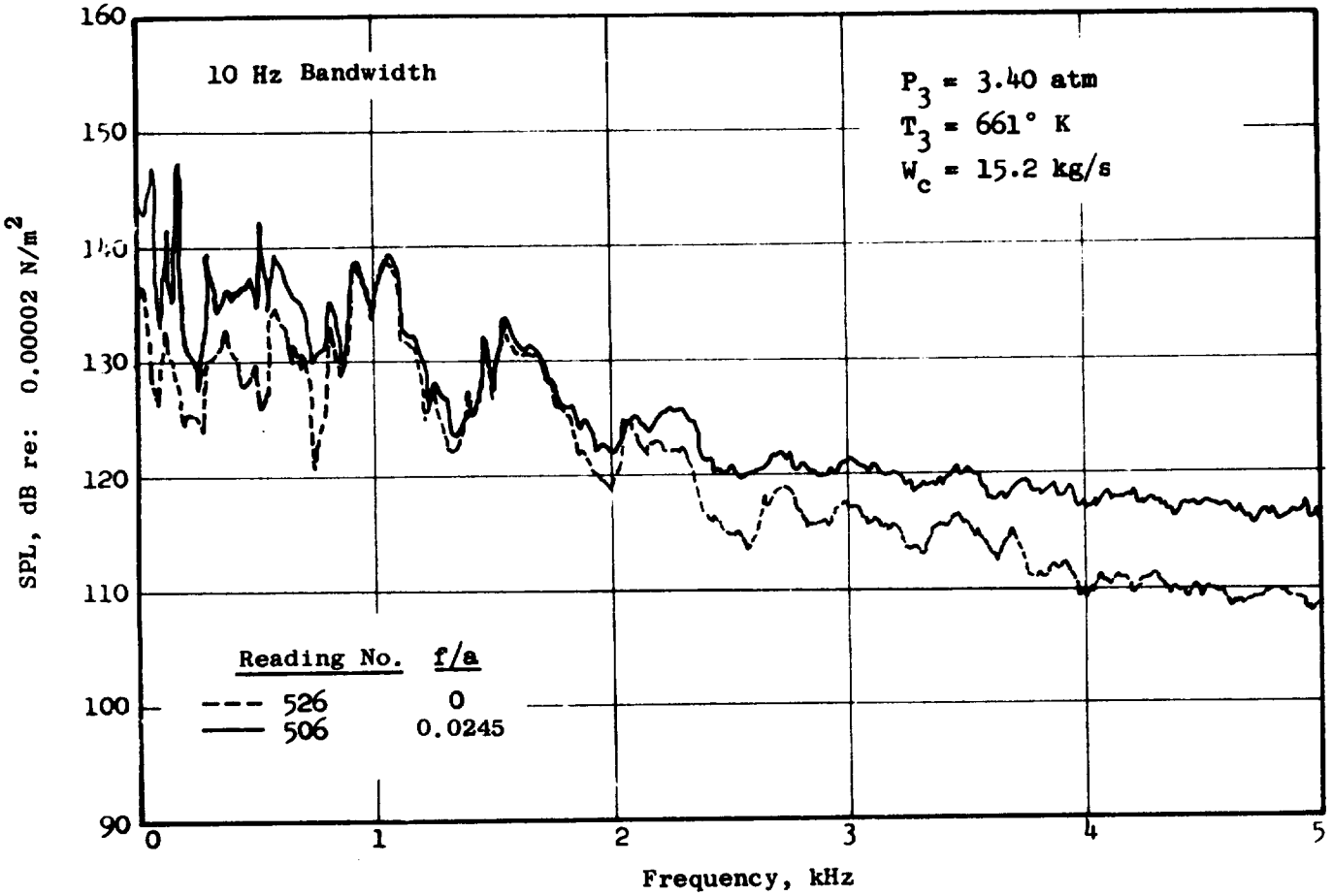

Figure 49. Comparison of Narrowband Spectra for Two Fuel-Air Ratios at Approach Inlet Conditions, Radial/Axial Staged Combustor, Configuration II-12, Upstream Probe.

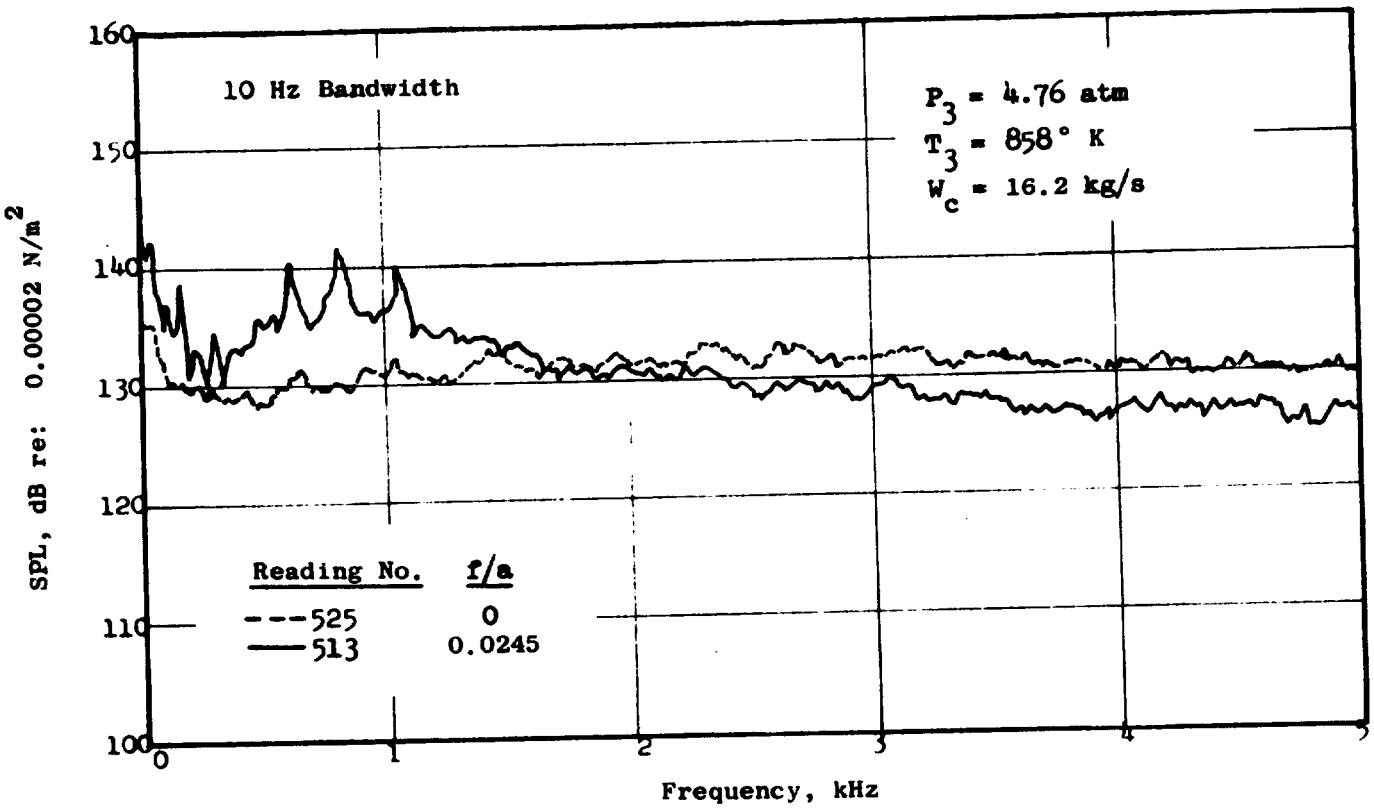

Figure 50. Comparison of Narrowband Spectra for Two Fuel-Air Ratios at Takeoff Inlet Conditions, Radial/Axial Staged Combustor, Configuration II-12, Downstream Probe.

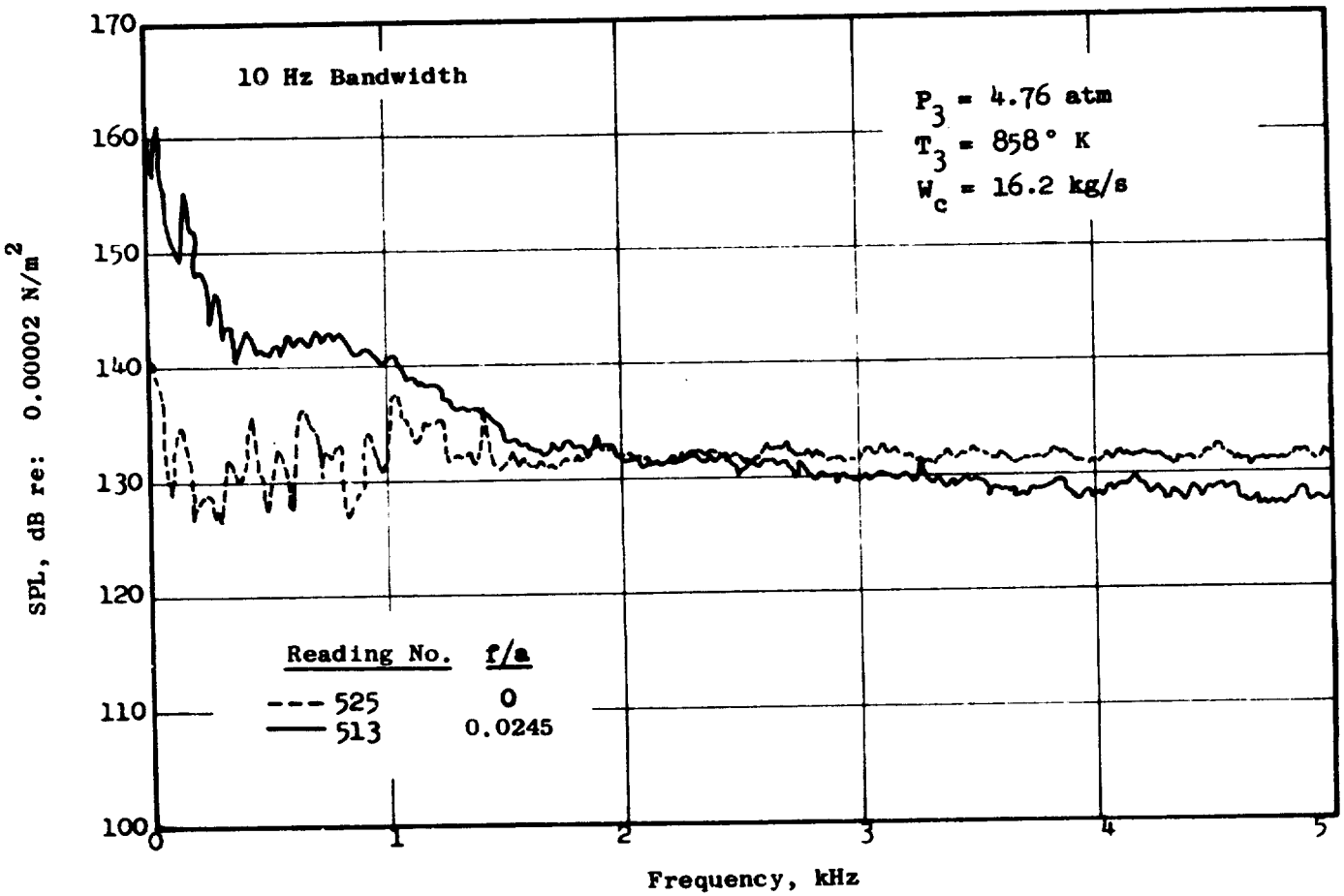

Figure 51. Comparison of Narrowband Spectra for Two Fuel-Air Ratios at Takeoff Inlet Conditions, Radial/Axial Staged Combustor, Configuration II-12, Upstream Probe.

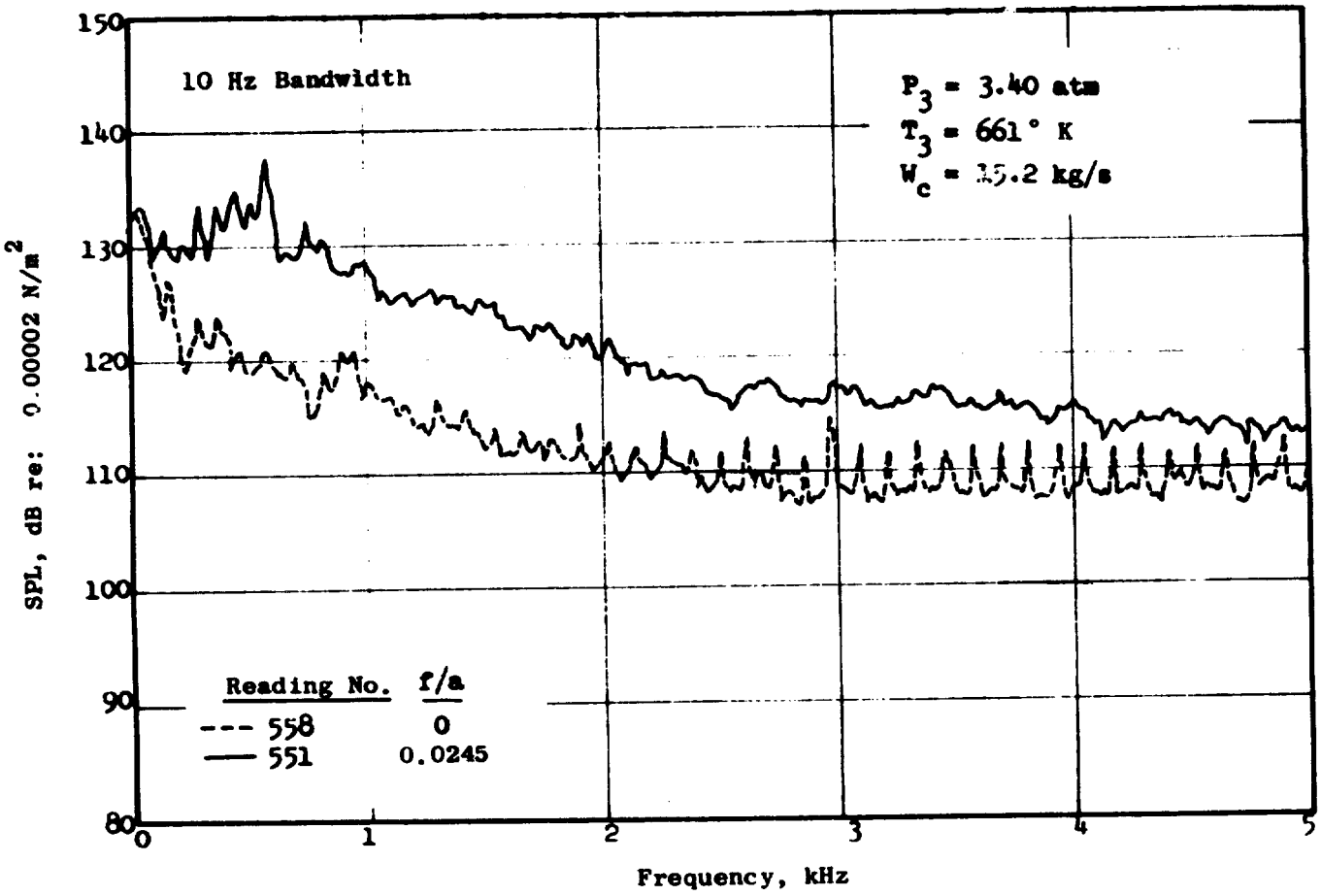

Figure 52. Comparison of Narrowband Spectra for Two Fuel-Air Ratios at Approach Inlet Conditions, 90-Swirl-Can/Sheltered Flameholder, Configuration I-12, Downstream Probe.

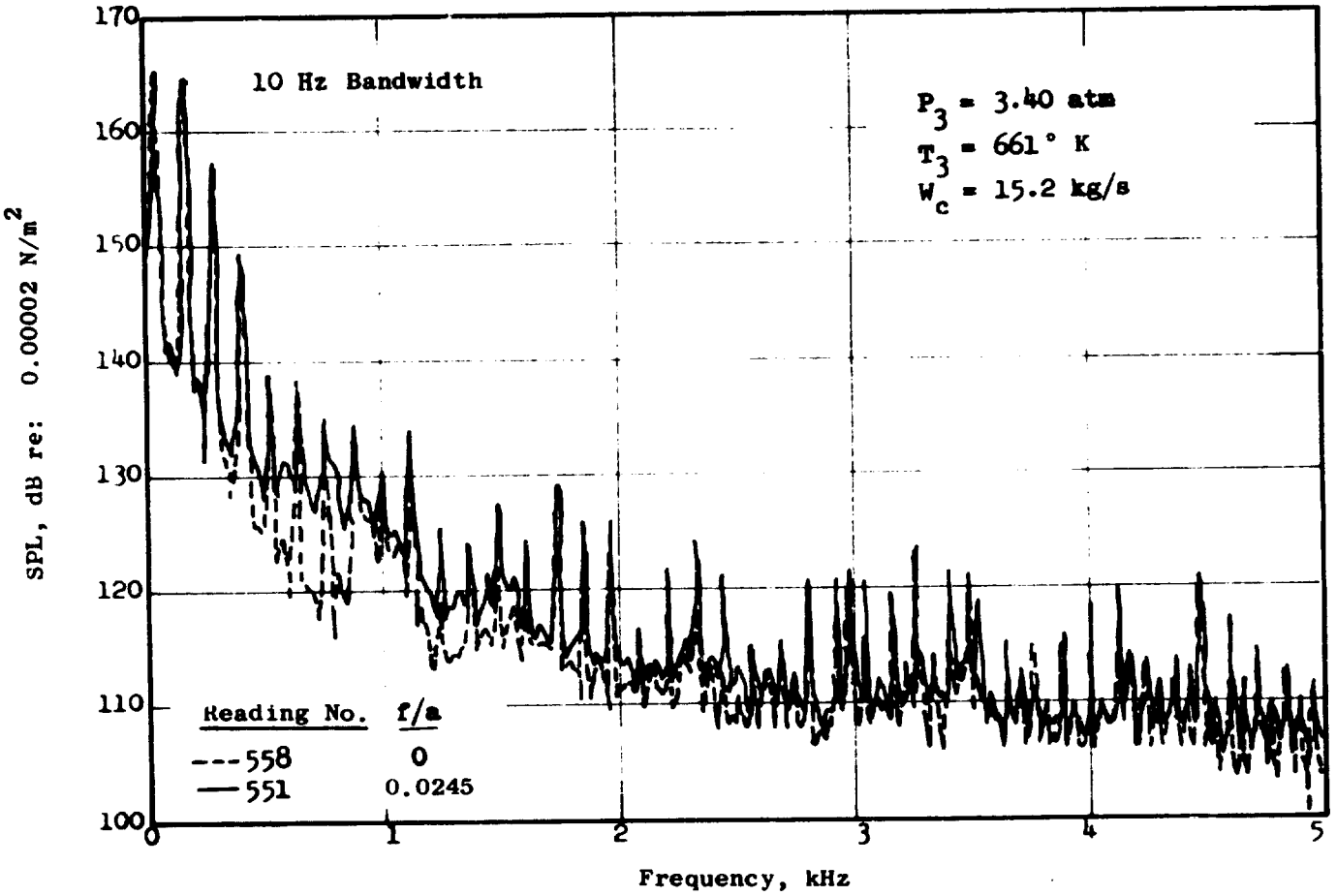

Figure 53. Comparison of Narrowband Spectra for Two Fuel-Air Ratios at Approach Inlet Conditions, 90-Swirl-Can/Sheltered Flameholder, Configuration I-12, Upstream Probe.

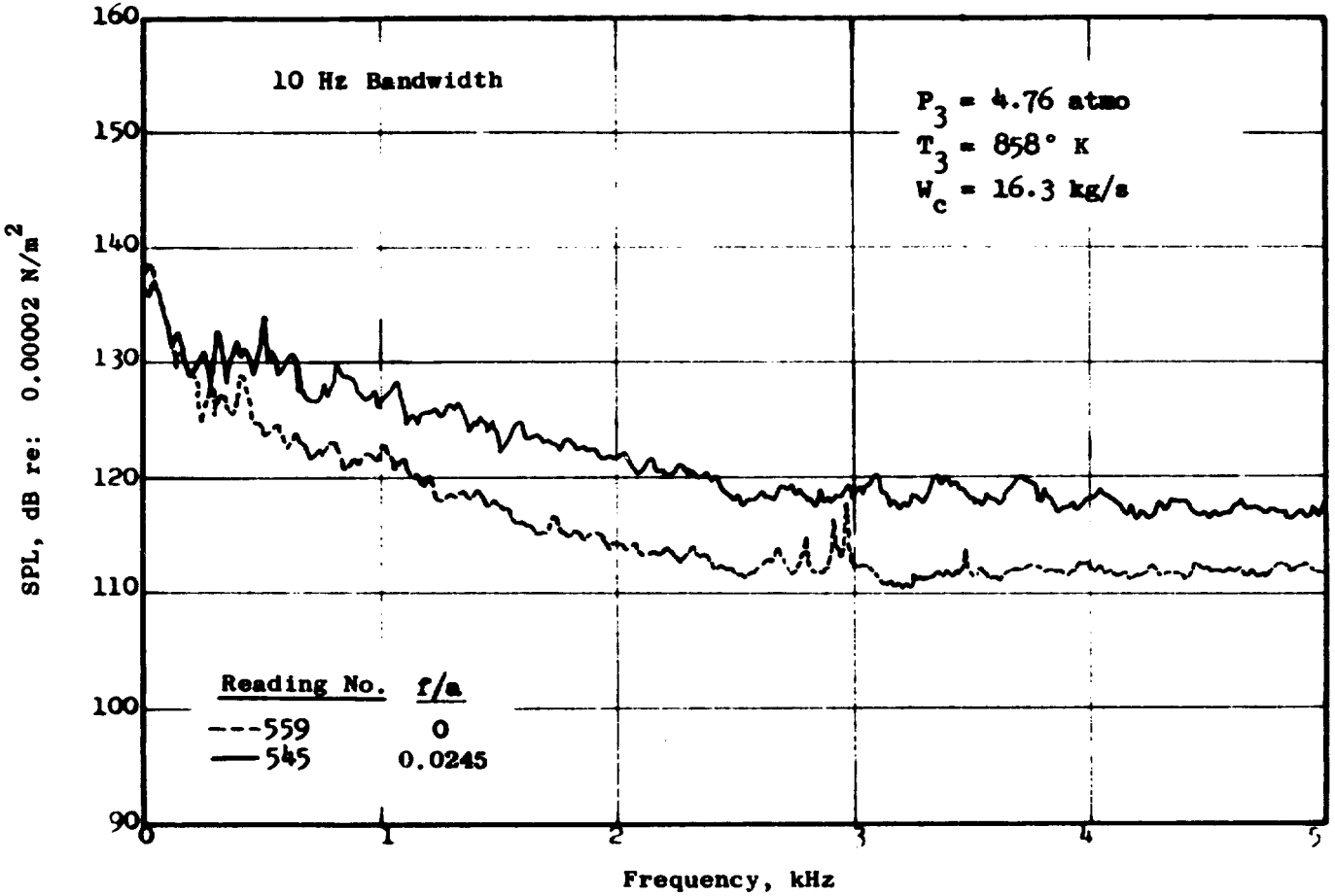

Figure 54. Comparison of Narrowband Spectra for Two Fuel-Air Ratios at Takeoff Inlet Conditions, 90-Swirl-Can/Sheltered Flameholder, Configuration I-12, Downstream Probe.

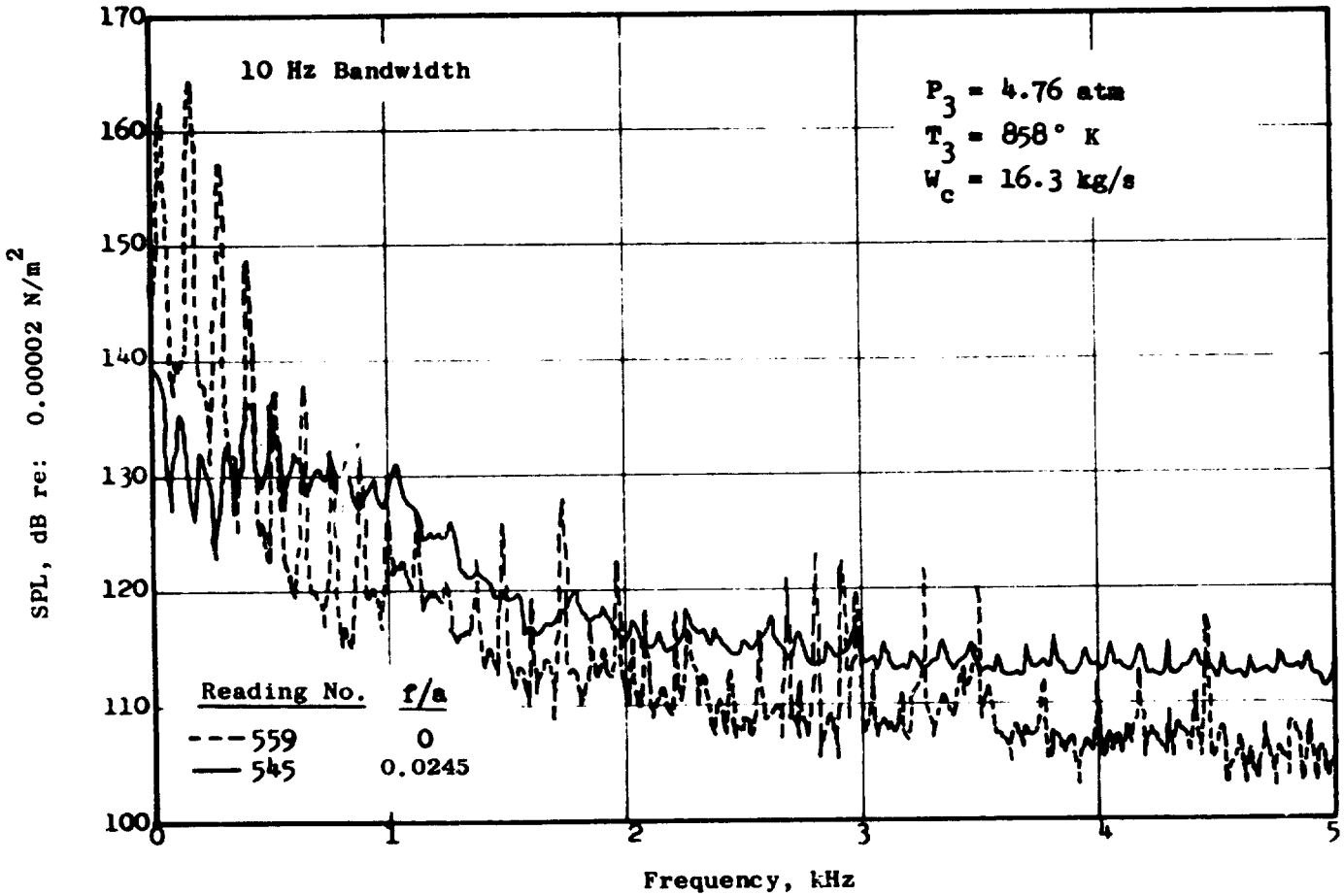

Figure 55. Comparison of Narrowband Spectra for Two Fuel-Air Ratios at Takeoff Inlet Conditions, 90-Swirl-Can/Sheltered Flameholder, Configuration I-12, Upstream Probe.

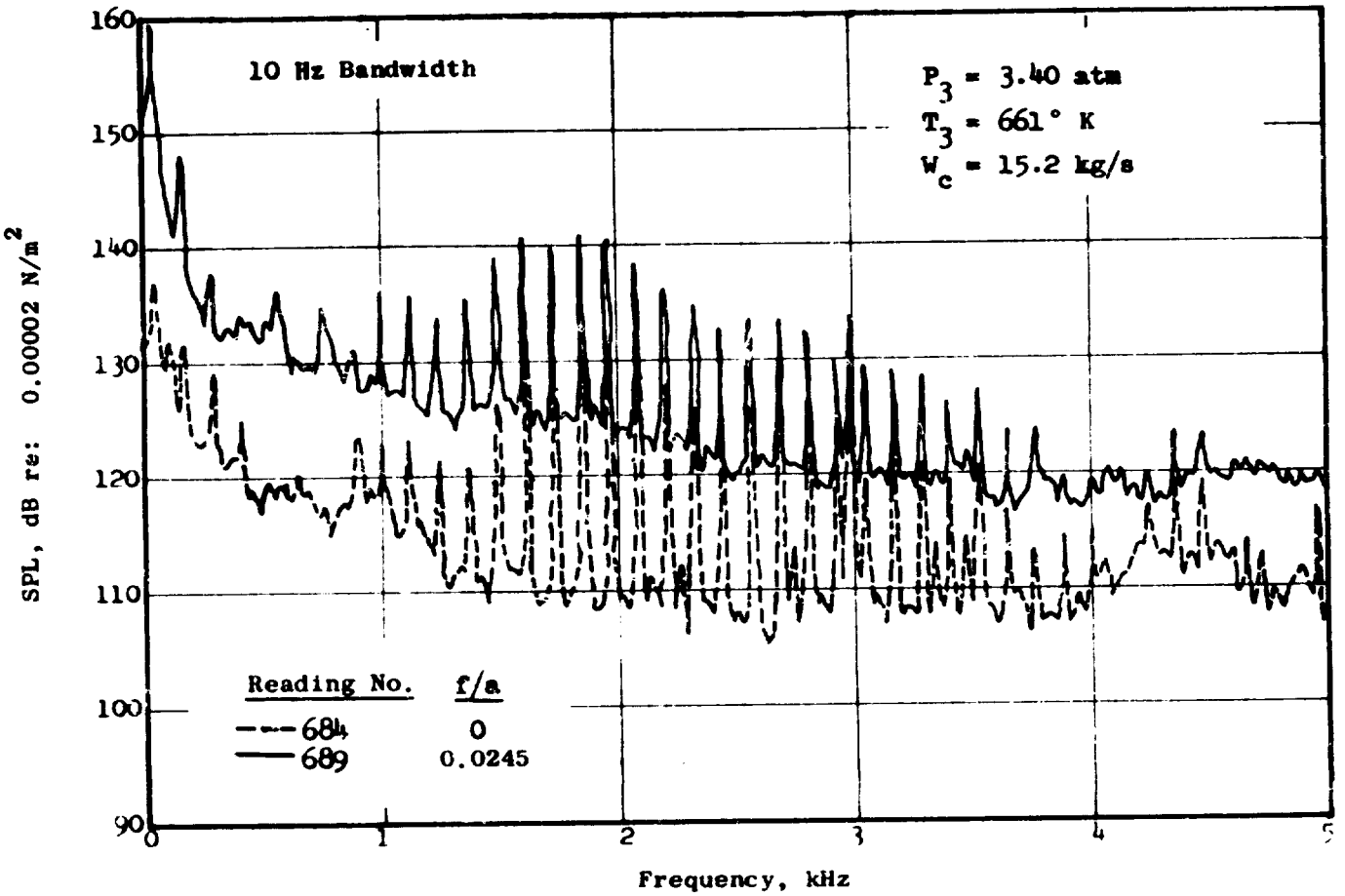

Figure 56. Comparison of Narrowband Spectra for Two Fuel-Air Ratios at Approach Inlet Conditions, 90-Swirl-Can/Sheltered Flameholder, Configuration I-14, Downstream Probe.

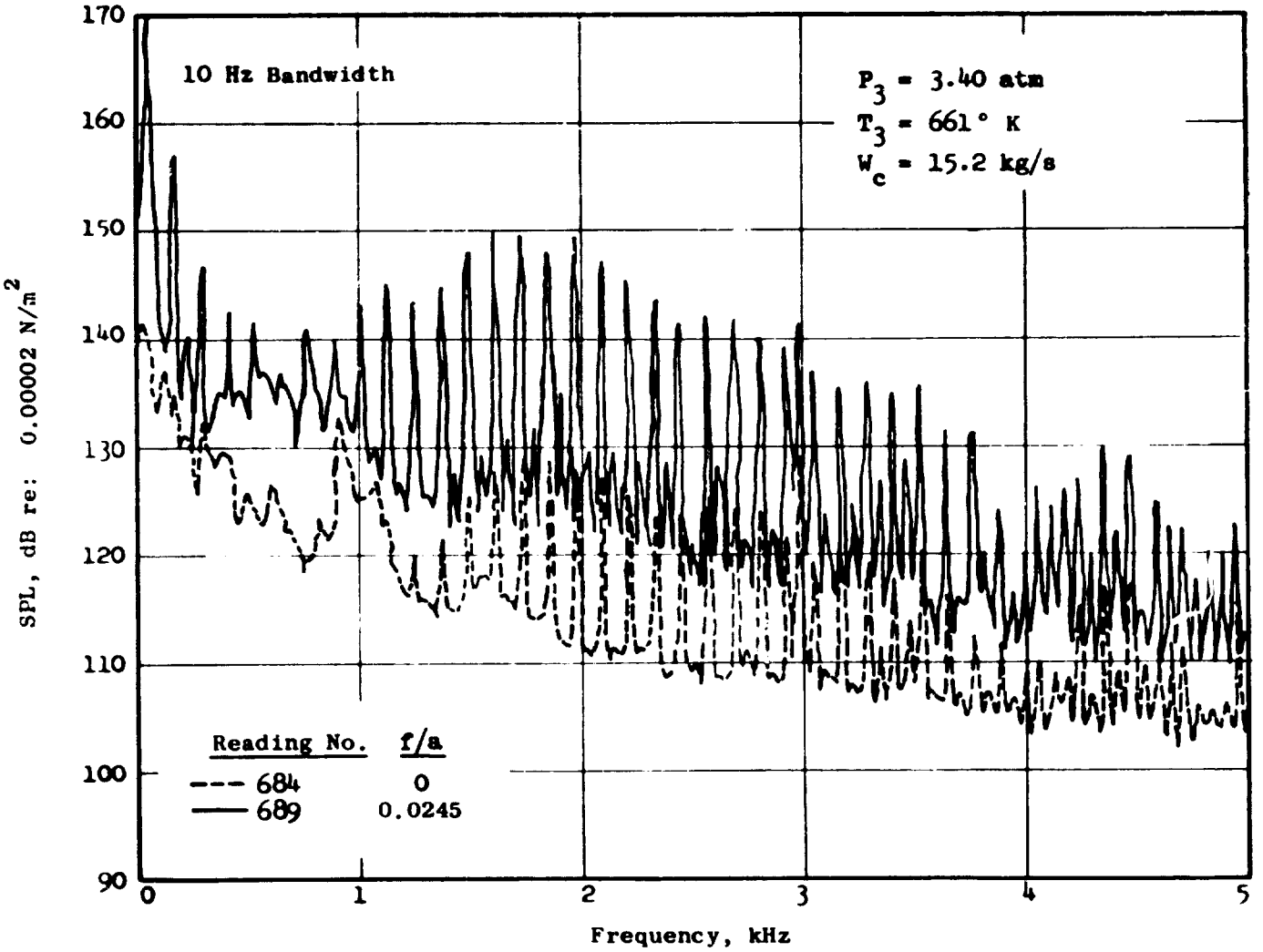

Figure 57. Comparison of Narrowband Spectra for Two Fuel-Air Ratios at Approach Inlet Conditions, 90-Swirl-Can/Sheltered Flameholder, Configuration I-14, Upstream Probe.

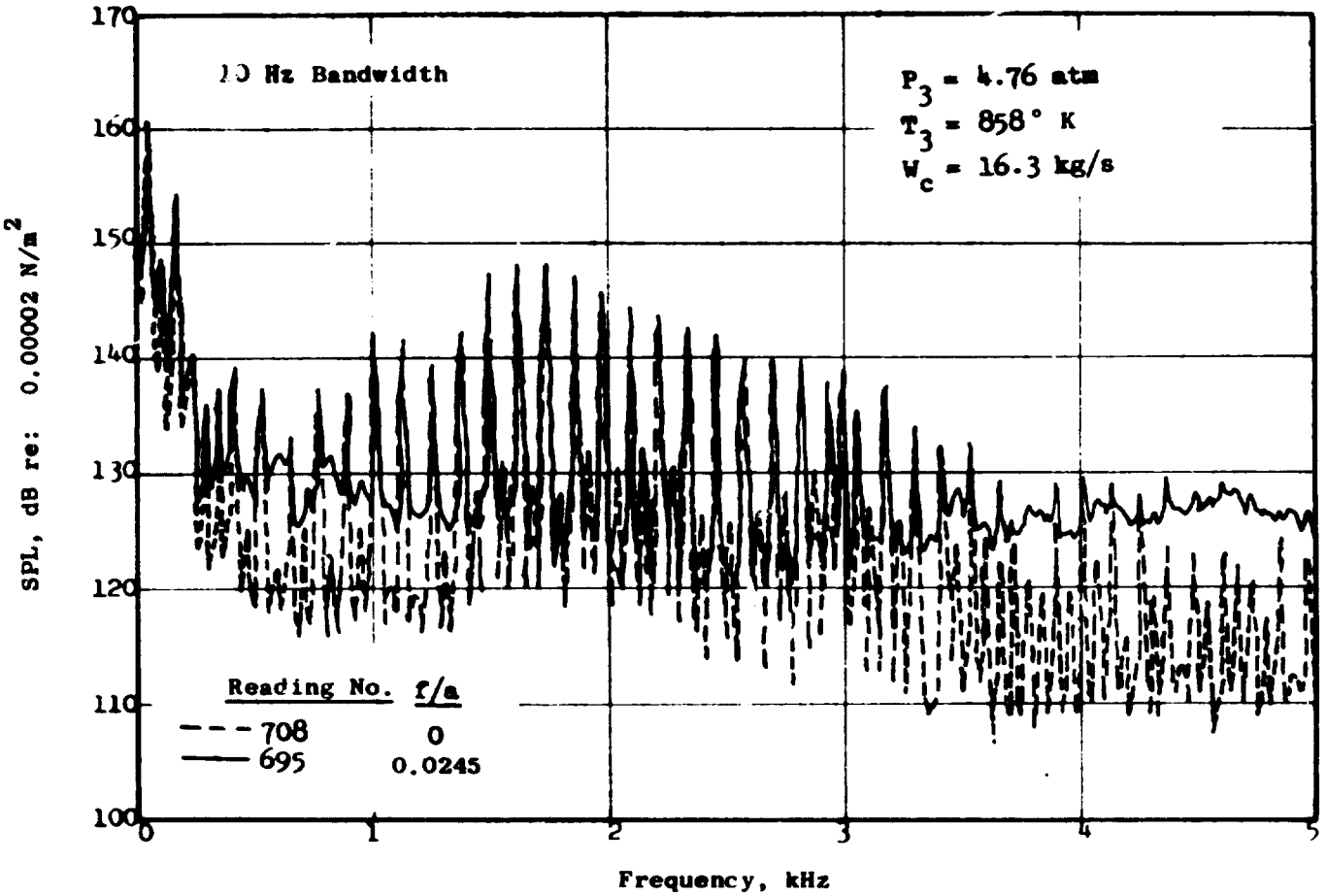

Figure 58. Comparison of Narrowband Spectra for Two Fuel-Air Ratios at Takeoff Inlet Conditions, 90-Swirl-Can/Sheltered Flameholder, Configuration I-14, Downstream Probe.

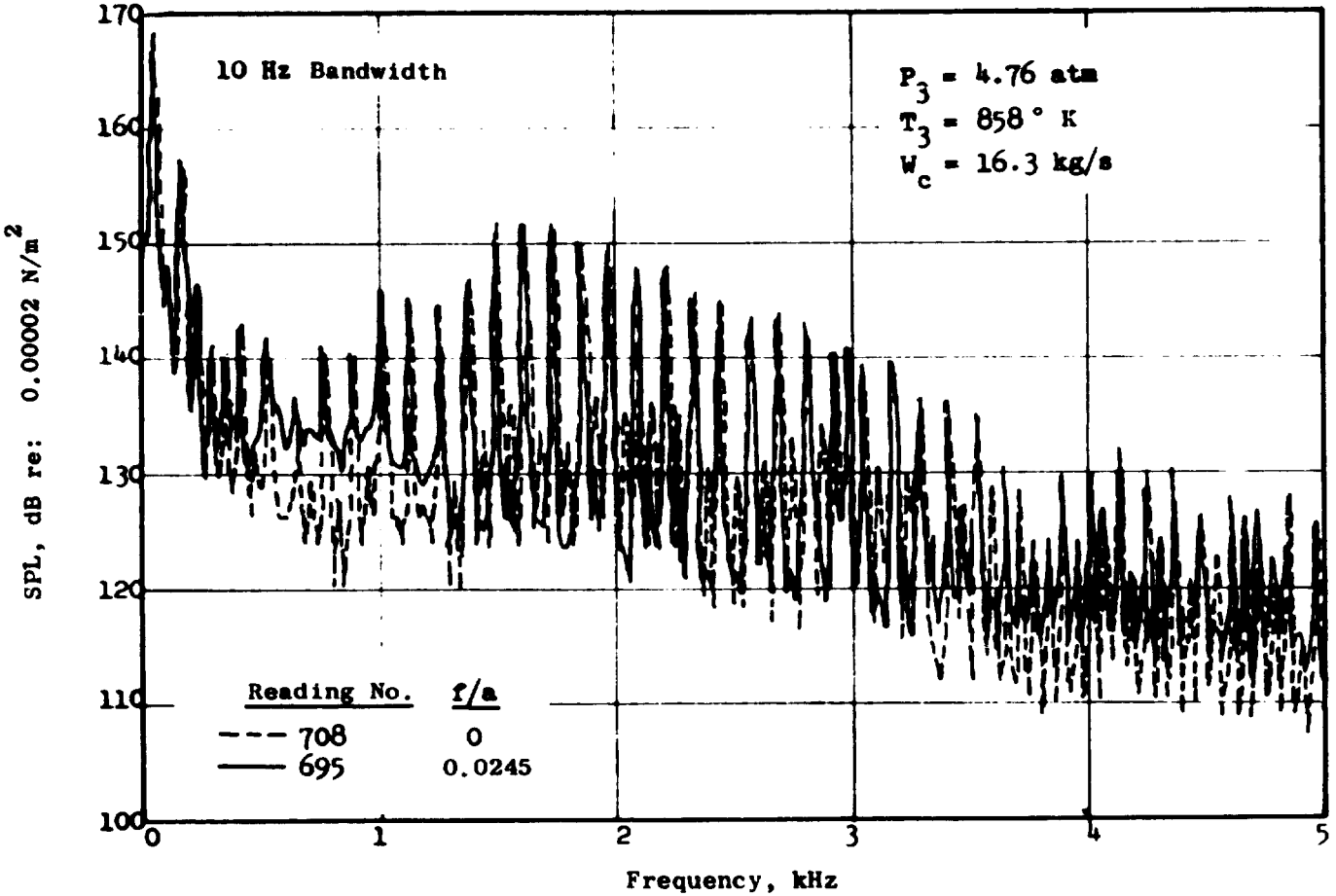

Figure 59. Comparison of Narrowband Spectra for Two Fuel-Air Ratios at Takeoff Inlet Conditions, 90-Swirl-Can/Sheltered Flameholder, Configuration I-14, Upstream Probe.

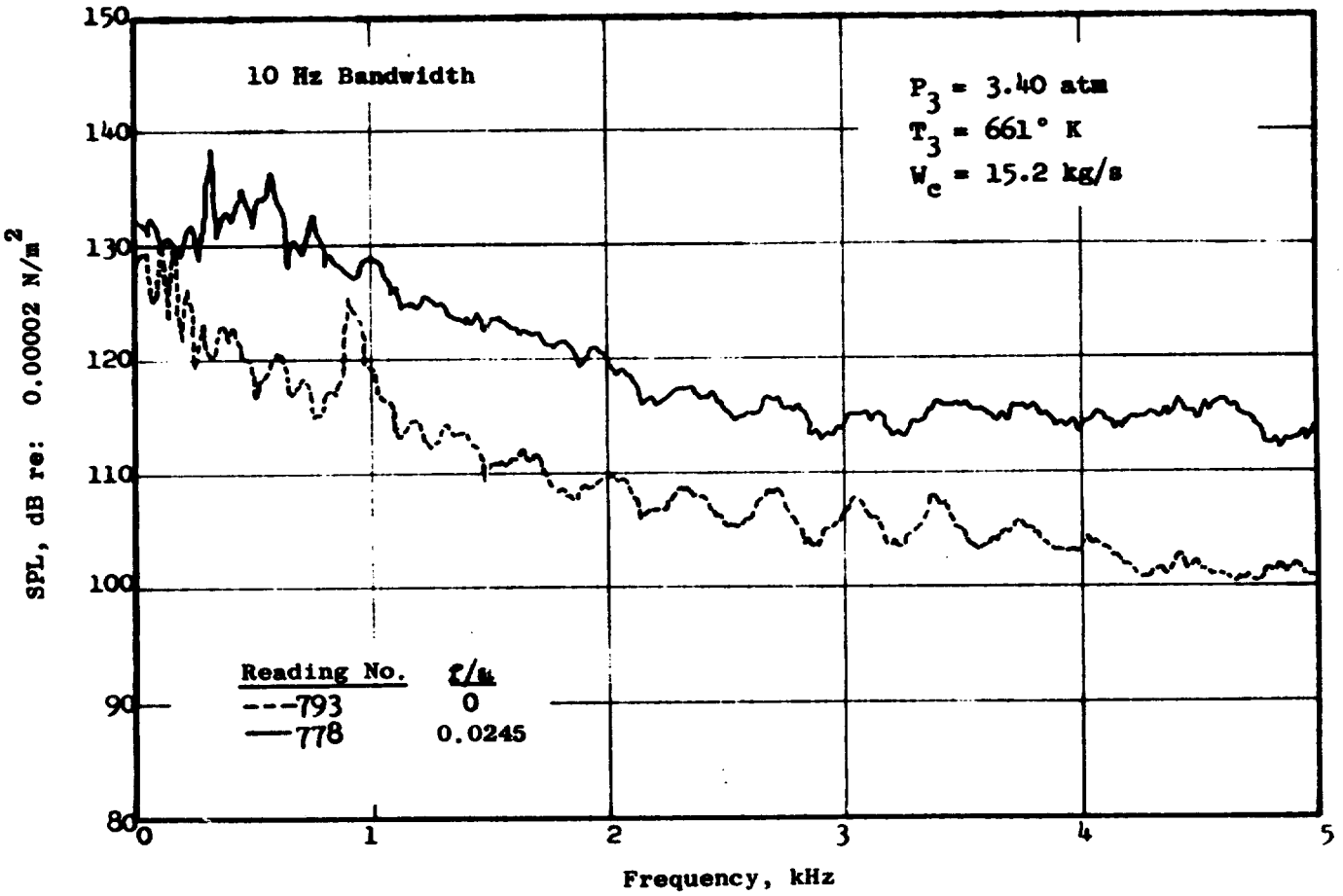

Figure 60. Comparison of Narrowband Spectra for Two Fuel-Air Ratios at Approach Inlet Conditions, 60-Swirl-Can/Slotted Flameholder, Configuration III-1, Downstream Probe.

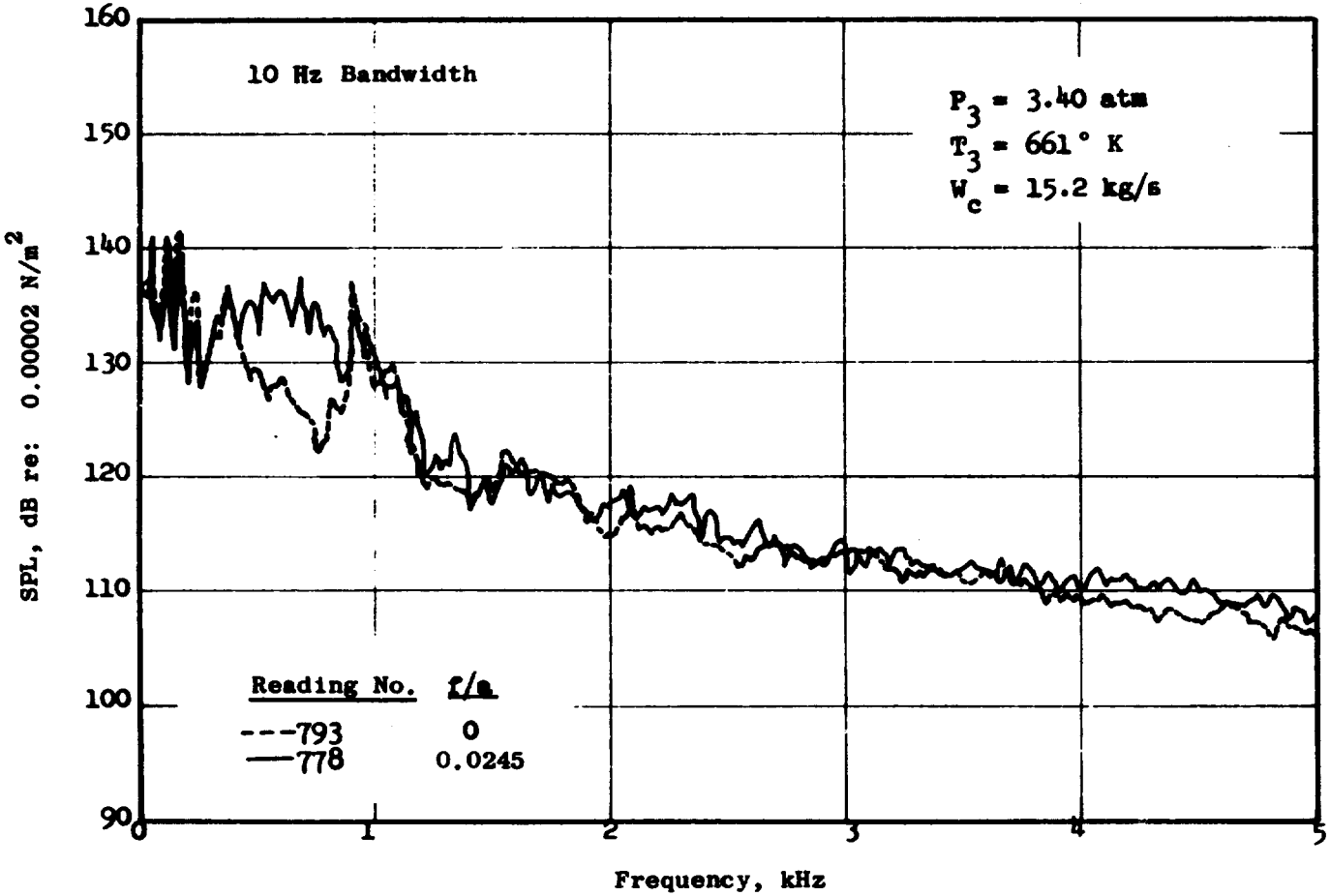

Figure 61. Comparison of Narrowband Spectra for Two Fuel-Air Ratios at Approach Inlet Conditions, 60-Swirl-Can/Slotted Flameholder, Configuration III-1, Upstream Probe.

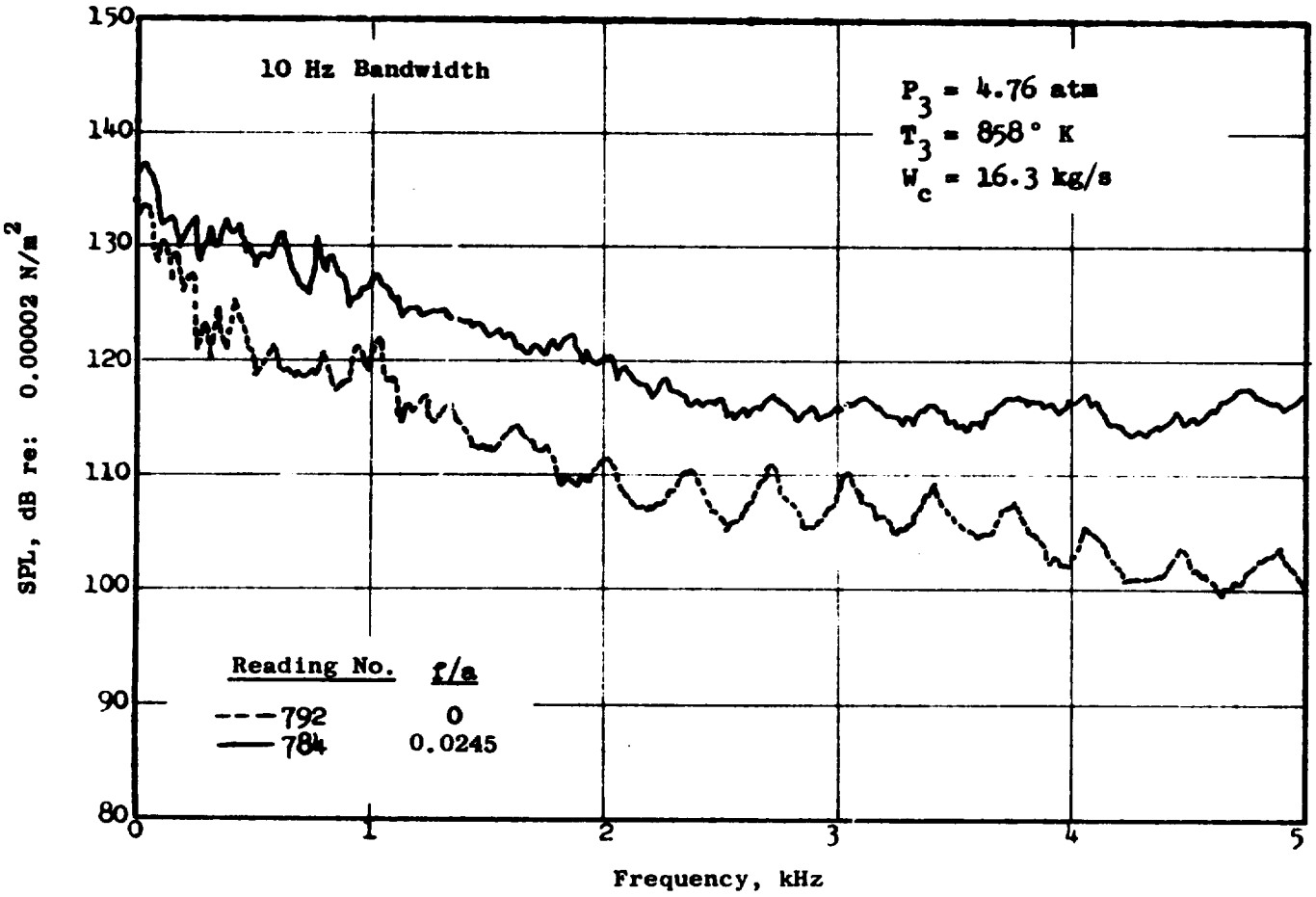

Figure 62. Comparison of Narrowband Spectra for Two Fuel-Air Ratios at Takeoff Inlet Conditions, 60-Swirl-Can/Slotted Flameholder, Configuration III-1, Downstream Probe.

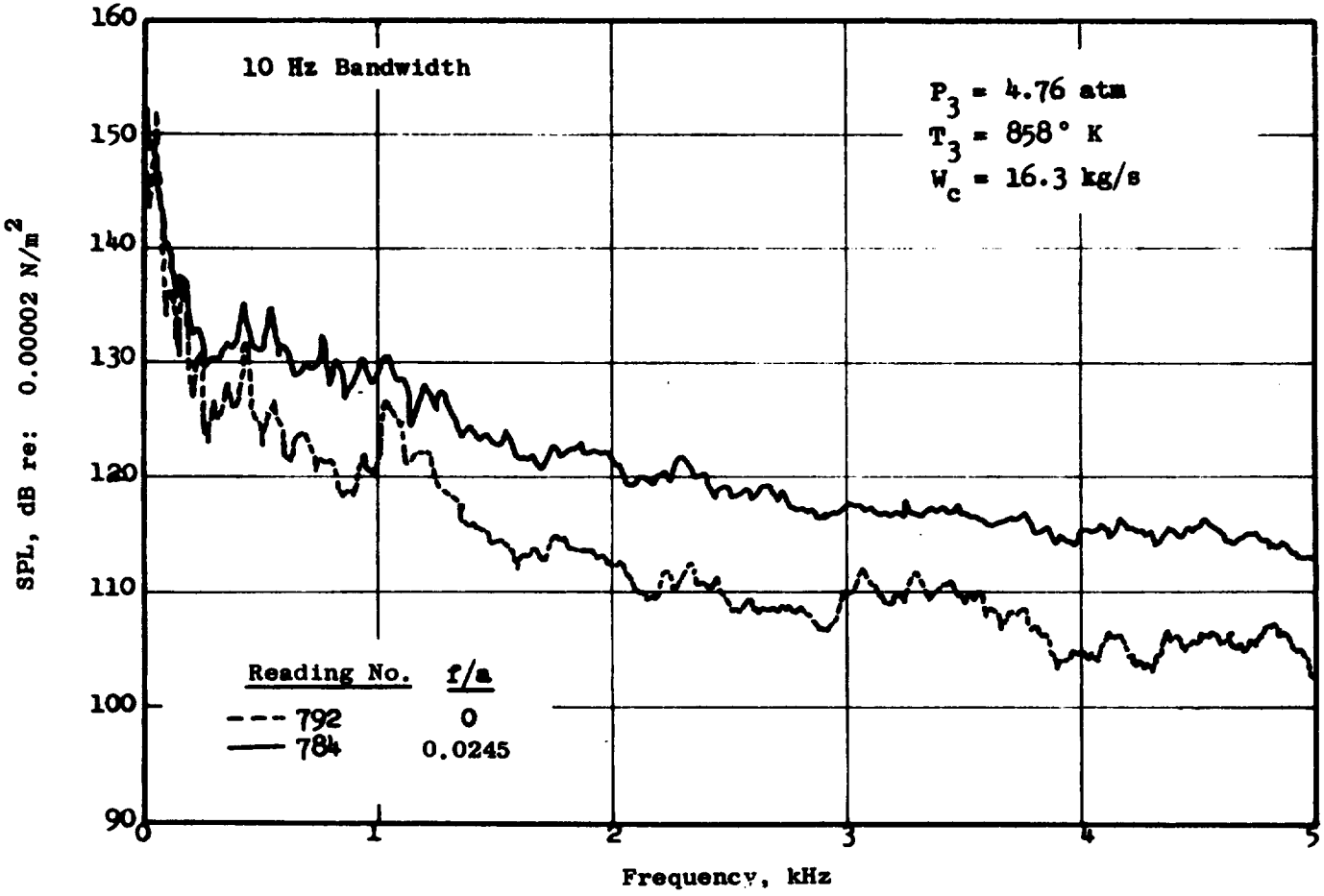

Figure 63. Comparison of Narrowband Spectra for Two Fuel-Air Ratios at Takeoff Inlet Conditions, 60-Swirl-Can/Slotted Flameholder, Configuration III-1, Upstream Probe.

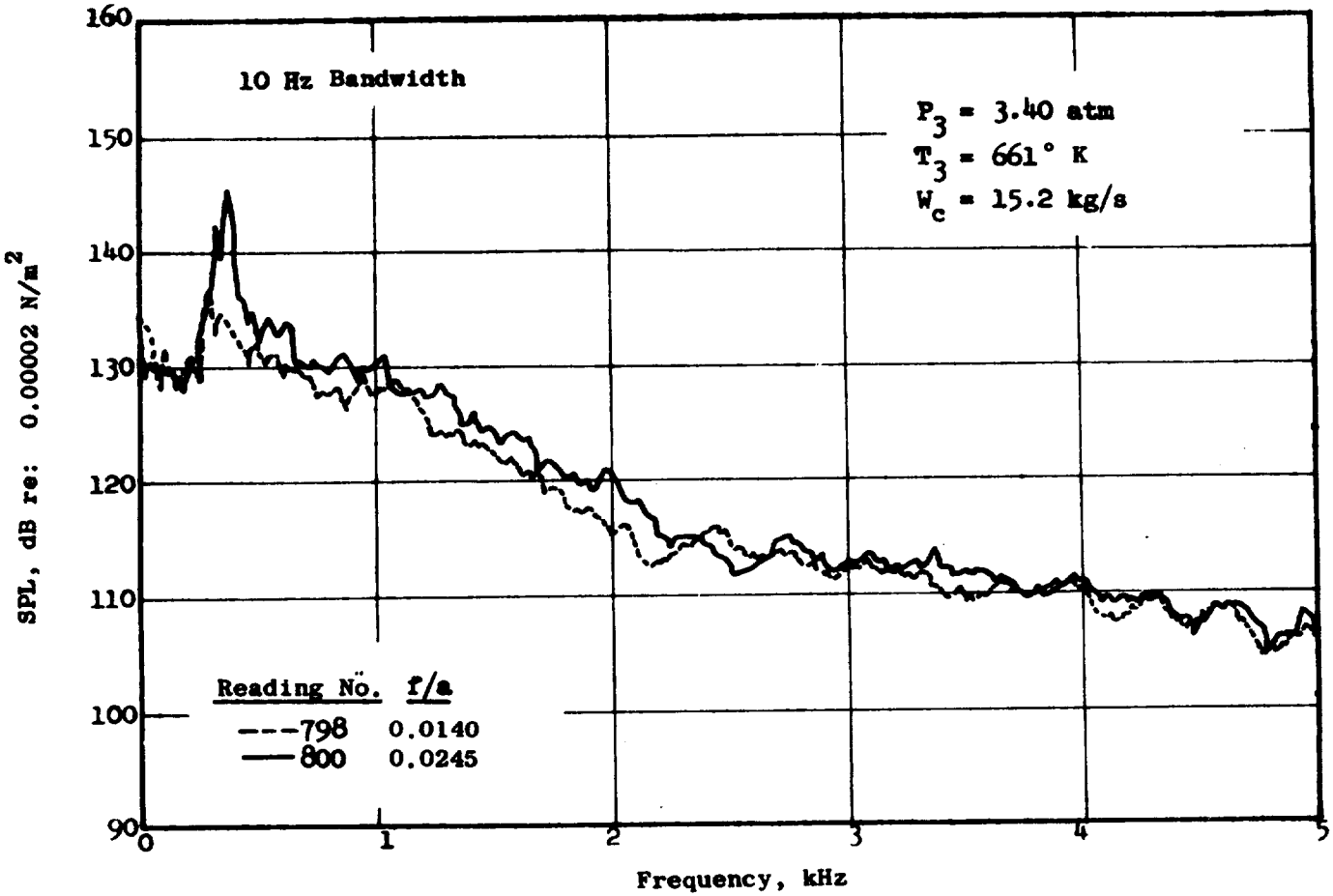

Figure 64. Comparison of Narrowband Spectra for Two Fuel-Air Ratios at Approach Inlet Conditions, 72-Swirl-Can/Counterswirl Flameholder, Configuration I-16, Downstream Probe.

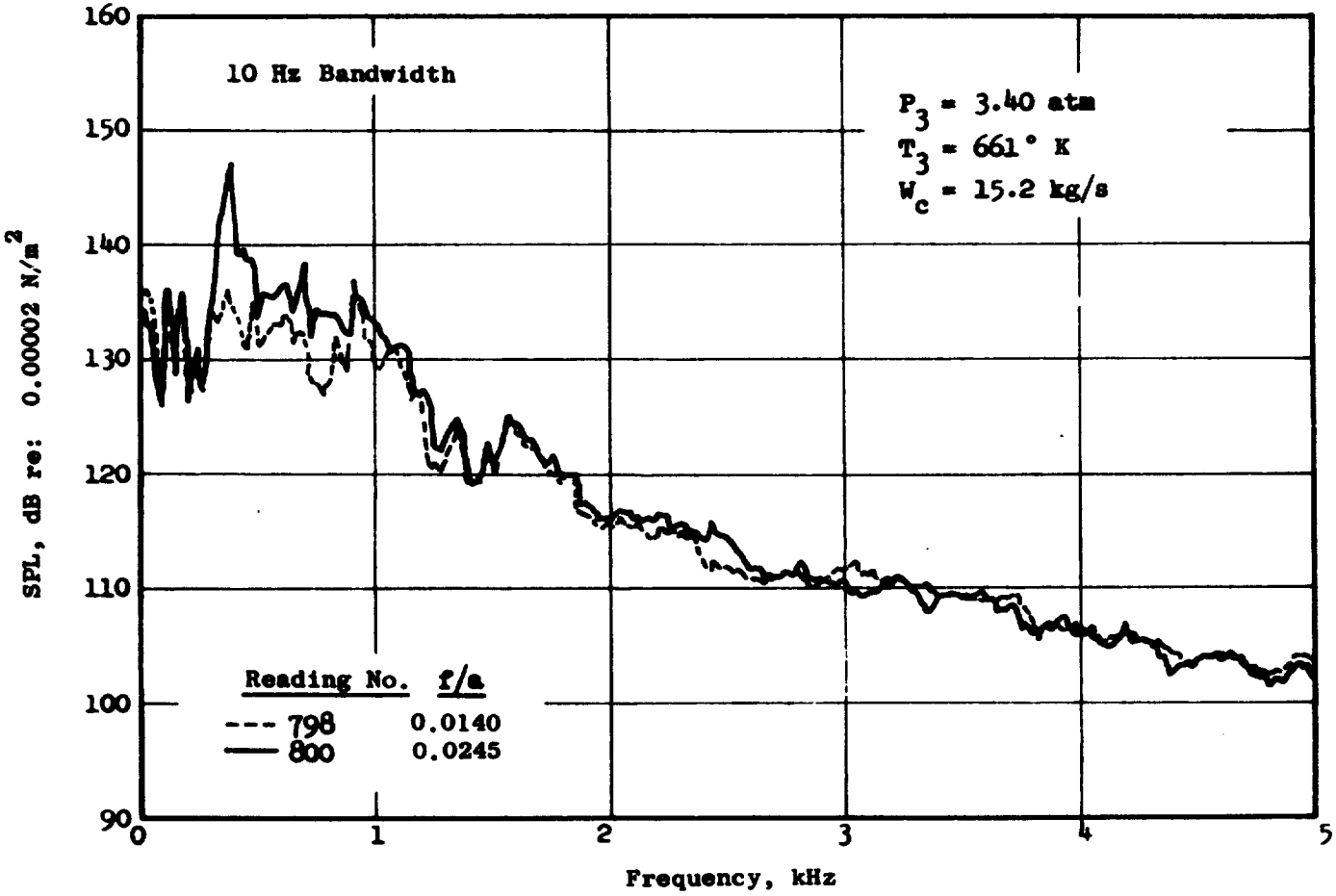

Figure 65. Comparison of Narrowband Spectra for Two Fuel-Air Ratios at Approach Inlet Conditions, 72-Swirl-Can/Counterswirl Flameholder, Configuration I-16, Upstream Probe.

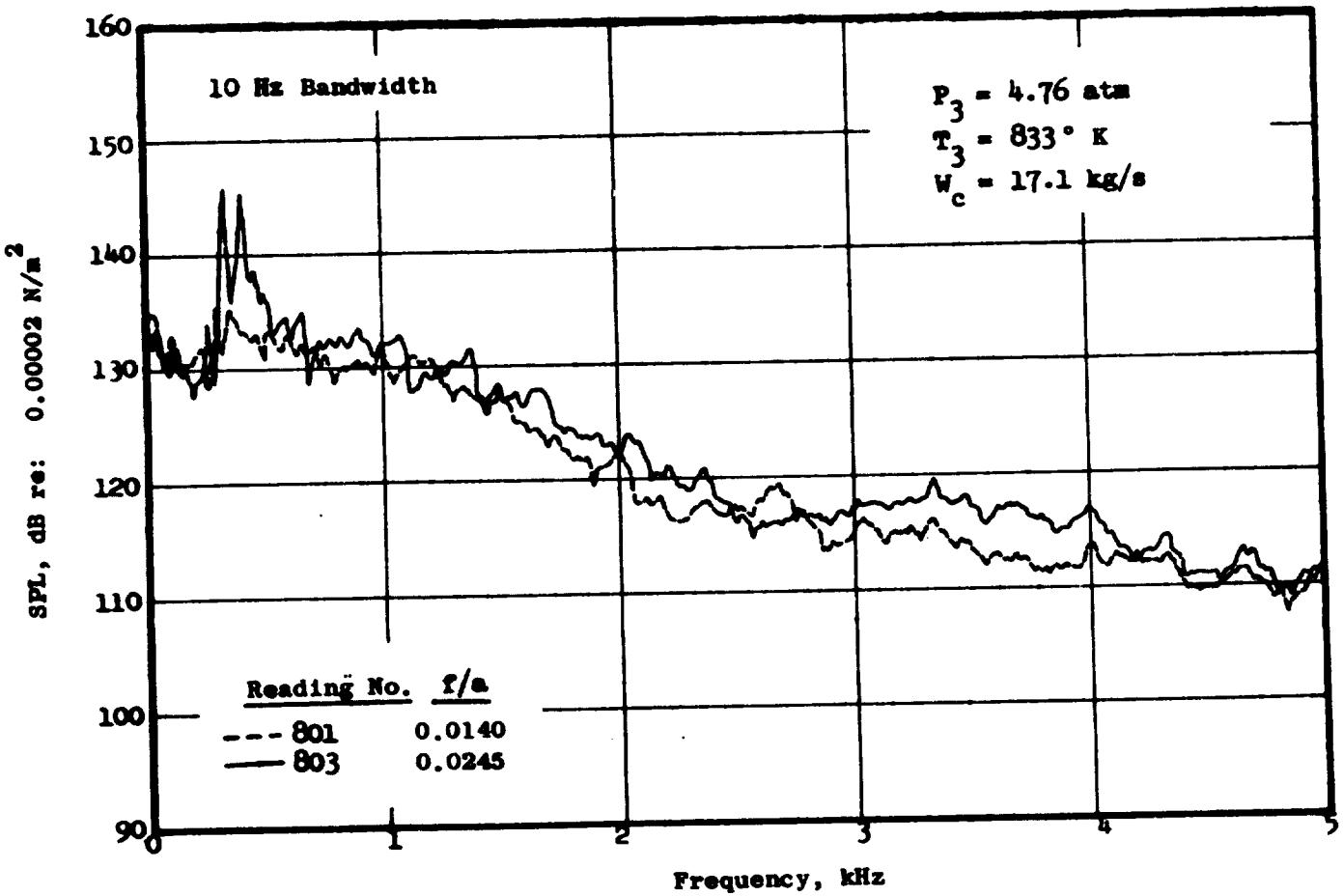

Figure 66. Comparison of Narrowband Spectra for Two Fuel-Air Ratios at Cruise Inlet Conditions, 72-Swirl-Can/Counterswirl Flameholder, Configuration I-16, Downstream Probe.

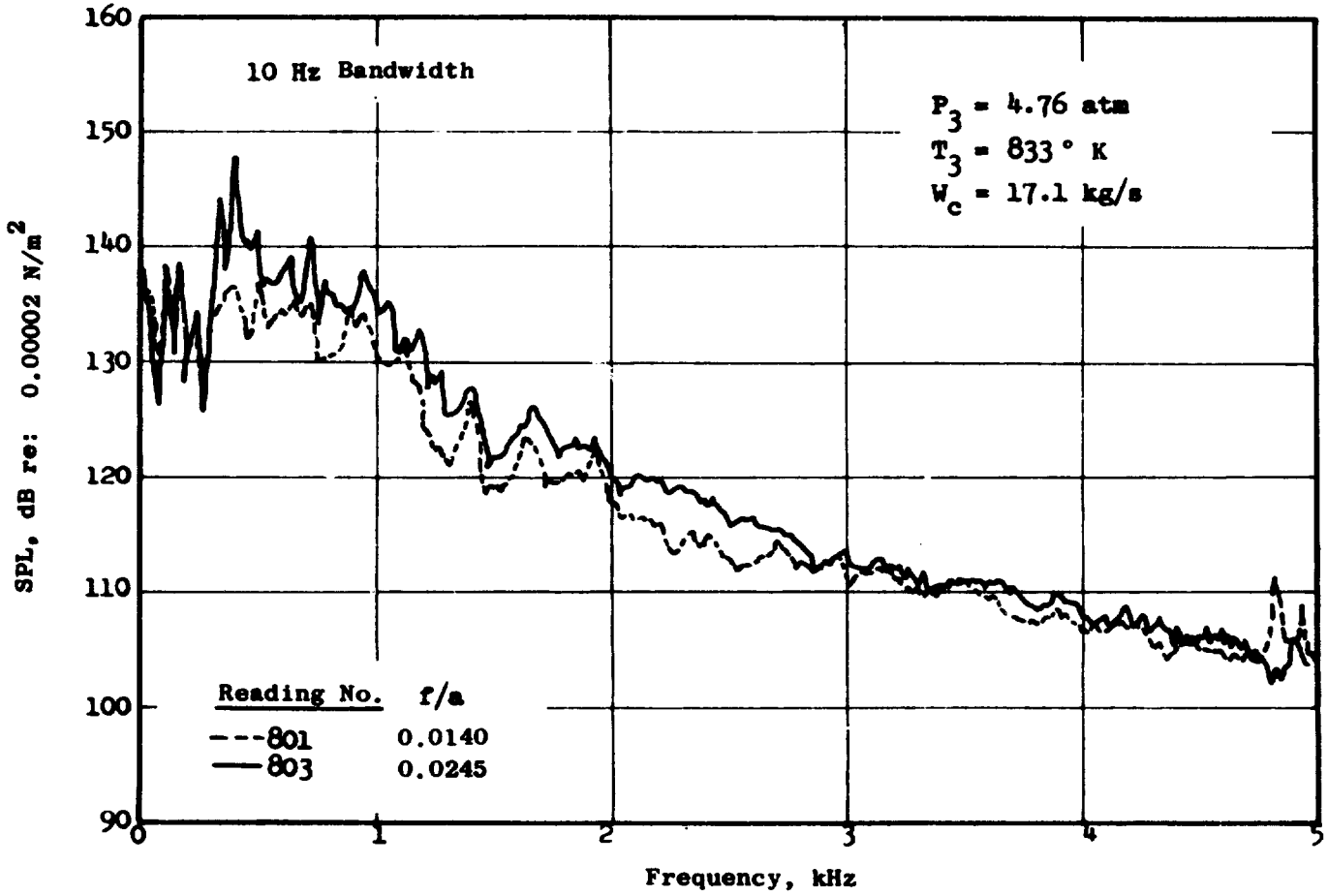

Figure 67. Comparison of Narrowband Spectra for Two Fuel-Air Ratios at Cruise Inlet Conditions, 72-Swirl-Can/Counterswirl Flameholder, Configuration I-16, Upstream Probe.

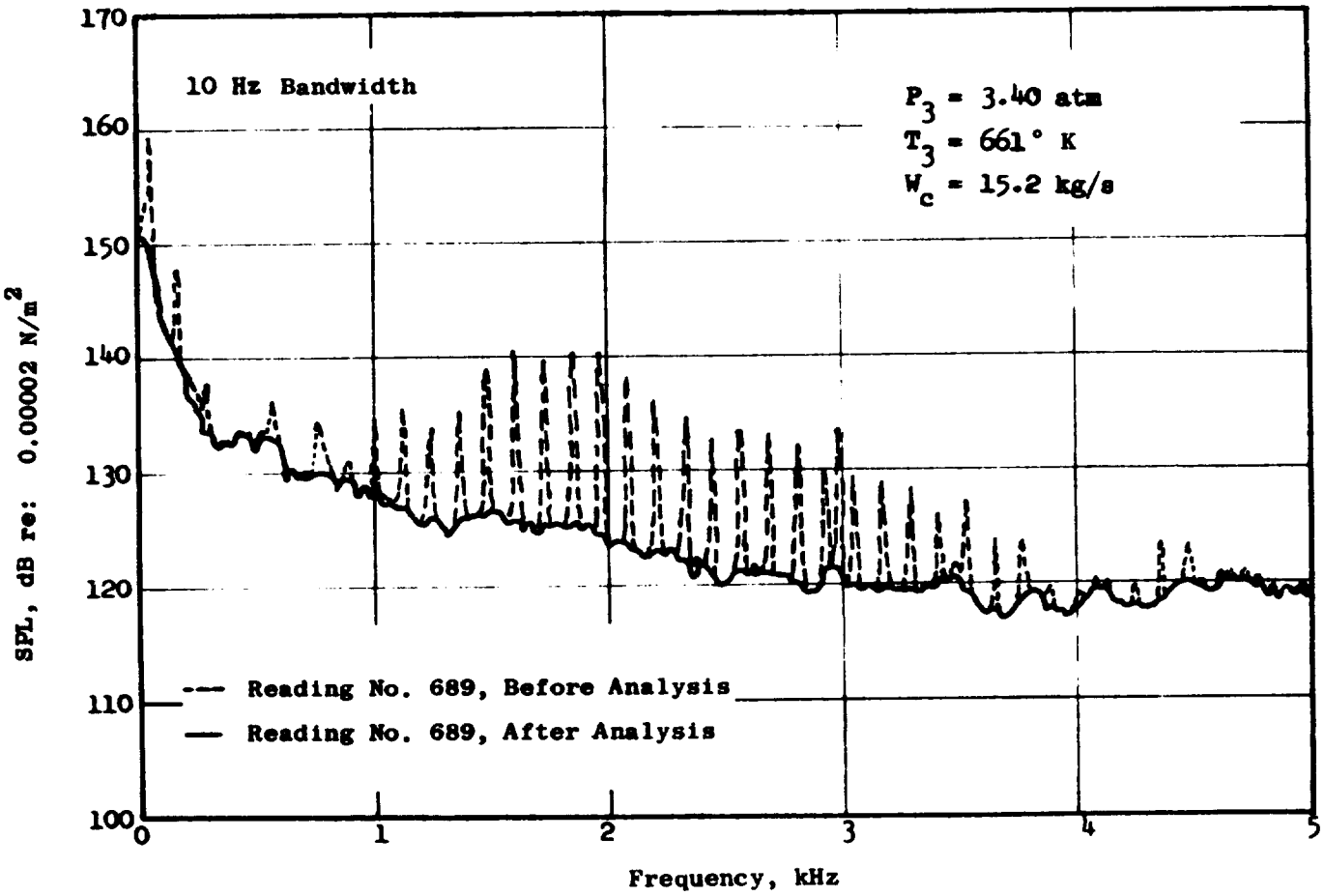

Figure 68. Typical Narrowband Spectrum Before and After Analysis, 90-Swirl-Can/ Flat Flameholder Combustor, Configuration I-14, Downstream Probe.

APPENDIX B

SYMBOLS

c	Speed of sound
e	Mass density
B	Fuel nozzle spacing
f/a	Fuel-to-air ratio
H	Height
k	Constant
L	Length
P	Pressure
T	Temperature
$\dot{W}$	Air weight flow rate
ρ	Density of air
OAPWL	Overall power level
OASPL	Overall sound pressure level
SLTO	Sea level takeoff

Subscripts

B	Fuel nozzle spacing
c	Combustor
D	Dome
o	Standard day reference
s	Static
t	Total
3	Inlet to the combustor
3.9	Exit from the combustor

REFERENCES

1. Bahr, D.W. and Gleason, C.C., "Experimental Clean Combustor Program - Phase I Final Report," NASA CR 134737.

2. Iberal, Arthur S.; "Attenuation of Oscillatory Pressures in Instrument Lines", Journal of Research of the NBS, Vol. 45, p. 85-108, July 1950.

3. Marble, Frank E. and Candel, S.M.,; "Acoustic Attenuation by Vaporization of Liquid Droplets - - Application to Noise Reduction in Fans and Ducts," AIAA Paper No. 74-526, June 1974.

4. Motsinger, R.; "Prediction of Engine Combustor Noise and Correlation With T64 Engine Low Frequency Noise", General Electric Report R72AEG313.

5. "Core Engine Noise Control Program, Final Report", Report No. FAA-RD-74-125, prepared for U.S. Department of Transportation, Federal Aviation Administration, System Research and Development Service, Washington, D.C. 20590. To Be Published.

6. Kazin, S.B.; Emmerling, J.J.; "Low Frequency Core Engine Noise", ASME 74-WA/AERO-2, November 1974.